DEVELOPMENT OF A SETUP FOR IN-SITU MEASUREMENT OF REINFORCEMENT CORROSION

BY

MOHAMMED ABDUL AZEEM JIBRAN

A Thesis Presented to the

DEANSHIP OF GRADUATE STUDIES

KING FAHD UNIVERSITY OF PETROLEUM & MINERALS

DHAHRAN, SAUDI ARABIA

In Partial Fulfillment of the
Requirements for the Degree of

MASTER OF SCIENCE

In

CIVIL ENGINEERING

December, 2011

KING FAHD UNIVERSITY OF PETROLEUM AND MINERALS
DHAHRAN, 31261, SAUDI ARABIA

DEANSHIP OF GRADUATE STUDIES

This thesis, written by **MOHAMMED ABDUL AZEEM JIBRAN** under the direction of his Thesis advisor and approved by his Thesis Committee, has been presented to and accepted by the Dean of Graduate Studies, in partial fulfillment of the requirement for the degree of **MASTER OF SCIENCE IN CIVIL ENGINEERING**.

Committee members

Dr. ShamshadAhmad (Advisor)

Dr. AbulKalam Azad (Co-advisor)

Dr. Mohammed Maslehuddin (Member)

Dr. Ahmad SaadAlgahtani(Member)

Dr. Salah U. Al-Dulaijan (Member)

22 FEB 2012

Dr. Nedal T. Ratrout
Departmental Chairman

Dr. Salam A. Zummo
Dean of Graduate Studies

25/2/12

Date

IN THE NAME OF ALLAH, MOST GRACIOUS, MOST MERCIFUL

DEDICATED

TO

MY FAMLIY & FRIENDS

ACKNOWLEDGEMENTS

In the name of Allah, the Beneficent, the Most Merciful. All praises and thanks are due to Allah, the Lord of the world for the successful completion of this research work. May His peace be upon the last messenger, Prophet Muhammad, his family and companions.

Acknowledgement is due to the King Fahd University of Petroleum and Minerals for providing facilities towards this research.

My gratitude and acknowledgment are due to Dr. Shamshad Ahmad, my thesis Advisor, for his constant support, encouragement and inspiration. Also, I am very grateful to Dr. AbulKalam Azad, my Co-Advisor; and Dr. Mohammed Maslehuddin, my committee member for their guidance and continuous support in all the phases of this work. Similarly, the support and guidance of Dr. Ahmad SaadAlgahtani and Dr. Salah U. Al-Dulaijan as committee members are highly appreciated.

My thanks go to the Chairman, Dr. Nedal T. Ratrout, and the entire Faculty and Staff of Civil Engineering Department for various assistance rendered to me during the course of my MS program. I want to particularly acknowledge the tremendous assistance I received from Dr. Mohammed Essa, Engr. Mukarram M. Khan and Engr. Syed Imran Ali all in the departmental laboratories. Similarly, thanks are due to Engr. Mohammed Shameem, Engr. Mohammed Ibrahim and Engr. Barry M. Salihu of University Research Institute for their assistance in all the stages of my experiments.

I extend my regards to the Indian community in KFUPM, my colleagues in the Department and all my friends for providing me with wonderful company.

My sincere appreciation goes to my parents, brothers, sisters and my entire family for their love, encouragement, patience and prayers.

Finally, I pray to Almighty Allah to reward all those who contributed, either directly or indirectly, towards the success of this work.

TABLE OF CONTENTS

LIST OF TABLES

LIST OF FIGURES

THESIS ABSTRACT

Name: **MOHAMMED ABDUL AZEEM JIBRAN**

Title: **DEVELOPMENT OF A SETUP FOR IN-SITU MEASUREMENT OF REINFORCEMENT CORROSION**

Department: **CIVIL ENGINEERING**

Date: **DECEMBER, 2011**

Deterioration and damage of reinforced concrete structures due to reinforcement corrosion is a widely reported subject in the literature. The rate of reinforcement corrosion is one of the essential factors required for assessing the extent of damage in a corroded reinforced concrete member and also for predicting its residual service-life. The rate of reinforcement corrosion is generally evaluated by the linear polarization resistance technique. However, the available commercial equipment do not predict the rate of reinforcement corrosion due to the high resistive medium of concrete. Thus there is a need to develop a reliable setup to measure reinforcement corrosion in concrete. The objective of this study was to develop a reliable and simple set-up and procedure for determining the rate of reinforcement corrosion utilizing the linear polarization resistance method.

Reinforced concrete specimens 500 × 500 × 80 mm with three 12 mm diameter steel bars were prepared. The steel bars in the concrete slabs were corroded to varying degree by the impressed current method. Corrosion current density (I_{corr}) was measured using the developed setup and two commercial equipment and the results were compared with the gravimetric weight loss.

The corrosion current density determined using the developed setup and other two commercial equipment without Ohmic drop compensation compared very well with the gravimetric weight loss. However, the best trend was noted in the data obtained from the developed setup. A good correlation was noted between the corrosion current density values determined with the developed setup with Ohmic drop compensation and the gravimetric weight loss. However, the correlation between the corrosion current density measured using the commercial equipment with Ohmic drop was poor indicating that the commercial equipment are not able to measure the corrosion rate with Ohmic drop compensation. These results indicate the usefulness of the developed setup in both types of measurements, namely with and without Ohmic compensation. A good correlation was noted between the moisture content, electrical resistivity and corrosion current density.

ملخص الرسالة

الاســـــــــــم: محمد عبد العظيم جبران

عنوان الرسالة: تطوير نظاما لقياس تآكلِ حديد التسليح في الموقع

التخصـــــــص: الهندسة المدنية

تاريخالتخـرج: ديسمبر 2011م

تدهوروضررالمنشات الخرسانية المسلحة بسببتآكلِحديد التسليح موضوعواسعالانتشارفيالدراسات الأخرى. معدل تآكلِحديد التسليح هو أحدالعواملالضروريةلتَقييممدىالضررِفي صَدّأ حديد التسليح للعنصر الخرساني وأيضاًلتَوقُّعحياةِالخدمةالمتبقيةِ. الهدف منهذهالدراسةِكَانَلتُطوّيرإعدادوإجراءبديلموثوقوبسيطلتحديد نسبةتآكلِحديد التسليحباستخدامطريقةَمقاومةِالاستقطابالخطيّةِ.

تم إعداد نماذجخرسانية 500 × 500 × 80 ممسلحةبثلاثقضبانمِنْ 12 مم. حيث حديد التسليح في البلاطات الخرسانية تم تعريضه لدرجات مختلفة من التآكل باستخدام التيار الانودي. كثافة تيارالتآكلِ (Icorr)تم قياسها باستخدام الإعداد الذي تم تطويرهوالجهازينالتجاريينوالنَتائِجتم مقارنتها َباستخدام الوزن المفقود للحديد (gravimetric weight loss).

الإعداد وإجراءالحسابَ تم تطويره بحيث تكون قادرة لتحديد نِسَبالتآكلِعلى نطاق واسع من درجة تأكل حديد التسليح. كثافة تيارالتآكل(I_{corr})حددت باستخدام الإعداد الذي تم تطويرهوالجهازينالتجاريينالآخرين بدون هبوط الاومية المعوضة قورنت بشكل جيد مع الوزن المفقود للحديد (gravimetric weight loss). وفي كل حال، أفضلاتجاه في البيانات حَصلَعليهمِنْالإعدادِالذي تم تطويره. كما لوحظَارتباطجيدبينمحتوىالرطوبةً،مقاومةنوعيةكهربائيةوكثافة تيارالتآكلِ.

CHAPTER 1

INTRODUCTION

1.1 Reinforcement Corrosion

Corrosion of reinforcing steel is one of the most dominant causes of concrete deterioration. Several billions of dollars are being spent for the repair and rehabilitation of the deteriorated concrete structures. However, prior to repair or restoration, it is necessary to determine the extent of corrosion of the reinforcing steel so that corrective measures can be planned. The corrosion potentials measurement only provides qualitative information, whereas measurement of corrosion current density gives quantitative information. The latter technique estimates the rate of corrosion which can be used for predicting the remaining service-life of a structure.

Various *non-destructive* methods, based on electrochemical techniques, have been used to detect the initiation and rate of corrosion at an early stage, and to predict residual lives and accordingly decide what preventive or repair systems are to be applied [1]. Both Direct Current (DC) and Alternate Current (AC) methods have been utilized as non-destructive methods for measuring the rate of corrosion in reinforced concrete. The electrochemical polarization methods are used to monitor quantitatively general corrosion and galvanic corrosion. They can also be used qualitatively to monitor localized corrosion (pitting and crevice). The main advantages of electrochemical techniques include: sensitivity to low corrosion rates, short experimental duration, and well-established theoretical understanding. On the other hand, the gravimetric weight loss measurement is a *destructive technique* for

obtaining the corrosion rate [2]. Due to the destructive nature of the gravimetric weight loss method, the non-destructive linear polarization resistance (LPR) method is commonly utilized for assessing the rate of reinforcement corrosion.

In the LPR measurements, the steel bar is *polarized* by the application of a small perturbation to the equilibrium potential through a counter electrode. The *polarized surface area* of the reinforcing steel is assumed to be that area which lies directly below the counter electrode. However, there is considerable evidence that current flowing from the counter electrode is not confined and can spread laterally over an unknown large area of the reinforcing steel, also the value of Stern- Gery constant (B) is unknown; it is taken as 26mv for active state of corrosion and 52mv for passive state of corrosion that may lead to the inaccurate estimation of the corrosion rate. On the other hand, gravimetric (weight loss) measurement as a *destructive test*, when conducted in controlled laboratory conditions serves as the most reliable reference method. It is simple, but is also a time-consuming technique for the determination of corrosion rate [2]. The weight loss measured is converted to a uniform corrosion rate over the exposure period. It has been proposed that the combination of the weight loss method and the polarization resistance method offers means of quantitative corrosion analysis. However, studies on the relationship between the weight loss method and the polarization resistance method are limited and most studies were conducted on different set of specimens [3].

1.2 Need for this Research

There are many commercially available instruments in the market for measuring the corrosion current density of rebar in concrete, but many of the instruments are very expensive and their accuracy has also not been verified with the other equipment (or) by gravimetric weight loss method. Also, the fact that matters is that many instruments can only be used in laboratory. However, the accuracy of the reinforcement corrosion rate measured electrochemically is invariably doubtful because of the difficulties and errors frequently involved in the experimental measurements. Due to this reason, a setup needs to be developed, which can predict the corrosion rate reliable and should less expensive. To check the accuracy of the developed setup it is needed to compare the electrochemically measured corrosion rates with gravimetrically measured corrosion rates, so as to see which among the developed setup and commercially instrument is closer to gravimetric weight loss method.

1.3 Objectives

The primary objective of this work was to develop a corrosion measurement setup which can be of low cost and can give the same or better results as obtained with the commercial instruments and gravimetric weight loss method.

The specific objectives are the following:

1) Develop a corrosion measurement setup for measuring reinforcement corrosion,

2) Correlate the electrochemically measured reinforcement corrosion rates with the gravimetric weight loss method, and

3) Correlate the corrosion rates measured using the developed setup and commercial instruments and compare the results with gravimetrically measured corrosion loss on a number of reinforced concrete specimens.

CHAPTER 2

LITERATURE REVIEW

2.1 Mechanism of Corrosion of Steel

When a rebar corrodes, the deterioration is usually very slow, but it is always progressive and the rust occupies a much larger volume than the steel and finally exerts force on the concrete to cause cracks. These cracks grow as rebar continues to corrode. Finally the crack grows leading to delamination and spalling of concrete. Remedial measures can be taken when we can know the cause of corrosion and also the rate of corrosion (corrosion current density). Corrosion rate helps in predicting the residual service life of the structure.

In reinforced concrete, the rebar may have many separate areas at different energy levels. Concrete plays the role of electrolyte, wire ties provide the metallic connection, the Corrosion is an electrochemical process which involves the flow of electrons and ions (charges). Active sites on the bar are called anodes, at these locations iron atoms lose electrons and move into the surrounding concrete as ferrous ions. This process is called a half-cell reaction or the anodic reaction which is represented as:

$$2Fe \rightarrow 2Fe^{2+} + 4\,e^{-} \qquad (1)$$

The electrons flow from anode to cathode, where they combine with moisture and oxygen in the concrete to form hydroxyl ions. The reaction at the cathode is called a cathodic reaction (or) reduction reaction .A common cathodic reaction is:

$$2\,H_2O + O_2 + 4e^- \rightarrow 4\,OH^- \quad (2)$$

To maintain electrical neutrality, the hydroxyl ions move through the concrete pore water to the cathodic site where they combine with ferrous ion to form iron hydroxides (or) rust as shown in Eq. 3.

$$Fe^{2+} + 2\,OH^- \rightarrow Fe\,(OH)_2 \quad (3)$$

The above formed hydroxide tends to react further with oxygen to form higher oxides. The increases in volume as the reaction products react further with dissolved oxygen leads to internal stress within the concrete that may be sufficient to cause cracking and spalling of the concrete cover. The loss of bond between concrete and rebar's and the loss of cross-section of rebars due to corrosion result into loss of load bearing capacity.

2.1.1 Concrete and the passive layer

Initially the concrete has a very high degree of alkalinity (pH of 12 to 13) which prevents steel from corrosion. At high pH, a thin oxide layer forms on the steel and prevents it from corroding. This protective (or) passive layer does not actually stop corrosion; it only reduces the corrosion rate to an insignificant level. For steel in concrete, the passive corrosion rate is typically 0.1 μm per year. Without the protective layer, the steel would corrode at rates at least 1,000 times higher.

Because of protection provided by the concrete, reinforcing steel does not corrode in the majority of concrete structures. However, corrosion can occur when the protective layer is destroyed. The destruction of the passive layer occurs when the alkalinity of the concrete is reduced or when the chloride concentration in concrete is increased to a certain level. An indicator termed as chloride/hydroxyl ion ratio is used to indicate the initiation of rebar corrosion when its value increases beyond 0.6 [4].

Corrosion of rebar in concrete structures occurs due to two reasons

- Carbonation
- Chloride Penetration

These two issues are discussed briefly in the following sub-sections:

2.1.2 Carbonation

Carbonation of concrete is mainly caused due to carbon dioxide (CO_2) present in air or from the pollutants such as vehicles, industries, etc.. Carbonation destroys the alkalinity (i.e., OH^- ions are destroyed) of concrete which results into breaking of the passive layer causing corrosion of steel in concrete. Carbonation occurs when carbon dioxide from the air penetrates the concrete and reacts with hydroxides, such as calcium hydroxide, to form carbonates. In the reaction with calcium hydroxide, calcium carbonate is formed as shown in Eq.4.

$$Ca(OH)_2 + CO_2 \rightarrow CaCO_3 + H_2O \quad (4)$$

This reaction reduces the pH of the pore solution leading to the destruction of the passive film on the steel.

2.1.3 Chloride penetration

Chloride Penetration in concrete is mainly caused due to chloride contaminate ion in the concrete ingredients, use of deicing salts and exposure to marine environments. Free chloride ions corrode steel in concrete by breaking the passive layer competing with the OH^- ions. Although chlorides are directly responsible for the initiation of corrosion, they appear to play only an indirect role in the rate of corrosion after initiation. The primary rate-controlling factors are the availability of oxygen, the electrical resistivity and relative humidity of the concrete, and the pH and temperature [5].

2.2 Factors Affecting Reinforcement Corrosion

In addition to factors other than the carbonation and chloride effects, there are numerous external and internal factors that affect the rebar corrosion to a large extent.

External factors affecting the rebar corrosion are mostly the environmental parameters such as:

- Oxygen and moisture at rebar level
- Temperature
- Relative humidity
- Carbonation
- Chlorides penetration
- Stray current
- Bacterial action

Internal factors affecting the corrosion of rebar in concrete are as the following:

- Cement type
- Cement content

- w/c ratio
- Impurities in aggregates and water
- Use of chloride based admixtures
- Construction practices
- Cover

2.2.1 Environmental factors affecting reinforcement corrosion

Effect of Oxygen

Oxygen is an important factor for corrosion to occur. It is also mainly responsible for the progress and rate of corrosion. Oxygen acts as depolarizer at cathode opposing the cathodic polarization and consequently increases the rate of corrosion [6]. Oxygen has to be in a dissolved state for it to be consumed in the cathodic reaction [7]. Dissolved oxygen will accelerate corrosion in acid, neutral (or) slightly alkaline electrolytes. The rate of corrosion in a neutral solution is almost directly proportional to the oxygen concentration for all other variables remaining constant. The passivation process depends upon the amount of oxygen available at the concrete/steel interface, which depends upon the thickness of concrete cover over steel and other factors that affect the quality of concrete, such as curing methods, cement content and water-to-water/cement ratio [8].

The availability of oxygen is one of the important controlling factors for corrosion of steel, as mentioned above; however, there is little information on its diffusion effect in concrete. Some information is shown below in the Figure 2.1, where the rate of oxygen diffusion through water saturated concrete of varying quality and thickness is illustrated [7]. With increasing water saturation the diffusion of oxygen through cement decreases and for certain

saturation, with increase in w/c ratio diffusivity also increases because of the increase in total porosity and superior interconnectivity of the pores [9].

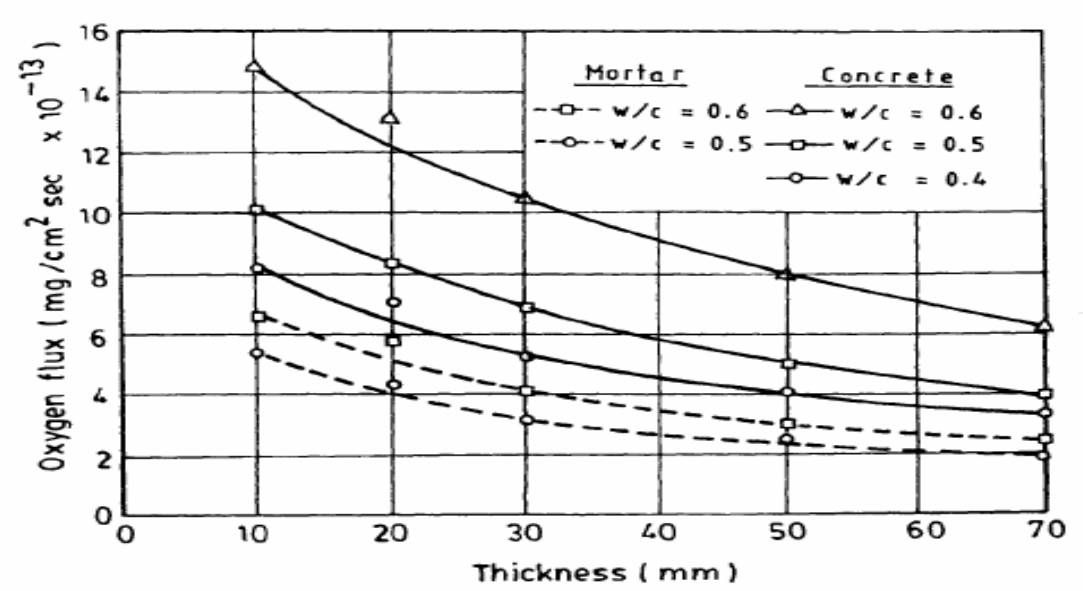

Figure2.1: Effect of water-cement ratio and thickness on the diffusion of oxygen through Mortar and Concrete [7].

The diffusion of O_2 to the concrete steel interface also depends upon the degree of saturation of concrete with water. In wet concrete, dissolved oxygen will be diffusing slowly in pore solution, while in partly dry concrete; the diffusion of gaseous oxygen is much faster**.** This is the reason for encountering enhanced corrosion rate in RC structures subjected to the condition of alternate wetting and drying cycles compared to that in a continuous saturated or dried structures, even in most aggressive conditions.

Effect of Moisture

Reinforcement corrosion in concrete is essentially a form of aqueous corrosion. The presence of moisture is extremely important for the corrosion reaction to take place. All corrosive factors are not effective in the absence of moisture [6] due to unavailability of electrolytic pore water. Additionally, moisture penetration is the means whereby any exterior

substances such as chloride salts, carbon dioxide and dissolved oxygen may gain access to the reinforcement.

Effect of Relative Humidity and Temperature

The relative humidity mostly affects the carbonation of concrete. Carbonation of concrete decreases with an increase in the environmental relative humidity in the range of 50–100%. Based on computations, in normal concentration of CO_2 even after a long period of exposure [10] have found that, within 50–30% RH, a decrease in environmental RH may not cause a decrease in carbonation of concrete. A rise in temperature may result in a twofold effect: (i) the electrode reaction rates are generally increased, and (ii) decrease in oxygen solubility resulting in a reduction in the rate of corrosion [6]. If the situation is favorable for corrosion to take place, the corrosion rate increases with high temperature and high humidity [11].

2.2.2 Effect of internal factors

Cement Composition

Concrete to resist the reinforcement corrosion it mainly depends on the C_3A in cement. By, using blended cements, such as micro silica-blended which consist of high-C_3A cement, it is established that it resists both reinforcement corrosion and sulfate attack [14].

Impurities in Aggregates

Aggregates containing chloride salts cause serious corrosion problems, particularly those associated with sea-water and those whose natural sites are in ground water containing high concentration of chloride ions [15].

Admixtures

Adding calcium chloride as an accelerator for hydration of cement is the most significant reason for the presence of chloride in concrete in the RC structures exposed to normal weather conditions. Some water reducing admixtures also contain chlorides [15].

w/c ratio

The w/c ratio mainly controls strength, and impermeability of concrete, and hence indirectly controls reinforcement corrosion. The penetration of chloride ions increases with an increase in the w/c ratio [16]. Carbonation depth has been found to be linearly increasing with an increase in the w/c ratio [17].

2.3 Corrosion Monitoring Techniques

A detailed literature review on the following topics will be made:

- Visual and physical appraisal
- Electrical resistance probe method
- A.C. Impedance technique
- Half-cell Potential measurement
- Electrochemical methods
  - Electrochemical noise
  - Polarization methods (Tafel plot and linear polarization resistance)
- Weight-loss (i.e., gravimetric) method

2.3.1 Visual and physical appraisal

In this category, there are techniques such as ultrasonic pulse velocity, Schmidt rebound hammer which can only determine the quality of concrete rather than the condition of the reinforcement. These methods indirectly show the signs of reinforcement corrosion by indicating whether the delamination has occurred on the surface or not. Sounding as a method of testing is best confined for locating the areas of difficulty. Further, hairline cracks which run parallel to the reinforcement may be first signs of corrosion or they may be due to shrinkage and thus visual inspection cannot provide conclusive information.

Physical methods, such as core samples, can indicate the state of reinforcement at a specific location but much more information is required to determine the durability and serviceability of a structure. But, visual inspection with various non-destructive testing like electrochemical and resistance measurements can provide useful information of condition of the structure [18].

2.3.2 Electrical resistance probe method

Resistivity of concrete can be determined using the following methods:

- Wenner four-probe method
- Two-probe method
- Disc method
- Core-clamping method
- Ohmic resistance method

Wenner Four-Probe Method

The resistivity of concrete can be measured non-destructively using Wenner's probe electrodes placed on the concrete surface, as shown in Figure 2.2. The current (I) is applied to the two outer probes (electrodes) and the resulting voltage drop (E) is measured between the two inner probes (electrodes). The resistance of concrete (R) is taken as E/I. Knowing the concrete resistance (R) and spacing of the probe electrodes (a), the resistivity of concrete (ϱ) can be calculated using the following formula:

$$\varrho = 2\pi.a.R$$

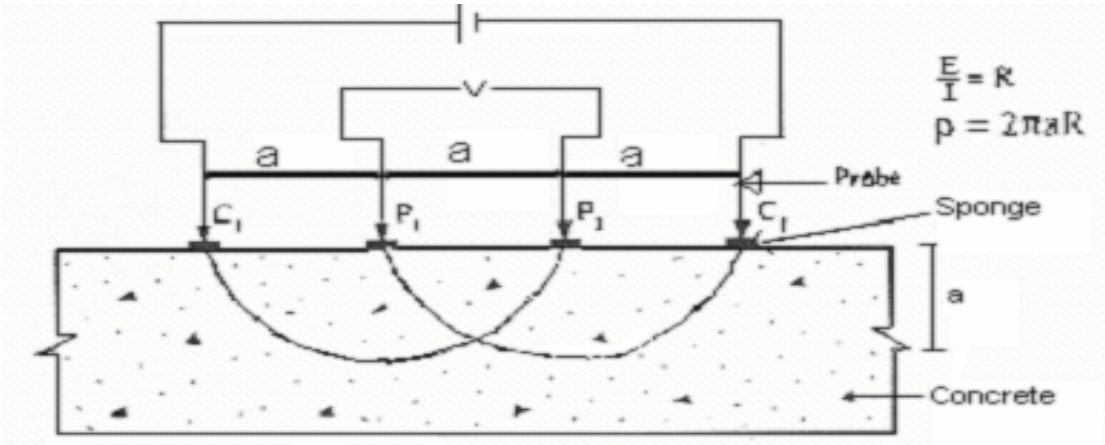

Figure 2.2: Scheme of the Wenner's technique to determine the electrical resistivity of concrete from the surface.

- Spacing of the probe electrodes (a) should always be greater than the maximum size of aggregate.
- Positioning of Wenner's probe electrodes should be as far as possible from the rebar [19].

Two-Probe Method

Hand-held two-probe equipment, as shown in Figure 2.3, is also available. This requires holes to be drilled and the procedure is as follows:

- Drill an 8mm deep hole in the concrete with the given 6mm drill bit and using the locating pin drill another hole at a distance of 5cm from the 1st one.
- Inject a small amount of conductive gel in the hole and insert the probes in it and press the button and on LCD the resistivity of concrete will be displayed.

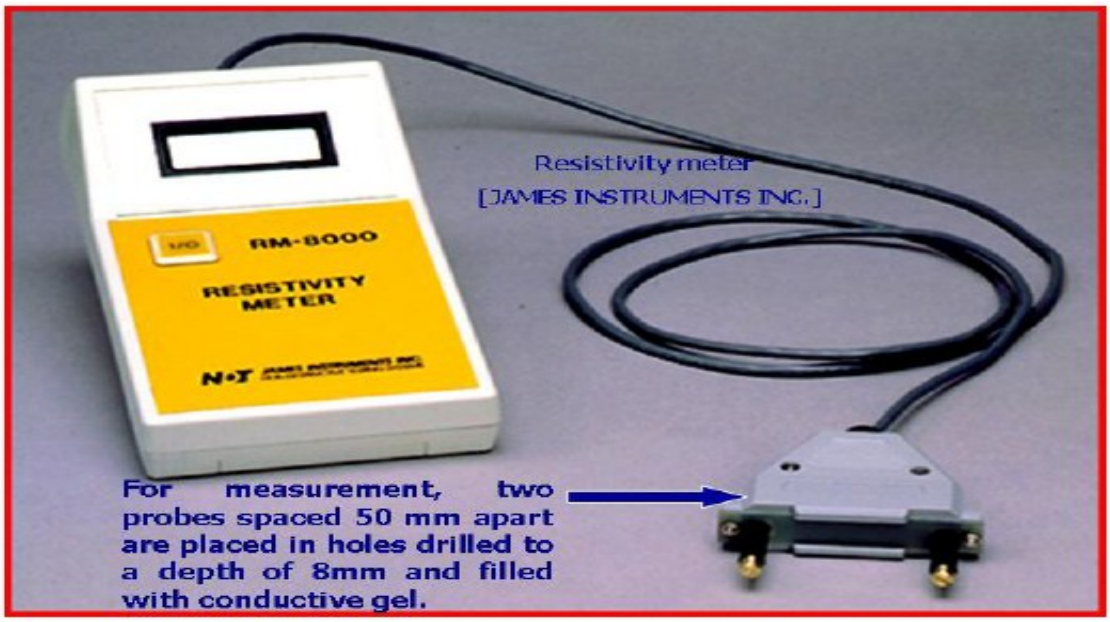

Figure 2.3: Resistivity measurement using two-probe method.

Disc method

One of surface electrical assessment testing methods is a disc-electrode method. This method involves an electrode-disc placed on the concrete surface over a rebar and it measures the resistance between the disc and the rebar. This method requires a connection to the reinforcement cage and full steel continuity [20] as shown in Figure 2.4.

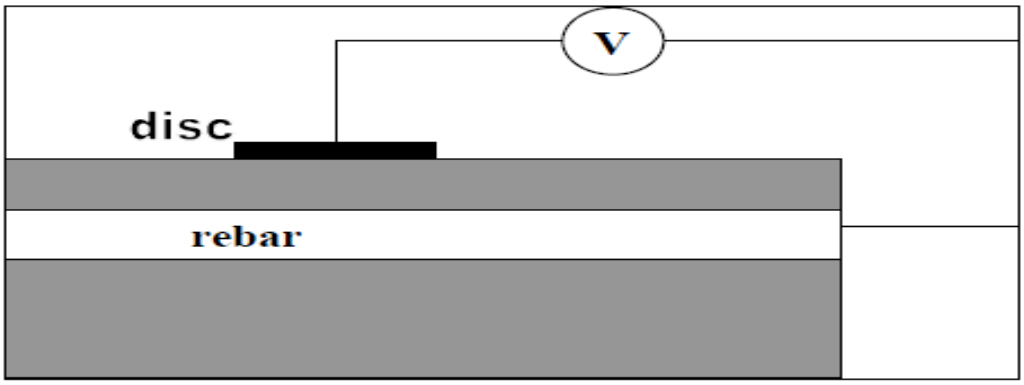

Figure 2.4: Setup of one electrode (disc) method of measurement of concrete resistivity.

The cell constant can be determined by applying this test method to several concrete slabs of known resistivity. For disc, cover depths and bar diameters being 10-50 mm, the cell constant is approximately 0.1 m [20]. Therefore, the resistivity measured using a disc electrode is approximately:

ρ (disc)= 0.1*R(disc –bar) = 0.1V / I

Where, V (or delta V is used sometimes) is the potential drop (V),

I is the current passed through covercrete (A), and

$\rho$is surface electrical resistivity (Ω-cm).

Core-clamping Method

In this method, steel plates are pressed to two parallel faces of a cube or cylindrical specimen with a wetted cloth for good electrical contact, as shown in Figure 2.5. Resistivity of concrete can be easily measured in laboratory using this method [20].

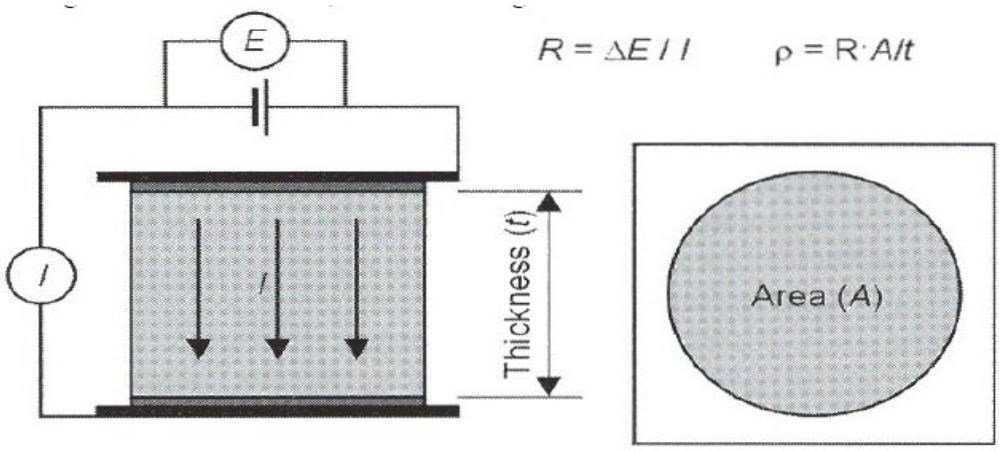

Figure 2.5: Measurement of electrical resistivity of concrete by two-electrode method.

The resistivity is calculated from the resistance measured between the plates by:

$$\varrho = R.C$$

Where:

ϱ = resistivity of concrete (ohm-m)

R = resistance between plates (ohm)

C = geometrical cell constant = A/t

A = area of parallel faces

t = thickness of specimen

Ohmic Resistance Method

The resistivity can be approximately determined through measured value of ohmic resistance (R) of concrete using the following expression:

$\varrho = 2\,RD$

where:

ϱ = resistivity of concrete (Ohm-m)

D = diameter of the metal disk (m)

R =Ohmic resistance of concrete between a metal disc (kept on the surface of concrete) and the rebar (Ohm)

The circuitry, as shown in Figure 2.6, is used to measure the value of R.

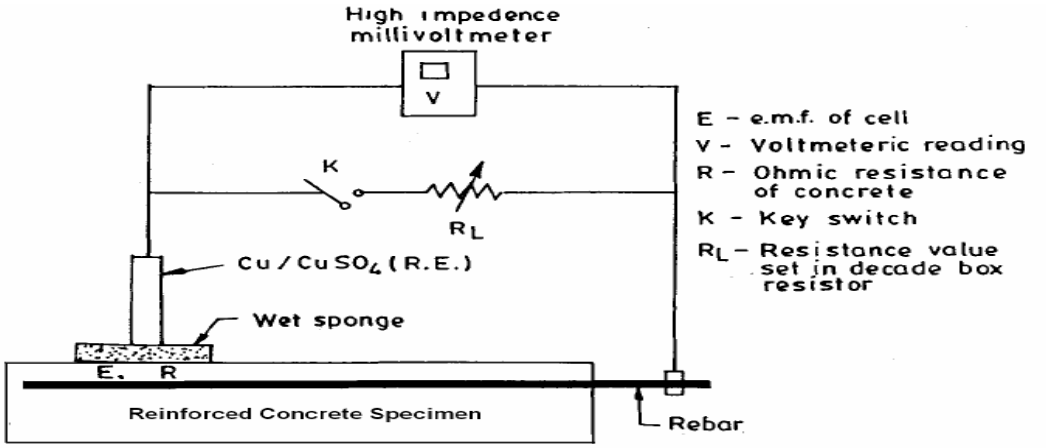

Figure 2.6: The circuitry for Ohmic resistance (R) measurement.

Referring to Figure 2.6, the procedure for measurement is as follows:

- R_L is fixed at several values one after another by connecting momentarily the switch K, just long enough to read the voltmeter reading (V) in each case of R_L.

- The R_L and V are related by the following equation:

$$\frac{1}{V} = \frac{R}{E}\frac{1}{R_L} + \frac{1}{E}$$

Where: E is open circuit potential (i.e. half-cell potential)

The R_L versus V data are plotted as $1/R_L$ versus $1/V$, as shown in Fig. 2.7.

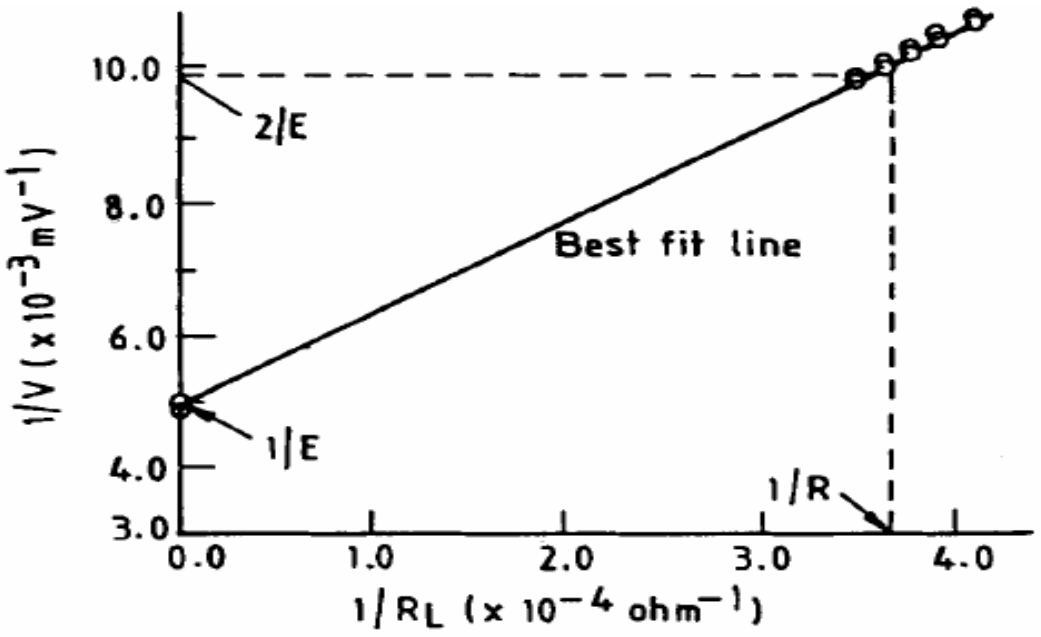

Figure 2.7: Method of determining the R by best fit of R_L versus V data points.

The slope (R/E) and intercept (1/E) of the best fit straight line joining these points (Figure 2.7) gives the solution for ohmic resistance R, as follows:

$$R = \frac{Slope\ (R/E)}{Intercept(1/E)}$$

The results of concrete resistivity measurements can be used for assessing risk of reinforcement corrosion [21]. Interpretation of results can be done using Table2.1.

Table 2.1: Relation between corrosion and resistivity [22].

Resistivity (Ohm-cm.)	Risk of Corrosion
Greater than 20,000	Negligible
10,000 to 20,000	Low
5,000 to 10,000	High
Less than 5,000	Very High

2.3.3 A.C. impedance

In recent years, A.C. Impedance technique has been a useful non-destructive method for determining the corrosion of steel embedded in concrete. Impedance (Z) is basically the ratio of A.C. voltage to A.C. current. An alternating voltage around 10 to 20 mV is applied to the rebar and the phase angle and resultant current are measured for different frequencies. The response to an A.C. input is a complex impedance that has both imaginary (capacitive or inductive) and real (resistive) component Z" and Z as shown in Figure 2.8. An equivalent electrical circuit can be determined by studying the variation of the impedance with frequency, which would give similar response as the corrosion system being studied. Plotting the real impedance against the imaginary impedance gives a semicircle, with a diameter equal to Rt. The semicircle is offset from the origin by a value Rs, which is the ohmic resistance of the concrete cover zone between the reference half-cell and the reinforcing bar being measured. At the highest point on the semicircle the frequency f can be determined and the double-layer capacitance value can be calculated by:

$$Cdl = \frac{1}{2\Pi\, Rt\, f}$$

In practice, due to different RC parallel components, an AC Impedance response will often be a combination of several different semicircles, which could arise from film effects, etc. The value of Cdl is useful because it may be used to understand the corrosion processes. The advantage of A.C. impedance technique is that, it can give more information than DC LPR Measurements, but disadvantage is that it is very time-consuming to perform. Due to this it can only be used in laboratory rather than in field works [23].

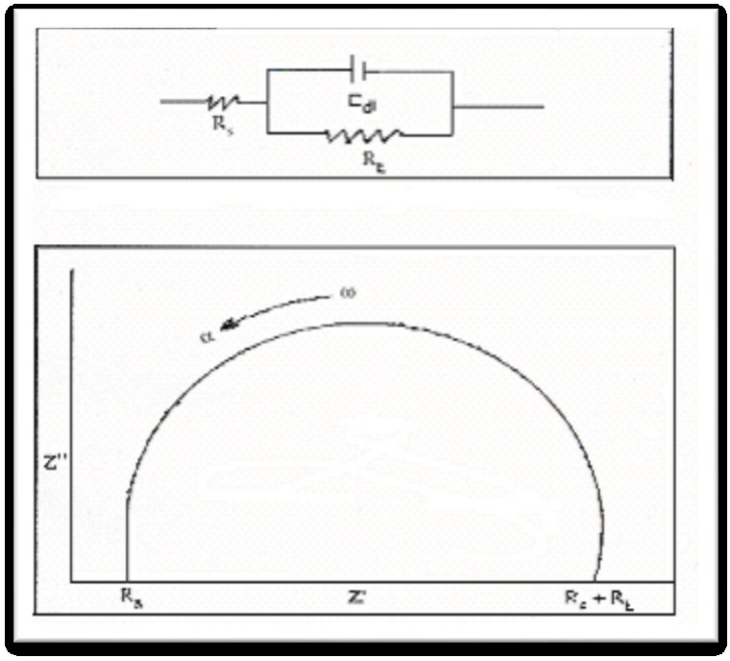

Figure 2.8: Nyquist Plot for steel in concrete.

2.3.4 Half-cell potential

In reinforced concrete, concrete acts, as an electrolyte and depending on the concrete environment the reinforcement will develop a potential, which may vary from place to place. The diagram for open circuit potential measurements is as shown in Figure2.9.

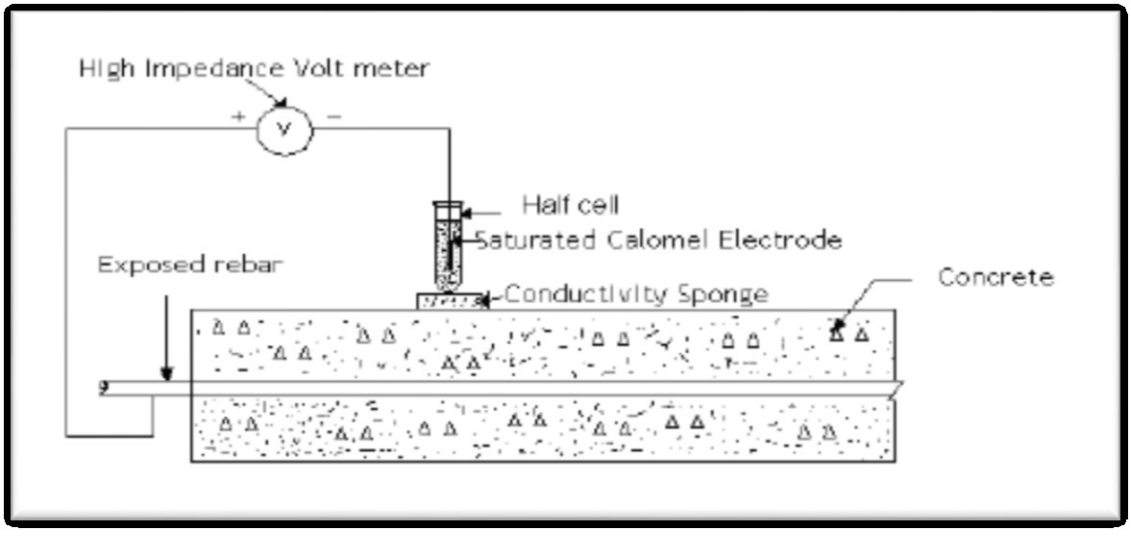

Figure 2.9: Schematic representation of open circuit potential (OCP) measurement.

In this technique it is essential to measure corrosion potential of rebar with respect to a standard reference electrode, such as copper/copper sulfate electrode (CSE), saturated calomel electrode (SCE), etc. As per ASTM C 876 [24] standards, the criteria for determining the probability of reinforcement corrosion are presented in Table 2.2.

Table 2.2: Corrosion condition related with half-cell potential (HCP) measurements [24].

Open circuit potential (OCP) values		**Corrosion condition**
(mV vs. SCE)	(mV vs. CSE)	
<-426	<-500	Severe corrosion
<-276	<-350	High (>90% risk of corrosion)
>-125 but < -276	>-200 but <-350	Intermediate corrosion risk
>-125	<-200	Low(10% risk of corrosion)

Identifying and measuring the corrosion in concrete structures is essential. Although there are several methods for the identification and measurement of corrosion in reinforcing steel, there is no agreement regarding which technique can measure the corrosion rate accurately. Various techniques for detecting and measuring corrosion will provide data on the causes, detection or rate of corrosion [25].

The key method of detecting corrosion is the half-cell potential (HCP) measurements. The corrosion process of steel in concrete can be followed using several electrochemical techniques. Monitoring by half-cell potential is the most common procedure for routine inspection of reinforced concrete structures [26],[27],[28] . Its use and interpretation are described in the ASTM C876 *Standard Test Method for Half-Cell Potential of Reinforcing Steel in Concrete* [24]. Half-cell Potential readings are insufficient as criterion, since they are affected by a number of factors, which include polarization by limited diffusion of oxygen [29], [30],

concrete porosity and the presence of highly resistive layers [31], [32]. According to this method if the potential of steel in concrete becomes more negative than -350mV vs. CSE there is a 90% probability that corrosion will occur. It is a non-destructive method but can still collect large quantity of data from a large structural area. Potential maps can be generated using the data , according to ASTM C876-91, is the most commonly applied electrochemical technique for diagnosing the corrosion risk of reinforced concrete structures [32], [33]. However it is generally accepted that corrosion potential measurements must be complemented by other methods [33], because in well-established conditions a reliable relationships between potential and corrosion rate can be found in the laboratory [34] , [35] but these cannot be generalized, since in very narrow range of potentials wide variations in the corrosion rate are possible [36]. Half-cell potential values can only provide information for corrosion probability but cannot determine the rate of corrosion [37].

2.3.5 Electrochemical methods

Electrochemical Noise Method

Electrochemical noise technique is a rising technique in measuring corrosion of reinforced concrete structures [38]. This method provides information on the mechanism and rate of corrosion processes at different areas in concrete structures. A low amplitude variation of the corrosion potential of steel in concrete is measured to obtain a noise data as a record of potential fluctuations in the form of power spectra. A noise source is located within the area of probability of corrosion. A time record at regular intervals is monitored over the frequency range (10 HZ to 1mHz) noise data is obtained as a potential fluctuation. Noise data is converted to frequency domain from time domain and displayed in the form of amplitude and frequency based on either Fast Fourier Transform or maximum entropy method of spectral analysis. The measurement interval is usually between 2-10 seconds depending upon the

frequency range. The instantaneous variations in current flow between two identical, electronically isolated bars in concrete coupled through a zero resistance ammeter are recorded, together with the fluctuations in the potential of one of them, measured against a reference electrode. The polarization resistance is then given by:

$$R_p = \sigma_E/\sigma_I$$

The corrosion rate may be obtained from Rp. In addition, the co-efficient of variance of the current noise σ_I/Iis said to indicate the type of corrosion, ranging from 10^{-3} for general corrosion to 1.0 for localized corrosion [39].

One of the most important advantages is that its application does not involve artificial disturbance of the system. Various authors have claimed that, it is possible to characterize different corrosion types: metastable pitting, pitting and crevice corrosion, uniform corrosion, and stress-corrosion cracking based on the results of these analyses [40],[41],[42]. To know the general characteristics of corrosion processes from the measured electrochemical noise (EN), numerous statistical parameters such as noise resistance [43], [44] are usually applied. In a number of cases, different quantities defined by the theory of chaos have been applied [41]. On the assumption of the stationarity of the signals all these parameters are calculated by means of mathematical techniques. EN signals, obtained from various corrosion processes usually do not satisfy the requirements for stationarity [45]. Wavelet transformation is the only mathematical technique, which can be used for the analysis of measured EN, and does not require the stationarity of signals [46].

There have been only a few studies of EN for measuring corrosion in concrete [47-49]. In general, no distinctive benefits of this technique comparing to the macro-cell current measurements were established.

Linear Polarization Resistance Method

The electrochemical methods consist of first measuring the corrosion current density (I_{corr} in $\mu A/cm^2$) and then converting I_{corr} into either corrosion penetration rate (P_r in μm/year) or instantaneous corrosion rate (J_r in g/cm^2/year) using Faraday' basic equation. I_{corr} values obtained at different points on a member may be plotted to obtain contours showing areas corroding at different rates. Instantaneous corrosion rate, J_r, which is the amount of rust being deposited per unit surface area of rebars per unit time, is used to predict time-to-corrosion cracking of cover concrete. Corrosion penetration rate, P_r, which is the loss of diameter of rebars per unit time, is used to predict residual load bearing capacity of a concrete structural member subjected to reinforcement corrosion.

Of all above techniques, linear polarization resistance (LPR) method is mostly used for measuring corrosion rate of rebar embedded in concrete, as it is non-destructive. Further, the LPR method is suitable for use in the laboratory as well as in the field for application to the corrosion of steel in concrete, whereas other methods are only suitable for use in the laboratory. The device used in the LPR method consists of a counter-electrode, a reference electrode, an electric signal supply unit, usually a potentiostat or galvanostat. The potentiostat/galvanostat is connected to rebar (the working electrode), counter-electrode, and the reference electrode. Using the device, polarization resistance, R_p, is measured which is used to calculate I_{corr}. The main difference in measuring the R_p on site and in the laboratory is the geometrical arrangement of the counter electrode. In the laboratory measurements on a small-size specimen, the specimen, counter electrode and reference electrode are immersed in a sodium chloride solution which ensures uniform current distribution on the steel bars. In the in-situ measurement or in case of a large-size specimen, a disk-shaped counter-electrode (having a central hole to accommodate the reference electrode) is placed on a water-soaked

sponge kept on the surface of the structure. The reference electrode passing through the central hole of the counter-electrode is also placed on the same water-soaked sponge.

LPR Method for In-situ Measurement of Reinforcement Corrosion Rate

In this section, test methods reported in the literature for on-site corrosion rate measurement of reinforcement corrosion in concrete using LPR are briefly reviewed. First the general LPR circuitry for in-situ measurement of corrosion rate of rebar is explained along with the procedure for the calculation of I_{corr}. Then the difficulties and errors encountered in the in-situ application of the LPR method for measuring reinforcement corrosion rate are described. Finally, ways and means for the elimination of the errors from I_{corr} estimation, as reported in the literature, are briefly outlined. Information on the use of some commercially available instruments for in-situ reinforcement corrosion rate measurements is also included.

Stern and Geary, for the first time, gave the following expression to calculate corrosion rate in terms of the corrosion current density Icorr using the linear polarization data [50].

$$I_{corr} = \frac{B}{R_p}$$

Where,

I_{corr} = corrosion current density ($\mu A/cm^2$),

B = Stern-Geary constant (mV)

Rp = polarization resistance ($k\Omega$-cm^2)

Determination of R_p

The polarization resistance (R_p) is determined using the slope of the linear portion of the polarization curve, as shown in Figure 2.10 below:

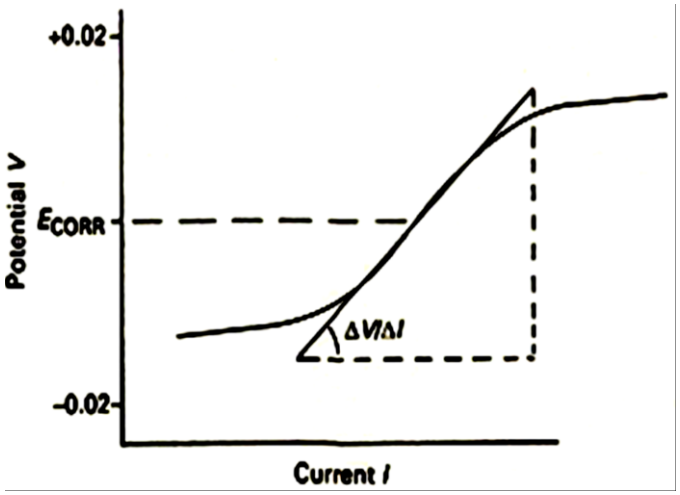

Figure 2.10: Polarization curve.

$$R_p = \frac{\Delta V}{\Delta I} A$$

Where,

$\Delta V/\Delta I$ = slope of the linear portion of the polarization curve, as shown in Figure 2.10

A = exposed surface area of the rebar

Determination of B

The value of Stern-Geary constant (B) can be determined using the values of Tafel coefficients from the following equation:

$$B = \frac{\beta_a \beta_c}{2.3(\beta_a + \beta_c)}$$

Where:

β_a = anodic Tafel coefficient

β_c = anodic Tafel coefficient

In the absence of Tafel constants, value of *B* may be assumed as 52 mV for steel in passive condition and 26 mV for steel in active condition. For on-site measurements a value of B equal to 26 mV is commonly utilized [51].

Set-up for In-situ LPR Measurements

A schematic set-up for LPR measurements in an in-situ reinforced concrete member is shown in Figure 2.11 [52].

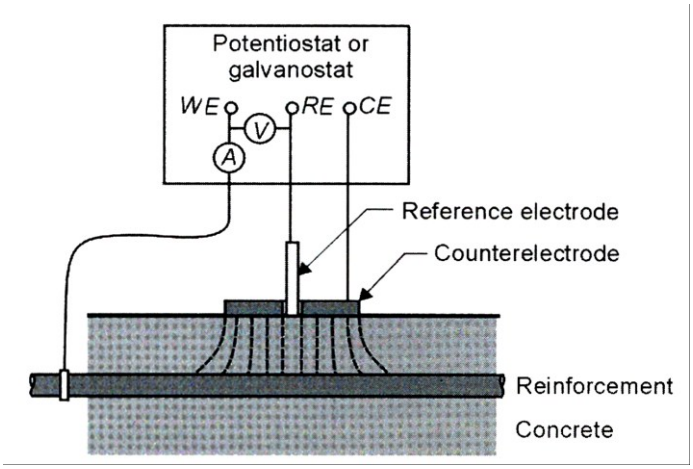

Figure 2.11: Schematic Set-up for LPR Measurements in Reinforced Concrete Members.

As shown in Figure 2.11, the set-up for LPR measurements in an in-situ reinforced concrete member consists of a counter-electrode disk (CE) and a central reference electrode (RE) placed on the surface of the structure. The potentiostat/galvanostat is connected to the reinforcement which works as the working electrode (WE), counter-electrode, and the reference electrode. The set-up is used to generate data for obtaining the polarization curve in

the linear range.

Difficulties and Errors Encountered in the In-Situ Application of the LPR Method for Measuring Reinforcement Corrosion Rate

Difficulties and errors encountered in the in-situ application of the LPR method for measuring reinforcement corrosion rate have been frequently reported in the literature [21,51,53-55]. The major difficulties, as reported by these researchers, are briefly described below:

- The polarization time needed to establish a stable polarization measurement depends on the steel surface, and it can be excessive.
- Where the Ohmic drop (IR) between the concrete and the reinforcing bar is high, this will result in a significant error in measuring R_p.
- The correct value of the Stern-Geary constant, B, depends on whether the steel is actively corroding or is passive. A value of B equal to 50 mV is sometimes adopted for both passive and actively corroding steel, and this could lead to some errors in evaluating I_{corr}.
- It is always assumed when evaluating I_{corr} that corrosion is occurring uniformly over the area of the steel. Where intense localized corrosion occurs (e.g. chloride pitting), averaging the localized corrosion rate over the whole measurement area may be a further source of error in the assessment of the corrosion severity. The corrosion rate of locally corroding area can be severely underestimated.
- The Rp value cannot be correctly determined if the steel is passive and exhibits corrosion potential, E_{corr}, value more cathodic than -300 mV SCE.
- One of the most important problems in evaluating I_{corr} in the field lies in evaluating the

area of the reinforcing bar that is being polarized by the test. There is non-uniform distribution of the electric signal between the small counter-electrode on the concrete surface and the large rebar network. The electric signal applied through the external counter-electrode not only polarizes the surface of the reinforcement below the counter-electrode itself but also spreads laterally or may reach deeper layers of the reinforcement. Due to the spread out of the applied electric signal the measured Rp is related to an unknown rebar surface area which would yield into an erroneous I_{corr}.

The measurement of corrosion rate of steel bars on site or in large-sized laboratory specimens using LPR method has been a challenging problem because of various practical difficulties encountered in the application of the available test methods and instruments resulting into significant errors in the estimation of the corrosion rate. The major sources of errors include: the ohmic drop due to the relatively high electrical resistivity of concrete; lack of information on the area of the rebar that is actually being polarized by applying electric signal through a small counter-electrode; and lack of the precise value of the Stern-Geary constant used for the calculation of the corrosion rate.

Recently, some commercial instruments have been marketed for in-situ monitoring of reinforcement corrosion. For example, Gecor™ corrosion rate meter from James Instruments Inc., USA, Galva Pulse© corrosion rate meter from German Instruments, Denmark and ACM Field Machine from UK. However, the reliability and accuracy of the data obtained through the use of these instruments is yet to be verified. Furthermore, these set-ups do not provide the values of Tafel's slopes required for calculating the Stern-Geary constant used for calculating the corrosion rate. In the absence of the actual values of Tafel constants the value of the Stern-Geary constant is arbitrarily assumed in the range of 26 to 52 mV which is another source of significant error in the determination of the corrosion rate, as mentioned

above.By following Table 2.3 results can be interpreted.

Table 2.3: Corrosion current vs. condition of the rebar [56].

Corrosion current (I_{corr})	Rate of corrosion
<0.1 μA/cm²	Passive
0.1 - 0.5 μA/cm²	Low to moderate
0.5 - 1.0 μA/cm²	Moderate to high corrosion
1.0 μA/cm²	High corrosion rate

2.3.6 Gravimetric weight-loss method

Weight-loss method is a simple way to determine the percentage weight of metal lost due to corrosion (i.e., weight of rust expressed as percentage of original weight of rebar). However, this method is destructive as many cores are to be taken to get the actual feel of the rate of corrosion. Preparation, cleaning and estimation of the weight loss are done according to ASTM G1-03 [57].The cleaning solution used was 1000 ml of hydrochloric acid with 20 g of antimony trioxide and 50 g of stannous chloride.

The weight loss W_l is calculated as:

$W_l = W_i - W_f$

Percentage weight loss(ϱ) = $\frac{Wi-Wf}{Wi}$ X 100

where:

W_i = initial weight of the bars before corrosion (g), and

W_f = weight of the bars after cleaning all rust products (g)

2.4 Linear Polarization Resistance Vs Gravimetric Weight Loss Method

Pradhan and Bhattacharjee [1] carried out an experimental investigation on a large number of concrete specimens in order to judge the performance of different types of rebar in chloride contaminated concrete made with different cement types by means of corrosion rate techniques. Reinforced concrete specimens with three different types of steel, three different types of cement, three different w/c ratios and four different admixed-chloride contents were prepared. The corrosion rate measurement techniques used in their work were AC impedance spectroscopy technique, LPR with guard ring arrangement, gravimetric weight loss method. They reported that the corrosion current density values obtained by LPR method and those corrosion current density values determined by gravimetric weight loss method do not vary by much. They obtained the relationship: I_{corr}(LPR) =0.99I_{corr}(gravimetric) and the regression coefficient (R-value) of 0.989 as indicated in Figure 2.12.

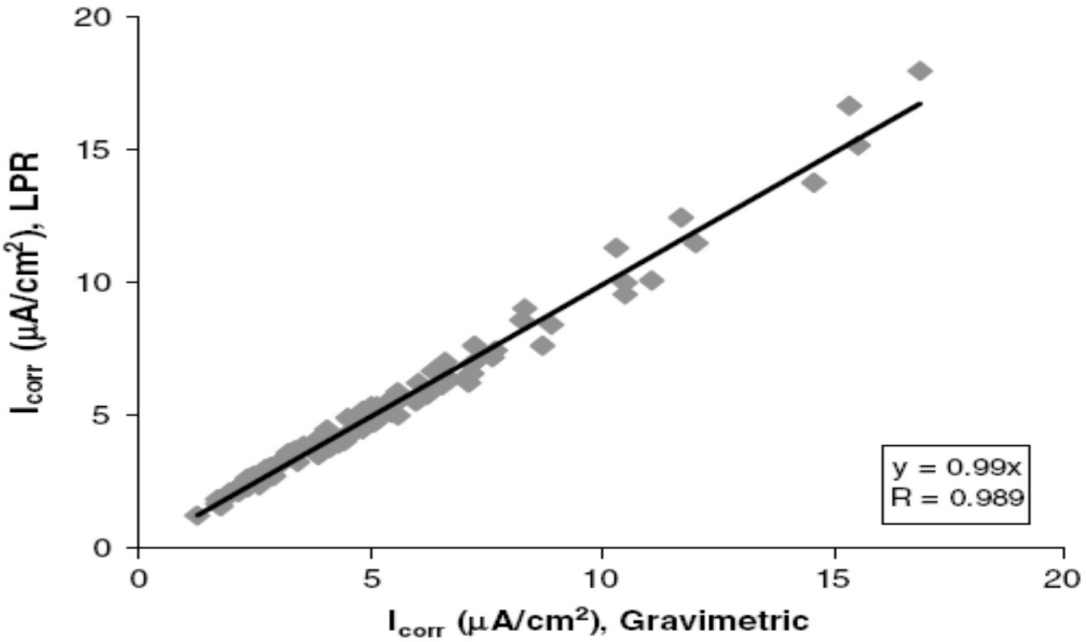

Figure 2.12: Relationship between I_{corr} measured by using LPRand Gravimetric method [1].

Sathyanarayanan *et al.* [2] carried out an experimental study of the corrosion of steel in concrete using different corrosion rate measurement techniques. They compared the results obtained by of galvanostatic pulse technique for monitoring the corrosion of steel in concrete with the corrosion rate values found using the gravimetric weight loss method. The concrete were of grades 15, 20, 30, and 35 MPa in which steel bars were embedded and exposed to chloride ion concentration values of 0 to 5%. They stated that the corrosion rate of steel in concrete depends upon the strength of concrete and the chloride concentration. They also reported that the corrosion rate values obtained by the LPR method were one order of magnitude lower than that of the gravimetric weight loss method due to ohmic drop in concrete.

Ganesan *et al.* [3] conducted an experiment to evaluate the performance of bagasse ash as corrosion resisting admixture for carbon steel in concrete. They burned boiler-fired ash at a controlled temperature of 650 ^{o}C for 1 hour for obtaining bagasse ash and grounded to fineness of Pozzolanic material and used in different levels in preparing concrete by replacing cement. The specimens were exposed to alternate dry-wet cycles in 3% sodium chloride (NaCl) solution for 18 months. The corrosion rate of steel in bagasse ash blended cement concretes was obtained using electrochemical impedance spectroscopy, linear polarization resistance and gravimetric weight loss methods. It was reported that the corrosion rate of reinforcing steel and chloride penetration was slightly lower and compressive strength was increased with the addition of bagasse ash up to 20% replacement of cement in concrete. Also, when compared with reference concrete the corrosion rate of rebar studied using gravimetric weight loss method showed a 3.6 times reduction for bagasse ash concrete with 10% cement replacement level. However, for all the cases, the corrosion rates measured by weight loss method were higher than those obtained on the basis of the corrosion rate

measured by the LPR and impedance methods. Nonetheless, they concluded that the corrosion rate measured using LPR method, impedance method and weight loss method gave the same trend in the corrosion performance of reinforcing steel in bagasse ash concretes.

CHAPTER 3

DEVELOPMENT OF A SET-UP AND A PROCEDURE FOR CALCULATION OF REINFORCEMENT CORROSION RATE MEASUREMENT

In this chapter, a simple arrangement and a calculation procedure developed for in-situ measurement of corrosion current density of rebar embedded in concrete based on linear polarization technique are presented. The proposed integrated circuitry of the set-up can be used to record half-cell potential (i.e., corrosion potential), data for determination of polarization resistance, and the data for determination of ohmic resistance of concrete, which enables to eliminate ohmic drop mathematically from the polarization data. An integrated calculation procedure has been proposed for determining: true polarization resistance, Tafel slopes for determining Stern-Geary constant, and finally calculation of reinforcement corrosion rate. The set-up having provision of ohmic drop elimination and calculation procedure with a provision of calculation of Stern-Geary constant (instead of assuming it), the proposed set-up and calculation procedure has advantage of determining reinforcement corrosion rate with a fair degree of accuracy.

3.1 Description of Proposed Set-up and Measurement Procedure

The circuitry developed for the proposed set-up for corrosion testing of R.C. specimens is based on linear polarization resistance method. The circuitry has been integrated in a way that the data can be generated to calculate ohmic resistance of concrete, true polarization

resistance, and Tafel slopes required for calculating reinforcement corrosion rate with more accuracy. The portion of integrated circuitry belonging to half-cell potential measurement is based on the circuitry developed by ASTM C 876-99 [24] for half-cell potential measurement using $Cu/CuSO_4$ reference electrode. The part of integrated circuitry for determination of ohmic resistance is based on the principle of determining the internal resistance of a cell [58]. The part of integrated circuitry for determination of the apparent polarization resistance is based on the usual constant current technique or galvanostatic, which is advantageous over potentiodynamic and potentiostatic methods [59]. One of the advantages of galvanostatic mode of operation is that it is found to be suitable for the mathematical correction of the Ohmic drop in this case. With this method, the electrochemical processes remain apparently unaltered and the potential drift whether in an active or noble direction is not affected by the polarization measurements. Potential variations due to localized crevice corrosion are not affected during the polarization measurements. The proposed integrated circuitry is shown in Figure 3.1 and a photograph showing different components of the circuitry is shown in Figure 3.2.

Before using the set-up for carrying out measurements, there should be good physical contact between the reference electrode tip and concrete surface point under test to avoid poor electrolytic contact of the reference electrode with the specimen. For this purpose, the concrete surface covering, if any, should be removed, either with abrasive paper or by a steel teeth brush. Then pre-wetting of the surface points under test is done through a tissue paper soaked with water, and allowed to be there for 20-30 minutes so that the moisture can soak in before beginning of the readings. For recording of the reading, the tip of the reference electrode is placed on the wetted tissue placed over the surface point under test and the rebar is connected to the circuitry.

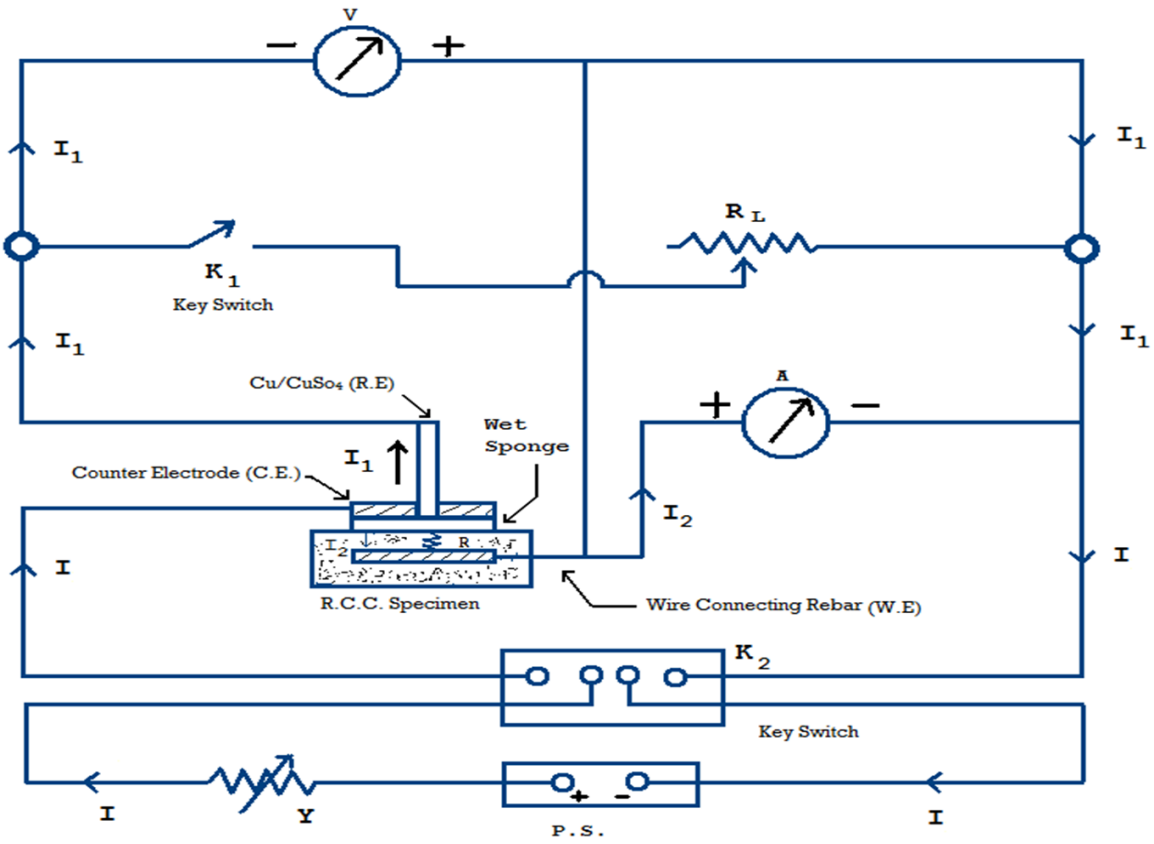

Figure 3.1: Arrangement for the determination of half-cell or corrosion potential, ohmic resistance and polarization resistance.

R_L = Standard decade box resistor;

V = Voltmeter capable of reading 0-l.0 V with a least count of 0.1 mV;

K_1&K_2 = Key switches;

R.E. = Standard Cu/$CuSO_4$ reference electrode as per ASTM C-876;

C.E. = Counter electrode;

W.E. = Working electrode (rebar);

A = Ammeter capable of reading 0-200, μA with a least count of 0.1, μA;

R = Ohmic resistance of concrete;

E = E.M.F. of corrosion cell;

I_2 = Cathodic current applied to the rebar for polarization;

P.S. = Constant voltage power supplier;

Y = Variable resistance to keep circuit resistance high enough to maintain constant current.

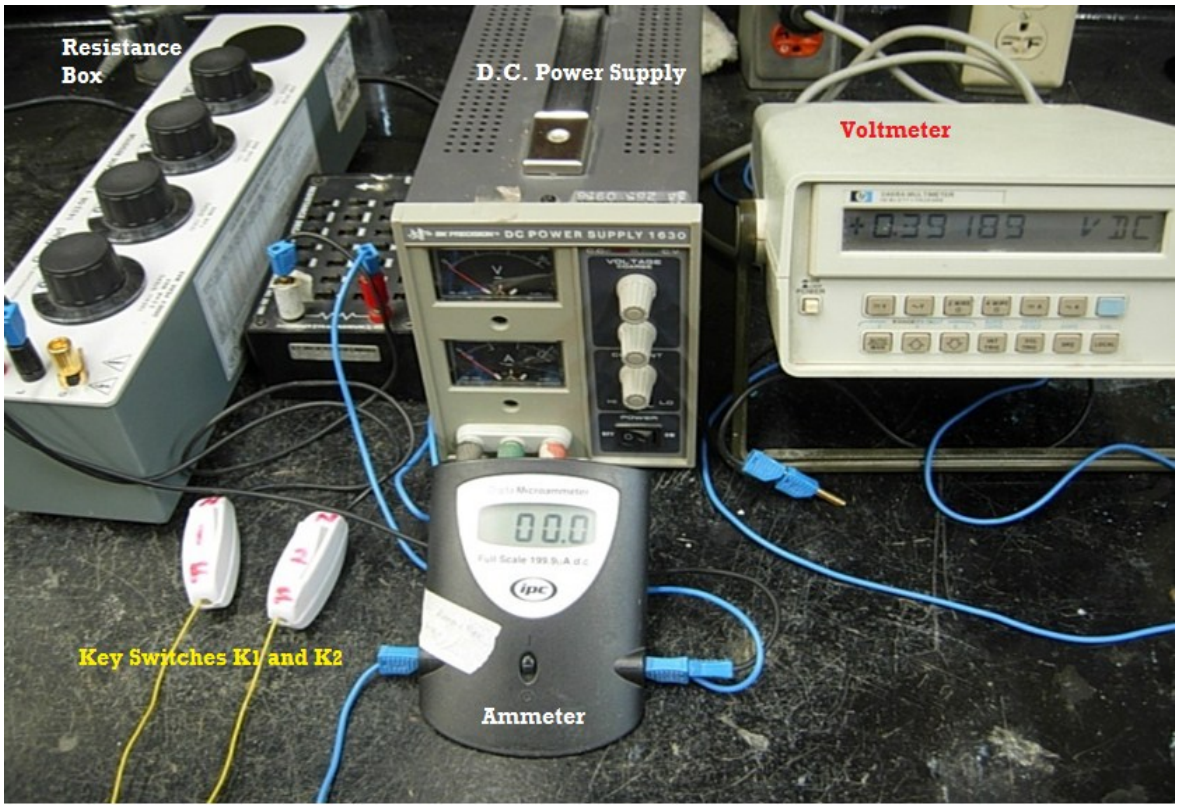

Figure 3.2 :Photograph showing components of developed setup.

Referring to Figure 3.1, the procedure for measurement of half-cell potential (E_{corr}) and generation of data required to determine Ohmic resistance (R), and polarization resistance (R_p) are as follows:

Half-cell potential (E_{corr})

Keeping key switches K_1 and K_2 off, the potential V is recorded (allowing a sufficient response time of 30-60 seconds for measurements to stabilize) and considered as half-cell potential. When the corrosion potentials are low, the Voltmeter reading is not stabilized and fluctuates, the reading after 30-60 seconds waiting period should be considered.

Ohmic resistance (R)

For determining Ohmic resistance, R_L vs. V data are generated keeping switch K_1on and K_2 off. The switch K_1 permits R_L to be connected momentarily, whenever a voltage reading is desired, thus avoiding excessive current drain over a prolonged period of time. The terminal

voltage of the cell, under load, is given by the voltmeter reading V, when the key switch, K_1, is closed.

Polarization resistance (R_p)

For determining polarization resistance, cathodic polarizing current, I, is applied and resulting potential V (which is more negative than E_{corr}) is recorded by keeping K_1 off and K_2 on. The current is applied in steps until the maximum value of the overvoltage (value of potential by which E_{corr} is shifted as a result of polarization) is reached, which is usually 10 to 20 mV for the polarization curve to be in the linear range, with the help of a variable resistor, Y, which helps to keep the resistance of circuit high enough to maintain a constant current. The initial cathodic polarizing current taken is usually 2 μA, and then the second current step is 4 μA, the third 6 μA, etc. After allowing a response time of 30 seconds at each current step the steady Voltmeter reading is recorded. After polarizing, at low corrosion the voltmeter reading fluctuates and hence response time of 30 seconds is used to note down the voltmeter readings.

3.2 Proposed Procedure for Calculation of Corrosion Rate

3.2.1 Determination of Ohmic resistance of concrete

R_L vs. V data are used to determine ohmic resistance of concrete by best-fitting the data in the following equation for straight line [21].

$$\frac{1}{V} = \frac{R}{E}\left(\frac{1}{R_L}\right) + \frac{1}{E} \tag{3.1}$$

The 1/V values are plotted against the values of 1/ R_L, to obtain a best-fitted straight line, as typically shown in Figure 3.3. The best fit straight line joining these points gives the solution for Ohmic resistance, R, as follows:

$$R = \frac{\text{slope } (R/E)}{\text{Intercept } (1/E)} \tag{3.2}$$

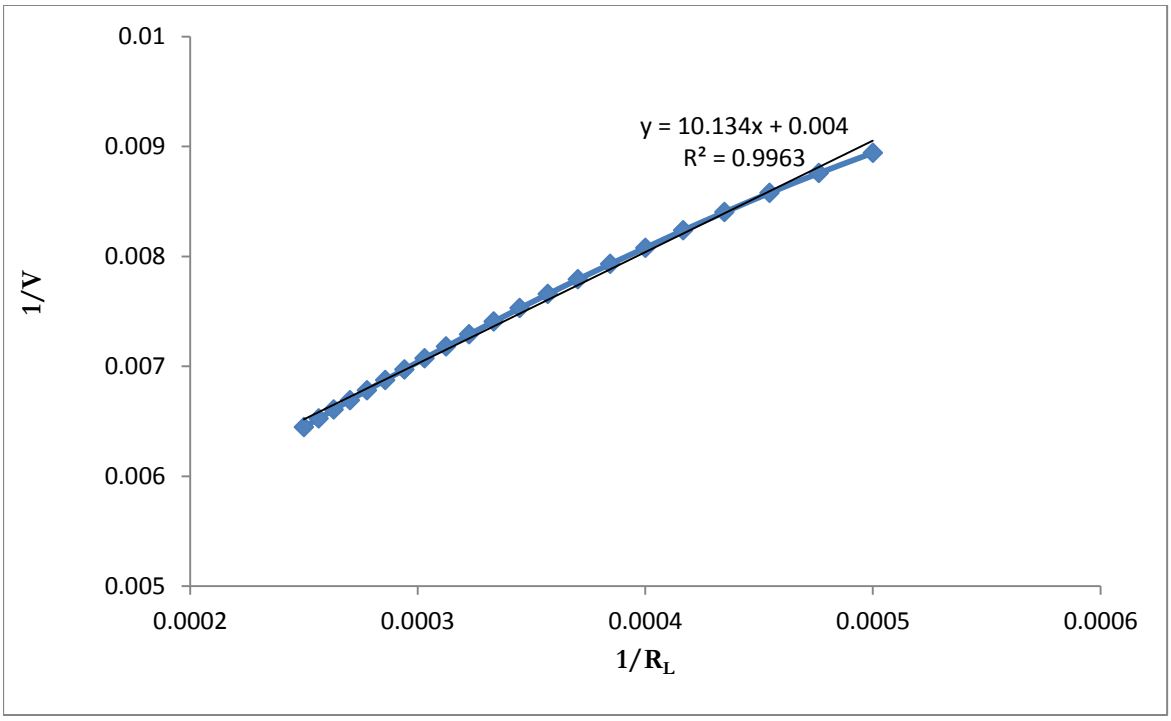

Figure 3.3: Method of determining the ohmic resistance R of concrete by best fit of $R_L$vs. V data points.

3.2.2 Determination of polarization resistance

With the help of the polarization data, i.e. *V* vs. $I_2$and the Ohmic resistance (*R*) obtained in the previous step, the polarized potential (*E*)with Ohmic drop being eliminated can be obtained as follows [21]:

$$E = V - I_2 R \tag{3.3}$$

The value of *E* given by equation (3.3) is the polarized potential of a cell with the ohmic drop (I_2R) being eliminated mathematically. The overvoltage (ε) induced by the cathodic polarizing current (I_2) is given by $\varepsilon = E - E_{corr}$ and the apparent polarization resistance, R_p is given by the initial slope of the polarization curve (i.e. I_2vsε), as follows:

$$R_P' = \frac{\Delta\varepsilon}{\Delta I_2} \tag{3.4}$$

The data pertaining to determination of polarization resistance is typically shown in Table 3.1.The plot of data to get a linear polarization curve is typically shown in Figure 3.4.

Table 3.1: Typical data pertaining to determination of polarization resistance.

E_{corr}(mV)	I_{app}(μA)	I_{app}(mA)	E (mV)	ε (mV) = E – E_{corr}
385.5	0.5	0.0005	386.22	0.72
	2	0.002	387.36	1.86
	3.2	0.0032	388.293	2.79
	5.2	0.0052	389.9	4.40
	6.3	0.0063	390.96	5.46
	7.1	0.0071	392.077	6.57
	9	0.009	393.9	8.40
	11.2	0.0112	395.9	10.40
	11.8	0.0118	396.82	11.32
	12.4	0.0124	397.8	12.30

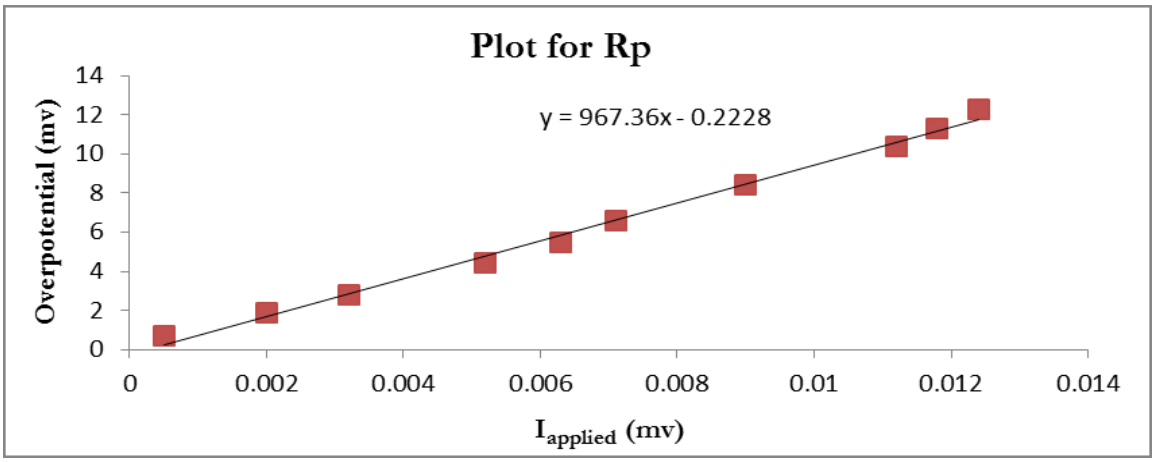

Figure 3.4: Plot of polarization data for determination of polarization resistance.

From Figure 3.4, the value of polarization resistance R_p can be taken as 967 ohm.

3.2.3 Determination of Tafel slopes and reinforcement corrosion rate

In order to determine the correct value of the Stem-Geary constant, *B*, Tafel slopes β_a and β_c should be determined using polarization data. The values of β_a and β_c can be determined by best-fitting the polarization data into Equation 3.5 [21]:

$$2.3\mathrm{R}_{\mathrm{P}}^{'}I_i = \frac{\beta a\, \beta c}{(\beta a+\beta c)}\left[\exp\left(\frac{2.3\,\varepsilon_i}{\beta a}\right) - \exp\left(\frac{-2.3\,\varepsilon_i}{\beta c}\right)\right] \quad (3.5)$$

The method of estimating β_a and β_c, described here consists of putting constraints on $1/\beta_a$ and $1/\beta_c$ values within the feasible domain, i.e. $(1/\beta_a + 1/\beta_c)$ values, are limited by the higher value

of the bound ($1/\beta_a + 1/\beta_c$) for an active state of corrosion and lower value of the bound ($1/\beta_a + 1/\beta_c$) for a passive state of corrosion of steel in concrete as shown below [21]:

$$\left(\frac{1}{\beta a}+\frac{1}{\beta c}\right)_{low} \leq \left(\frac{1}{\beta a}+\frac{1}{\beta c}\right) \leq \left(\frac{1}{\beta a}+\frac{1}{\beta c}\right)_{high}$$

Gonzalez and Andrade [63] have verified the values of the Stern-Geary constant, B, for the active state of corrosion of a rebar in concrete to be 26 mV and for passive state of corrosion of a rebar in concrete to be 52 mV [63].However, LeRoy [62] suggests that the value of the factor equation: $\left(\frac{2.3}{\beta a}+\frac{2.3}{\beta c}\right)$ seldom lies outside the range $0.02 < \left(\frac{2.3}{\beta a}+\frac{2.3}{\beta c}\right) < 0.12$

The above conditions yield the extreme bounds of the feasible region of the solution as shown in below equation (3.6).

$$8.312 \times 10^{-3} \leq \left(\frac{1}{\beta a}+\frac{1}{\beta c}\right) \leq 5.2115 \times 10^{-2} . \quad (3.6)$$

In equation (3.5), putting $2.3R'_P I_i = A_i$ and $B_i = 2.3\,\varepsilon_{i\ as}$ shown in Equation (3.7)

$$A_i = \frac{1}{\left(\frac{1}{\beta a}+\frac{1}{\beta c}\right)}\left\{\exp\left(\frac{B_i}{\beta a}\right) - \exp\left(\frac{-B_i}{\beta c}\right)\right\} \quad (3.7)$$

The sum of the error squares, for polarization data points, can be written as Equation (3.8)

$$Z = \sum_{i=1}^{n}\left[A_i - \frac{1}{\left(\frac{1}{\beta a}+\frac{1}{\beta c}\right)}\left\{\exp\left(\frac{B_i}{\beta a}\right) - \exp\left(\frac{-B_i}{\beta c}\right)\right\}\right]^2 \quad (3.8)$$

Where n is the number of data points.

The values of $1/\beta_a$ and $1/\beta_c$ which satisfy all the data points together are the values where the sum of error squares, *Z*, would be a minimum.

Using Solver in an MS Excel program, the *Z* can be minimized by using the constraints presented in Table 3.2.Once the values of β_a and β_c are determined corresponding to $Z_{minimum}$, the Stern-Geary constant, B, can be determined as [64]:

$$B=\frac{\beta a\ \beta c}{2.3\ (\beta a+\ \beta c)} \quad (3.9)$$

Table 3.2: Constraints used in the excel program.

βa ,βc	≥ 120 but ≤ 240
B (mV)	≥ 26 but ≤ 52
(1/βa)+(1/βc)	≥0.0083612
(1/βa)+(1/βc)	≤ 0.052115

Once the polarization resistance, Rp, and Stern-Geary constant (B) are determined, reinforcement corrosion rate I_{corr}, can be determined as:

$$I_{corr}=\frac{B}{R_P} \quad (3.10)$$

The typical results obtained by running the developed Excel program are shown below:

βa (mV)	120			
βc (mV)	188			
Rp (Ohm)	**967.3**			
B (mV)	**31.85**			
(1/βa)+(1/βc)	0.01364996			
Surface Area (cm^2)	158.33			
Iapp (mA)	ε (mV)	A		Z
0.0005	0.72	1.1124	1.656	-0.547
0.002	1.86	4.44958	4.278	0.1432
0.0032	2.793	7.11933	6.4239	0.630
0.0052	4.4	11.5689	10.12	1.285
0.0063	5.46	14.0162	12.558	1.202
0.0071	6.577	15.796	15.1271	0.2922
0.009	8.4	20.0231	19.32	0.0741
0.0112	10.4	24.9176	23.92	0.0085
0.0118	11.32	26.2525	26.036	-0.969
0.0124	12.3	27.5874	28.29	-2.11
			$Z_{minimum}$	**-5E-07**
I_{corr} (μA/cm^2)	0.208			

CHAPTER 4

EXPERIMENTAL PROGRAM

Following the development of the set-up and calculation procedure for measuring reinforcement corrosion rate, an experimental program was planned and carried out for assessing the viability and accuracy of the developed set-up. The experimental work consisted of preparing and corroding a set of 15 reinforced concrete slab specimens to different degrees using impressed current technique and measuring reinforcement corrosion rates using the developed corrosion monitoring setup and two more commercially available set-ups. Electrochemical measurements of reinforcement corrosion rates using all three set-ups were carried out for both scenarios, without and with Ohmic drop compensation. After completion of electrochemical non-destructive corrosion measurements, corroded bars were extracted from concrete and tested for percentage weight loss using gravimetric method. The electrochemically and gravimetrically measured reinforcement corrosion rate results were utilized to compare the accuracy of reinforcement corrosion rates measured by different set-ups without and with Ohmic drop compensation.

Additionally, some naturally corroded reinforced concrete specimens were tested for reinforcement corrosion rate and electrical resistivity at various moisture content levels for studying correlations between reinforcement corrosion rate, electrical resistivity, and moisture content.

4.1 Materials

4.1.1 Cementitious materials

ASTM C 150 Type I Normal Portland Cement was used to prepare the concrete specimens. The chemical composition of the Portland cement used in the preparation of the test specimens is shown in Table 4.1.

Table 4.1: Chemical Composition of Portland cement.

Constituent	weight,%
Silica (SiO_2)	19.92
Alumina (Al_2O_3)	6.54
Ferric oxide (Fe_2O_3)	2.09
Lime (CaO)	64.70
Magnesia (MgO)	1.84
Silicate (SO_3)	2.61
Potassium Oxide (K_2O)	0.56
Sodium Oxide(Na_2O)	0.28
Tricalcium silicate (C_3S)	55.9
Dicalcium silicate (C_2S)	19
Tricalcium aluminate (C_3A)	7.5
Tetracalciumalumino ferrite (C_4AF)	9.8

4.1.2 Aggregates

Crushed limestone aggregates were used for casting of reinforced concrete slab specimens and dune sand was used as fine aggregate. The specific gravity and water absorption of coarse and fine aggregates determined according to ASTM C 128 [65] are given in Table 4.2.

Table 4.2: Specific gravity, Absorption of the Coarse & Fine aggregate.

Aggregate	Specific gravity	Water absorption (%)
Coarse	2.43	1.1
Fine	2.56	0.6

4.2 Details of Test Specimens

Reinforced concrete slabs 15 in number were prepared. Figure 4.1 is the schematic representation of the concrete slab specimen. Reinforced concrete specimen was of size 500 × 500 × 100 mm reinforced with three 12mm ø bars. GFRP bars were used as transverse reinforcement to avoid corroding of reinforcement in transverse direction. Plastic tie wires were used to tie steel and GFRP bars to avoid corroding of the ties while corroding the specimen. Schematic representation is of the specimen is shown in Figure 4.1 and Figure 4.2 is a photograph of the specimen.

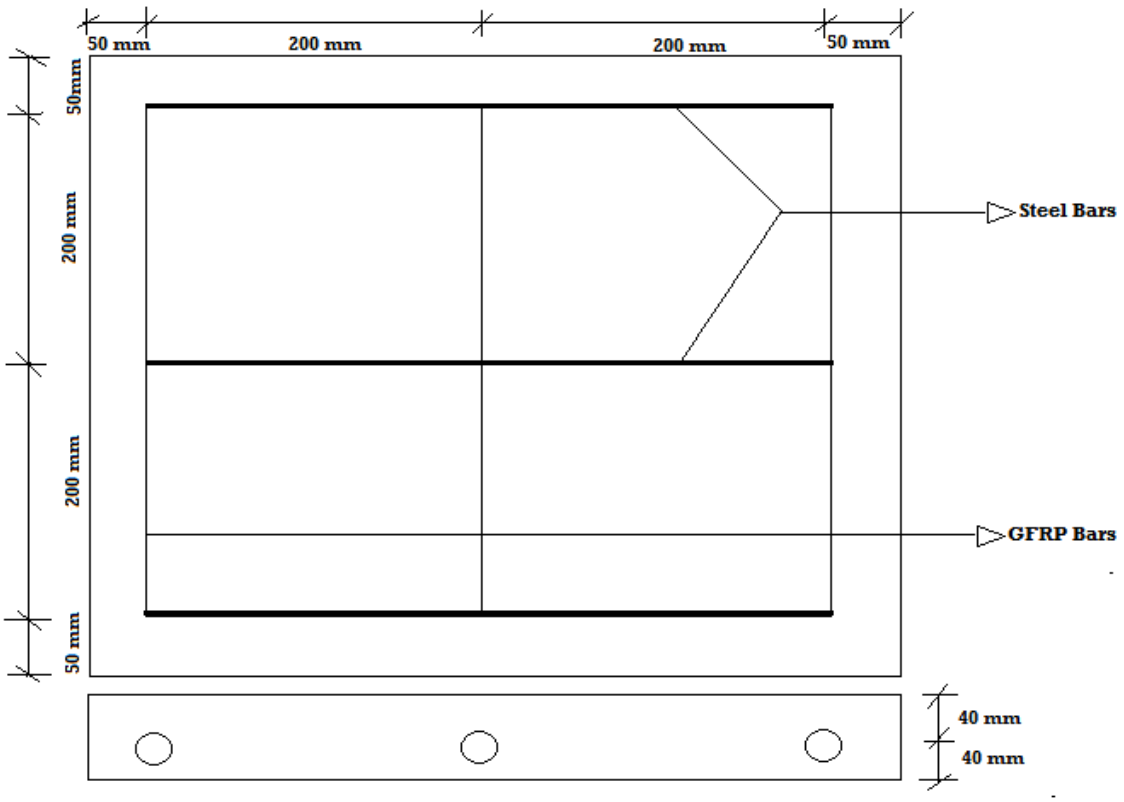

Figure 4.1: Details of reinforced concrete slab.

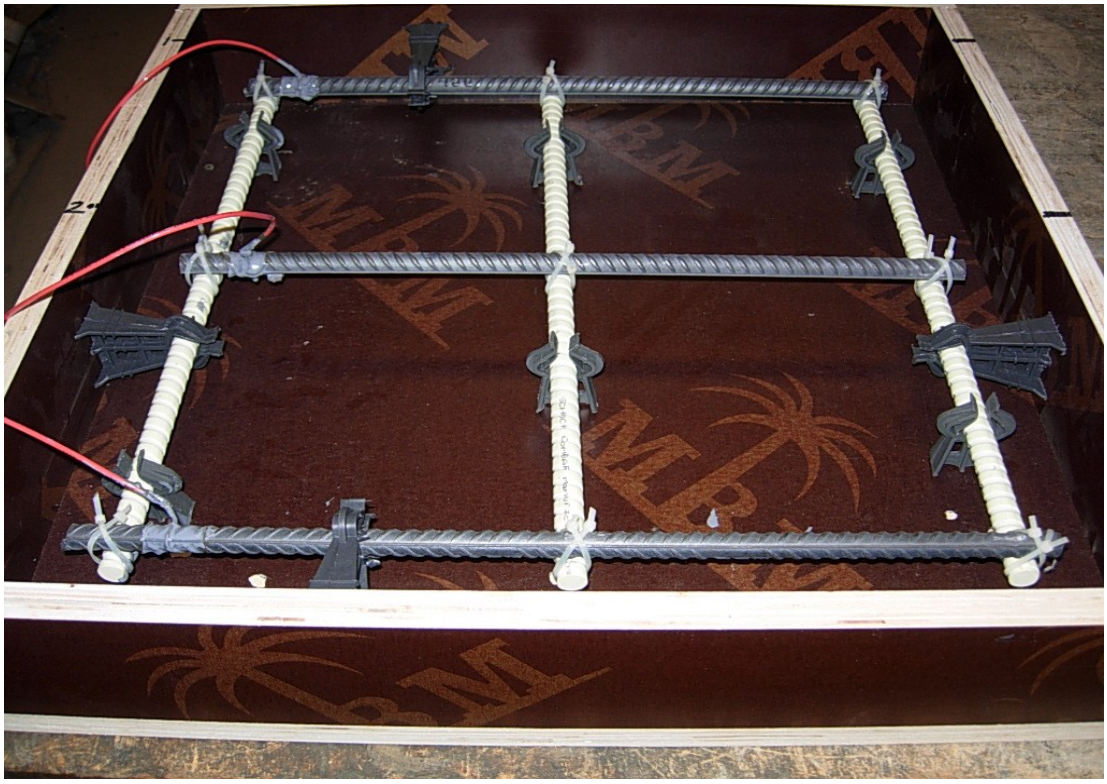

Figure 4.2: Photograph showing reinforcement details in concrete slab specimens.

4.3 Preparation of Test Specimen

4.3.1 Mix design

The absolute volume method [66] was used for the concrete mix design and the quantity of each constituent was calculated on the basis of weight. Parameters used for design the concrete mixtures are presented in Table 4.3. Superplasticizer SP-440 was used to achieve workability in the range of 50-75mm slump.

Table 4.3: Parameters for reinforced concrete slabs for measuring corrosion rate.

Parameter	Level
Effective water/cementitious materials ratio (by mass)	0.45
Cementitious materials content	370 kg/m^3
FA/TA ratio (by mass)	0.40
Aggregate type	Riyadh Road Aggregate
Cement type	Type-1
Cover thickness	35mm

4.3.2 Mixing of concrete and casting of test specimens

Firstly, coarse and fine aggregates were mixed together in the drum type mixer. Then, cement was added and homogenous concrete was obtained with all the constituents mixed together with the addition of potable water and then by adding super plasticizer, the constituents were mixed uniformly to achieve uniform consistency and cohesiveness without segregation.

The molds were oiled and the steel mesh was placed in position in the square molds. Concrete was then poured into the molds in three layers and the concrete was consolidated by placing

the molds on a vibrating table. This procedure was used to prepare all the 15 test specimens. Figure 4.3 shows the casting of the specimens.

Figure 4.3: Photographs showing casting and finishing of slab specimens.

4.3.3 Curing of Specimens

After casting the specimens were cured with plastic sheet to minimize evaporation of water. The specimens were demolded after 24 hours of casting. All the test specimens were then cured for a period of 28 days by placing water-soaked gunny bags.

4.3.4 Corroding of specimens

Rebars embedded in concrete were corroded using impressed current technique. A constant voltage of 47 V was maintained for corroding the three bars embedded in each slab for a defined duration. The positive terminal of the D.C. Power supply was connected to rebars while the negative terminal was connected to the three stainless steel plate on top of the specimen working as counter electrodes. Each specimen was corroded for a duration ranging from 27 to 280 hours to cause different degrees of rebar corrosion. Figure 4.4 shows a schematic representation of the accelerated corrosion set-up while Figure 4.5 shows the photograph of the set-up.

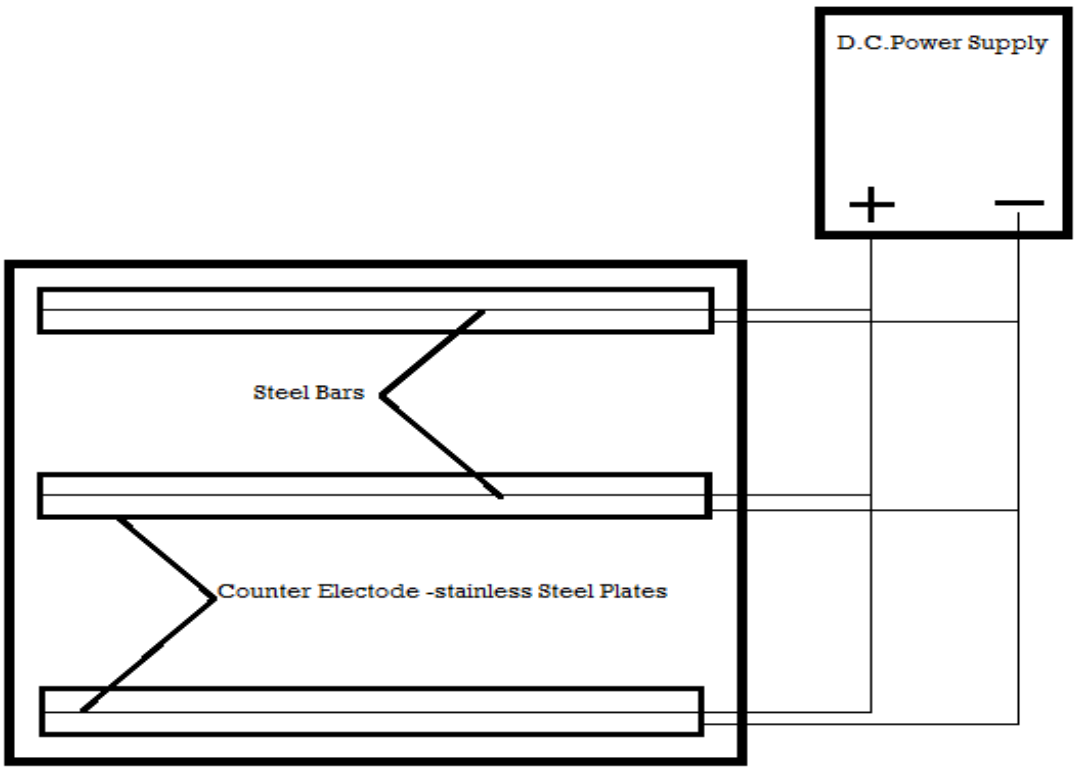

Figure 4.4: Schematic representation of the accelerated corrosion setup.

Figure 4.5: Photograph showing concrete specimen with the concrete electrode.

4.4 Corrosion Rate Measurements

4.4.1 Corrosion rate measurement using the developed setup

Corrosion current density was determined without Ohmic drop and with Ohmic drop compensation using developed set-up. The details regarding measurements steps and calculation procedure are described in Chapter 3. Figure 4.6 shows the photographs of developed set-up being utilized to measure the corrosion current density.

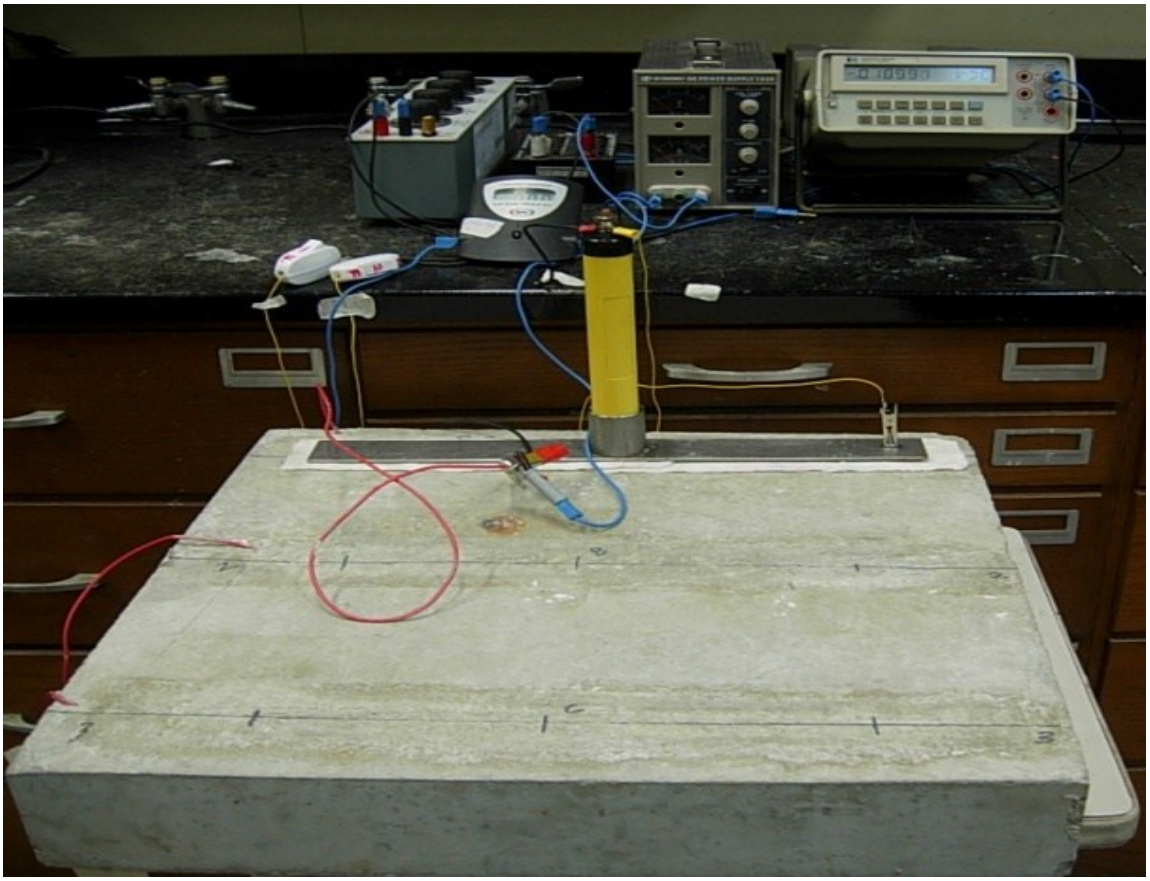

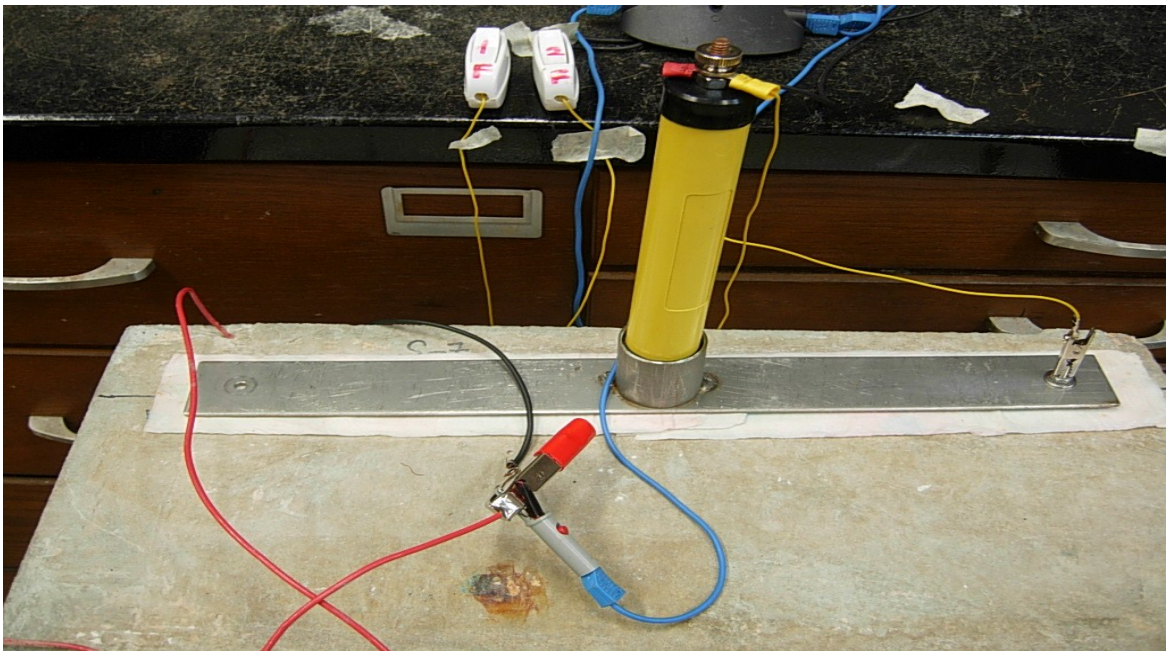

Figure 4.6: Photographs showing measurement of rebar corrosion rate using developed set-up.

4.4.2 I_{corr} measured using commercial equipment

Two different commercially available equipment used in this study are as follows: PARSTAT 2273 potentiostat, manufactured by PRINCETON (USA) [67] and ACM Gill AC, manufactured by Association for Computing Machinery UK. Photographs showing both instruments are shown in Figure 4.8.

Figure 4.7: Commercial Equipment ACM Gill AC (left) and PARSTAT 2273(right).

4.4.3 Gravimetric weight loss method (GWLM)

After conducting corrosion tests using the developed set-up and commercial equipment, the concrete specimens were broken to take out the corroded rebars for conducting the gravimetric weight loss test. The specimens were broken using jack hammer. Preparation, cleaning and estimation of the weight loss were done according to ASTM G1-03 [57].The cleaning solution used was 1000 ml of hydrochloric acid with 20 g of antimony trioxide and 50 g of stannous chloride.

The weight loss W_l was calculated as:

$$W_l = W_i - W_f$$

where:

W_i = Initial weight of the bars before corrosion (g), and

W_f = Weight of the bars after cleaning all rust products (g)

Percentage weight loss (ϱ) = $\frac{W_i - W_f}{W_i}$ X 100

Samples of the corroded steel bars obtained from the test specimens before cleaning are shown in Figures 4.8 through 4.14.

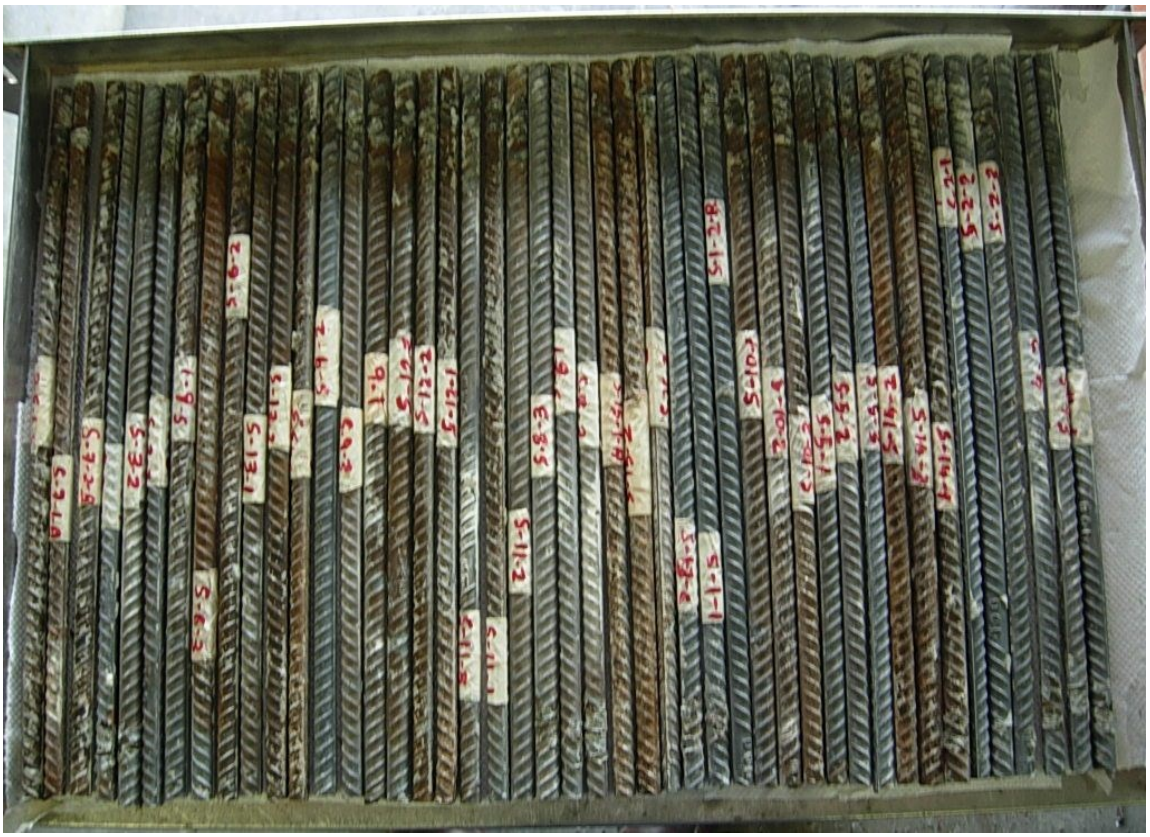

Figure 4.8: All the corroded steel bars before cleaning.

Figure 4.9 : Condition of steel bars after corroding for a duration of 64 hours-(Slab No-3).

Figure 4.10: Condition of steel bars after corroding for a duration of 96 hours-(Slab No-5).

Figure 4.11: Condition of steel bars after corroding for a duration of 144 hours-(Slab No-9).

Figure 4.12: Condition of steel bars after corroding for a duration of 192 hours-(Slab No-10).

Figure 4.13: Condition of steel bars after corroding for a duration of 240 hours-(Slab No-15).

Figure 4.14: Preparation before cleaning of steel bars.

CHAPTER 5

RESULTS AND DISSCUSION

5.1 Corrosion Current Density

The corrosion current density measured both with and without Ohmic drop compensation using developed setup and commercial equipment is summarized in Table 5.1. These data were utilized to compare I_{corr} measured using the developed setup and two commercial equipment with each other and finally with the gravimetric weight loss.

Table 5.1: Experimental results obtained using all three setups.

Slab ID	Impressed Current duration (hours)	$I_{corr}(\mu A/cm^2)$						Gravimetric (% wt. loss)
		D.S-W/O IR	D.S-With IR	C.E-1-W/O IR	C.E-1-With IR	C.E-2-W/O IR	C.E-2-With IR	
S-1-1-A	27	0.026	0.030	0.018	2.1	0.019	0.57	0.136
S-1-2-B	27	0.034	0.039	0.024	5.05	0.025	0.01	0.098
S-1-3-C	27	0.033	0.041	0.019	3.56	0.022	0.39	0.109
S-4-1-A	34	0.045	0.052	0.027	0.21	0.025	0.013	0.190
S-4-2-B	34	0.084	0.116	0.12	2.06	0.08	0.116	0.225
S-4-3-C	34	0.058	0.070	0.028	0.12	0.044	0.118	0.163
S-2-1-A	50.5	0.035	0.041	0.04	2.1	0.028	0.03	0.156
S-2-2-B	50.5	0.062	0.076	0.05	1.96	0.046	1.24	0.342
S-2-3-C	50.5	0.053	0.060	0.042	0.23	0.063	0.6	0.188
S-3-1-A	64	0.065	0.085	0.088	0.47	0.074	0.104	0.203
S-3-2-B	64	0.1	0.165	0.065	0.34	0.08	0.189	0.197
S-3-3-C	64	0.047	0.057	0.058	0.396	0.045	0.135	0.162
S-5-1-A	96	0.045	0.052	0.027	1.76	0.025	0.0567	0.249
S-5-2-B	96	0.045	0.055	0.15	2.08	0.042	0.0722	0.232
S-5-3-C	96	0.098	0.053	0.08	2.35	0.06	0.07	0.351
S-8-1-A	120	0.09	0.132	0.12	0.76	0.14	0.3	0.281
S-8-2-B	120	0.14	0.196	0.14	5.9	0.11	0.162	0.386
S-8-3-C	120	0.122	0.192	0.078	0.734	0.06	0.085	0.281
S-9-1-A	144	0.286	0.509	0.1	3.057	0.09	0.25	0.424
S-9-2-B	144	0.156	0.085	0.08	2.5	0.1	0.3	0.456
S-9-3-C	144	0.157	0.212	0.063	2.88	0.055	0.78	0.213
S-12-1-A	164.5	0.24	0.667	0.2	0.73	0.2	1.925	0.597
S-12-2-B	164.5	0.143	0.441	0.16	0.2	0.18	0.194	0.550
S-12-3-C	164.5	0.1	0.152	0.09	0.02	0.09	0.093	0.215
S-13-1-A	172.5	0.09	0.111	0.068	1.36	0.06	0.13	0.239
S-13-2-B	172.5	0.21	0.650	0.1	4.52	0.21	0.21	0.658
S-13-3-C	172.5	0.19	0.508	0.21	4.91	0.214	0.231	0.531
S-10-1-A	192	0.212	0.493	0.205	2.95	0.15	0.4	0.460
S-10-2-B	192	0.44	0.809	0.35	9.45	0.38	1.25	0.512
S-10-3-C	192	0.32	0.979	0.26	3.1	0.32	2.1	0.412
S-11-1-A	204	0.28	0.751	0.22	5.2	0.28	4.53	0.731
S-11-2-B	204	0.14	0.349	0.16	2.45	0.17	0.25	0.389
S-11-3-C	204	0.092	0.138	0.1	3.85	0.1	0.16	0.305
S-14-1-A	216	0.26	0.576	0.28	0.52	0.26	0.271	0.515
S-14-2-B	216	0.22	0.495	0.3	0.61	0.25	0.278	0.674
S-14-3-C	216	0.25	0.969	0.24	0.435	0.22	0.23	0.993
S-15-1-A	240	0.28	0.809	0.15	0.66	0.21	0.76	1.160
S-15-2-B	240	0.41	1.180	0.12	2.83	0.17	0.196	1.393
S-15-3-C	240	0.193	0.461	0.14	1.01	0.1	0.15	0.551
S-6-1-A	260	0.274	0.670	0.122	3.28	0.187	0.56	0.635
S-6-2-B	260	0.19	0.411	0.313	3.11	0.242	4.18	0.530
S-6-3-C	260	0.271	0.514	0.199	3.72	0.172	6.906	1.370
S-7-1-A	280	0.25	0.730	0.25	0.37	0.32	11.2	2.051
S-7-2-B	280	0.22	0.517	0.16	2.7	0.3	0.5	0.589
S-7-3-C	280	0.27	0.712	0.24	1.44	0.19	0.19	0.732

5.2 Variation of Polarization Trends with Degree of Corrosion

In order to show the variation of polarization curve within linear range, the I_{corr} data were classified into three groups according to the degree of corrosion (very low, low and medium). The applied current for polarization (I_{app}) versus over-potential (ε) plots corresponding to very low, low and medium degrees of corrosion are shown in Figure 5.1.

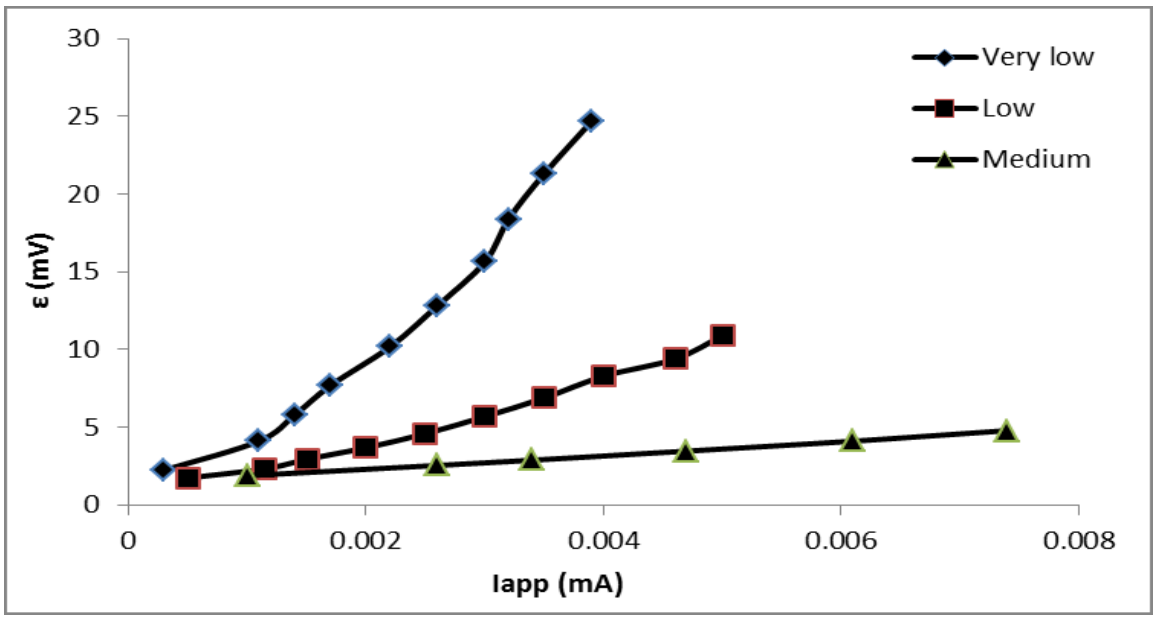

Figure 5.1: Linear polarization curve for very low, low and medium degrees of corrosion.

It can be seen from Figure 5.1 that polarization curve becomes linear with an increase in the degree of corrosion. The polarization data for each group is linearly fitted as shown in Figures 5.2 through 5.4.

From Figure 5.2 it can be concluded that when the corrosion rate is very low, i.e. passive state then the curve is not linear it forms a belly like shape and the value of polarization resistance (R_p)=8525 Ω and the value of I_{corr} obtained is 0.026 μA/cm^2 and value of R^2 =0.964.

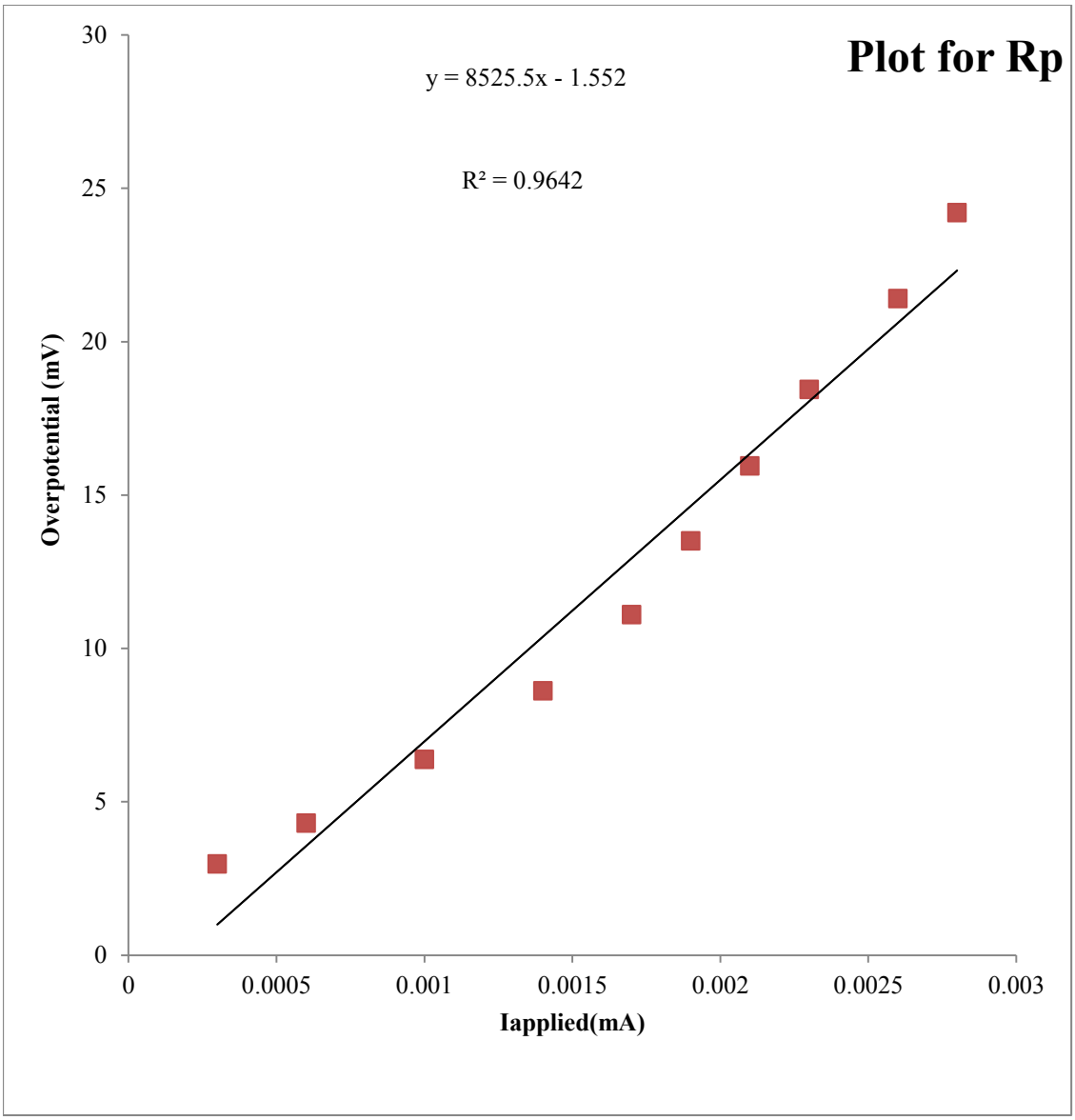

Figure 5.2: Linear polarization curve obtained for very low corrosion rate-(Sample-1-2-B).

From Figure 5.3, the Rp is 2059 Ω and the value of Icorr=0.084 μA/cm^2 with R^2=0.981,and the curve starts losing its belly like shape. Further, from Figure 5.4 the value of Rp is 504.2 Ω, Icorr=0.44 μA/cm^{2}and R^2=0.996, the curve is completely linear. Hence, it can be concluded that when the corrosion rate is low the polarization curve obtained is curved and when the corrosion rate increases the curve tends to become linear.

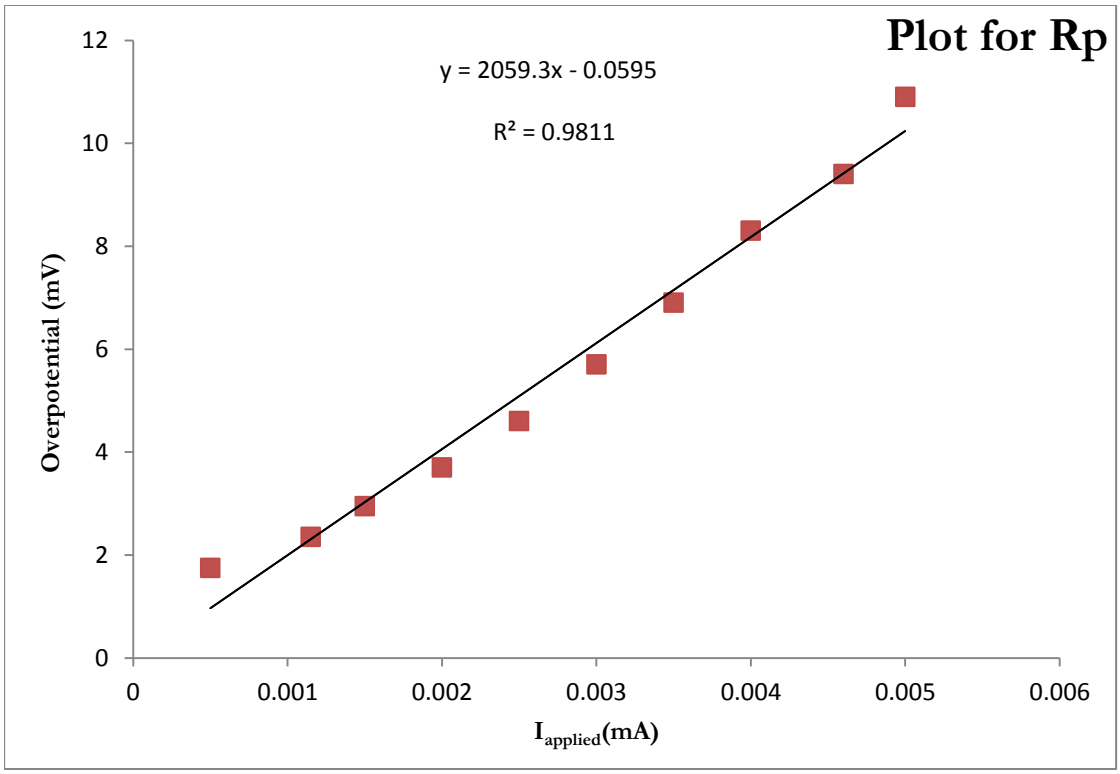

Figure 5.3: Polarization curve obtained for low corrosion rate-(Sample-4-2-B).

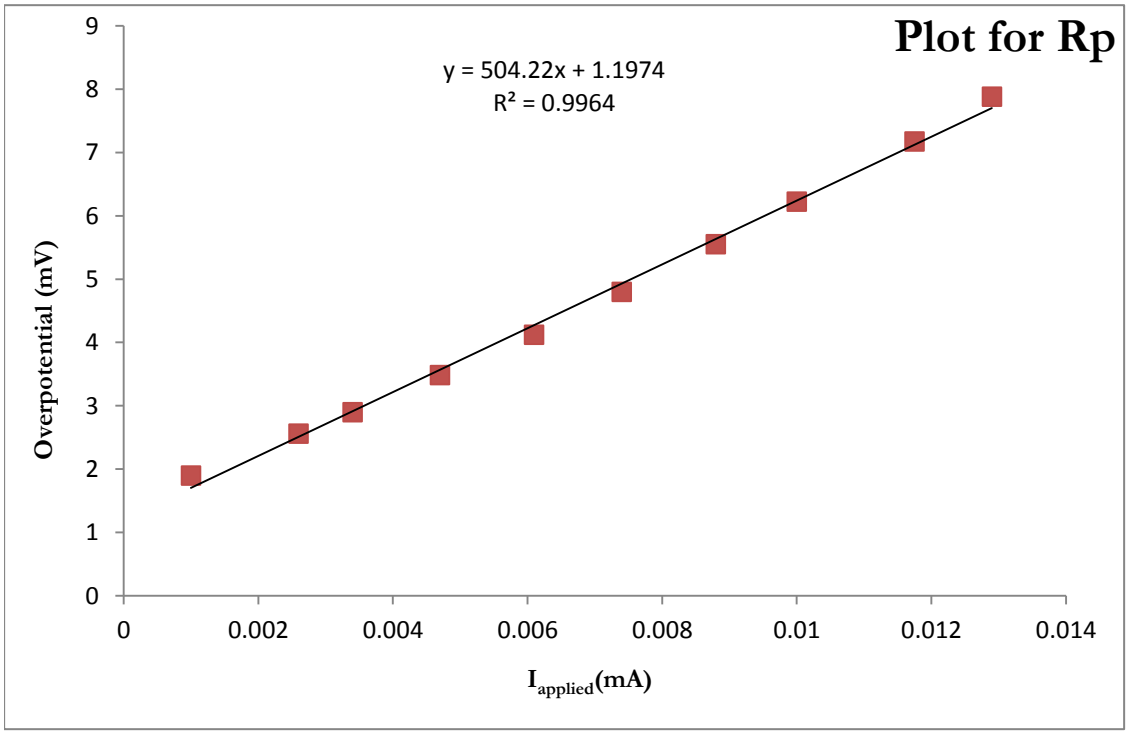

Figure 5.4: Polarization curve obtained for medium corrosion rate-(Sample-10-2-B).

It can be observed from Figure 5.5 and Figure 5.6 that the over potential decreases and current requirement for polarization increases with an increase in the degree of corrosion.

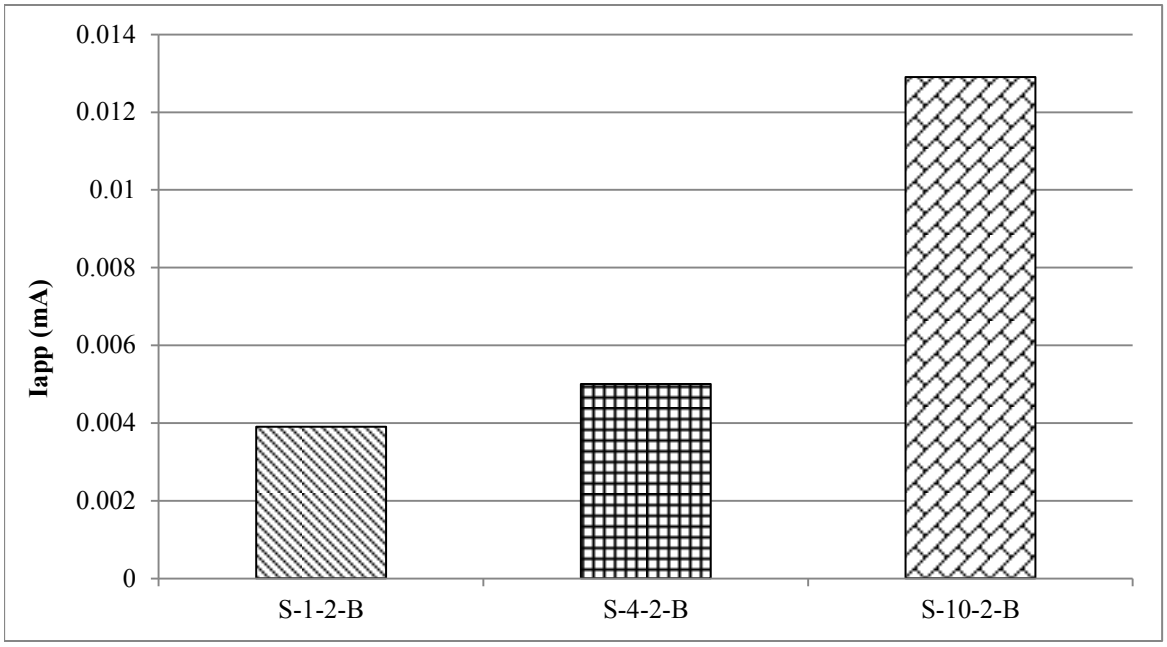

Figure 5.5: Current required for polarization for very low, low and medium corrosion rates.

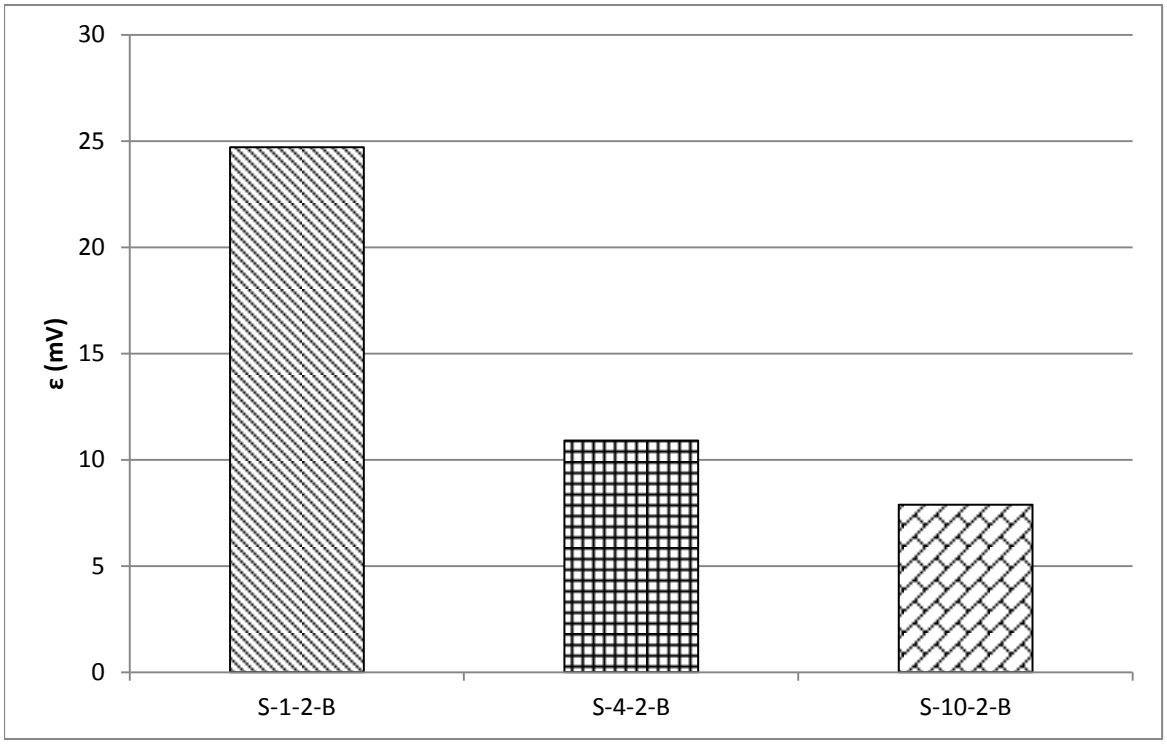

Figure 5.6: Over potentials obtained for very low, low and medium corrosion rates.

5.3 Variation of Corrosion Current Density with Duration of Impressed Current

Figure 5.7 shows the plot of duration of impressed current applied to the concrete specimen versus corrosion current density measured using the developed setup without Ohmic drop compensation. It can be observed from Figure5.7 that as the duration of impressed current increases, corrosion rate also increases almost linearly (R^2=0.88).

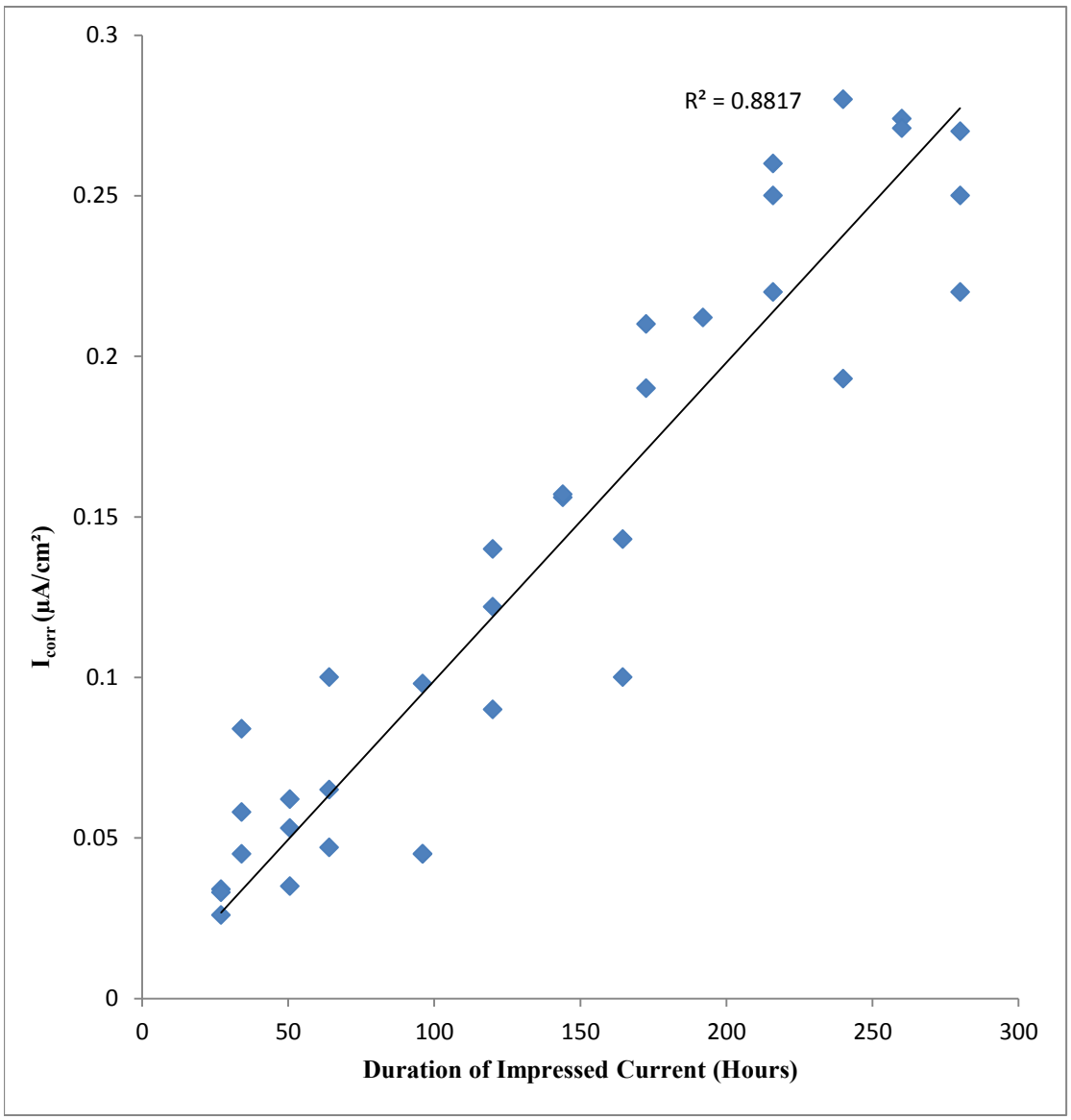

Figure 5.7: Duration of impressed current Vs corrosion current Density without Ohmic Drop compensation measured using developed setup.

Figure 5.8 shows the duration of impressed current applied to the concrete specimen and I_{corr} measured using the developed setup with Ohmic drop compensation. It can be observed from Figure5.8 that as duration of impressed current applied increases, Icorr with Ohmic drop compensation also increases. However, there was a scatter in the data as indicated by R^2=0.80.

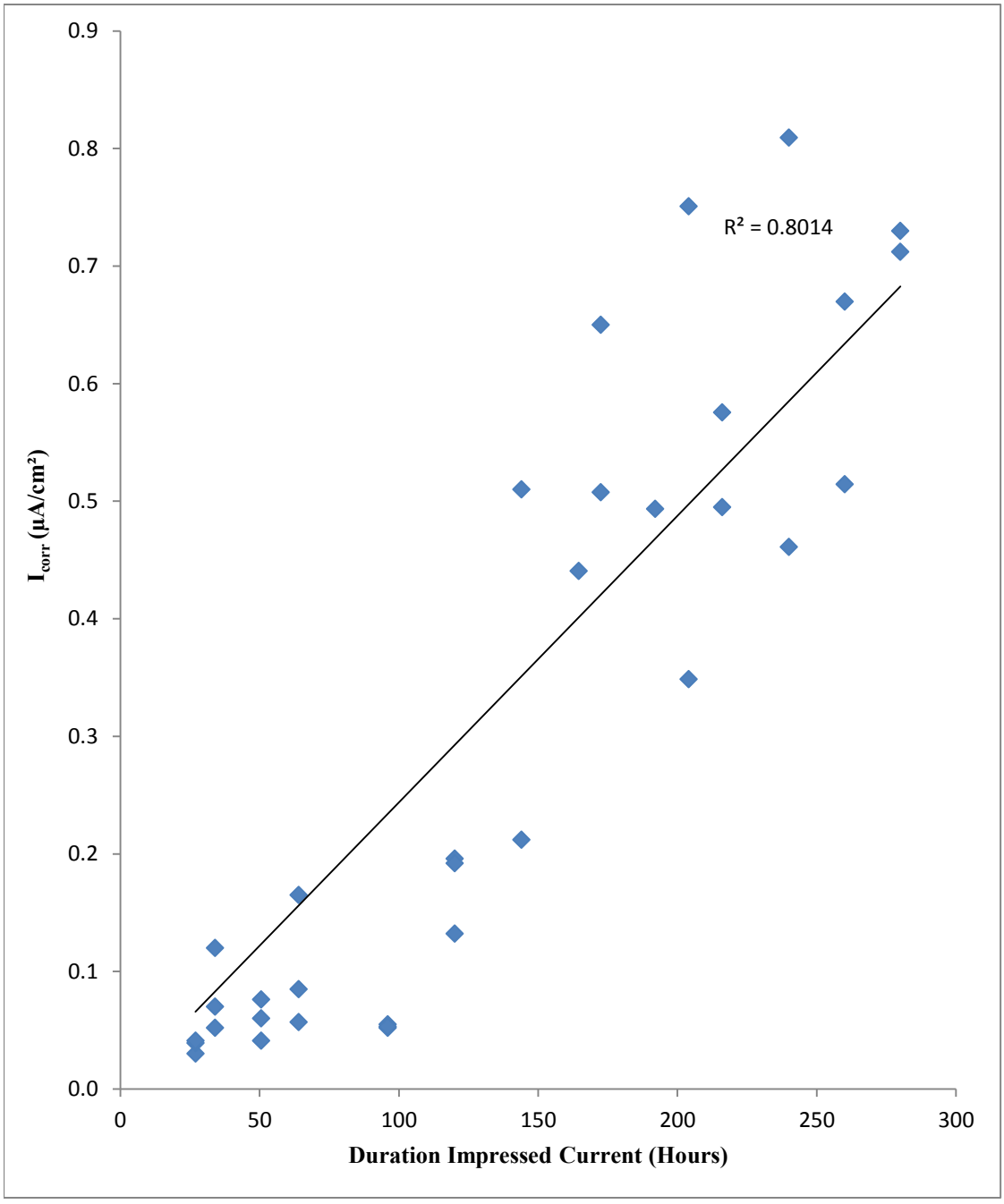

Figure 5.8: Duration of impressed current Vs corrosion current density with Ohmic drop compensation measured using developed setup.

5.4 Comparison of Electrochemical and Gravimetric Test Results

5.4.1 Measured using developed set-up without IR compensation

The corrosion current density measured using the developed setup, without Ohmic drop compensation, is compared with the gravimetric weight loss in Figure 5.9 it can be observed that I_{corr} measured using developed setup without Ohmic drop compensation compares very well with the gravimetric weight loss. The I_{corr} increases almost linearly with the extent of gravimetric weight loss, $R^2 = 0.89$.

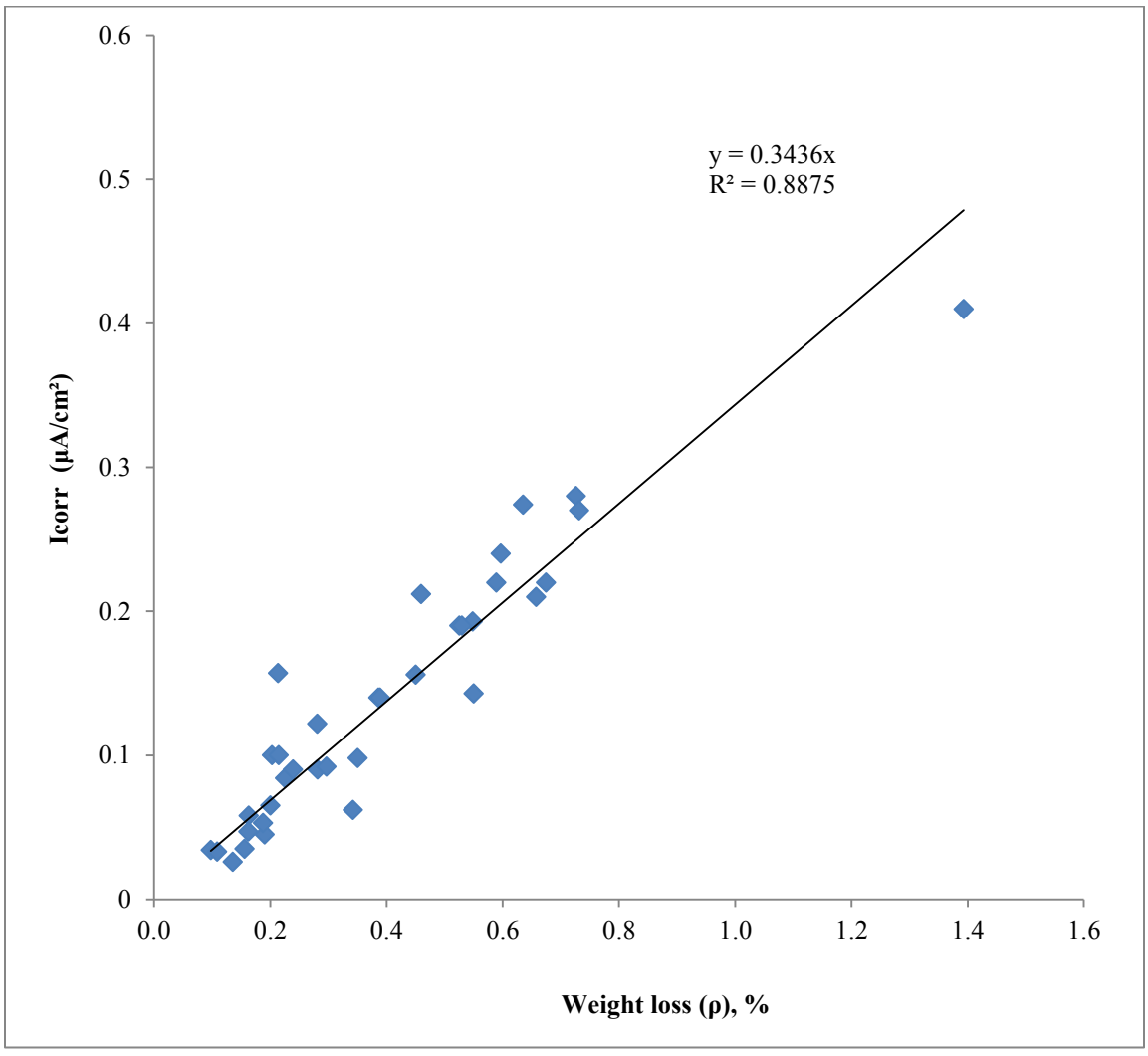

Figure 5.9: Comparison of I_{corr} measured without IR drop compensation using developed setup with gravimetric weight loss.

Although, above relation is fairly linear it cannot be concluded that Ohmic drop due to concrete can be neglected. Consequently, the weight loss was compared with I_{corr} obtained with Ohmic drop compensation using the developed setup.

5.4.2 Measured using developed set-up with IR compensation

The corrosion current density measured with the developed setup with Ohmic drop compensation is plotted against the gravimetric weight loss in Figure 5.10. From Figure 5.10 it can be observed that I_{corr} measured using developed setup with Ohmic drop compensation compares very well (R^2=0.877) with the gravimetric weight loss. The corrosion current density increases with an increase in the weight loss.

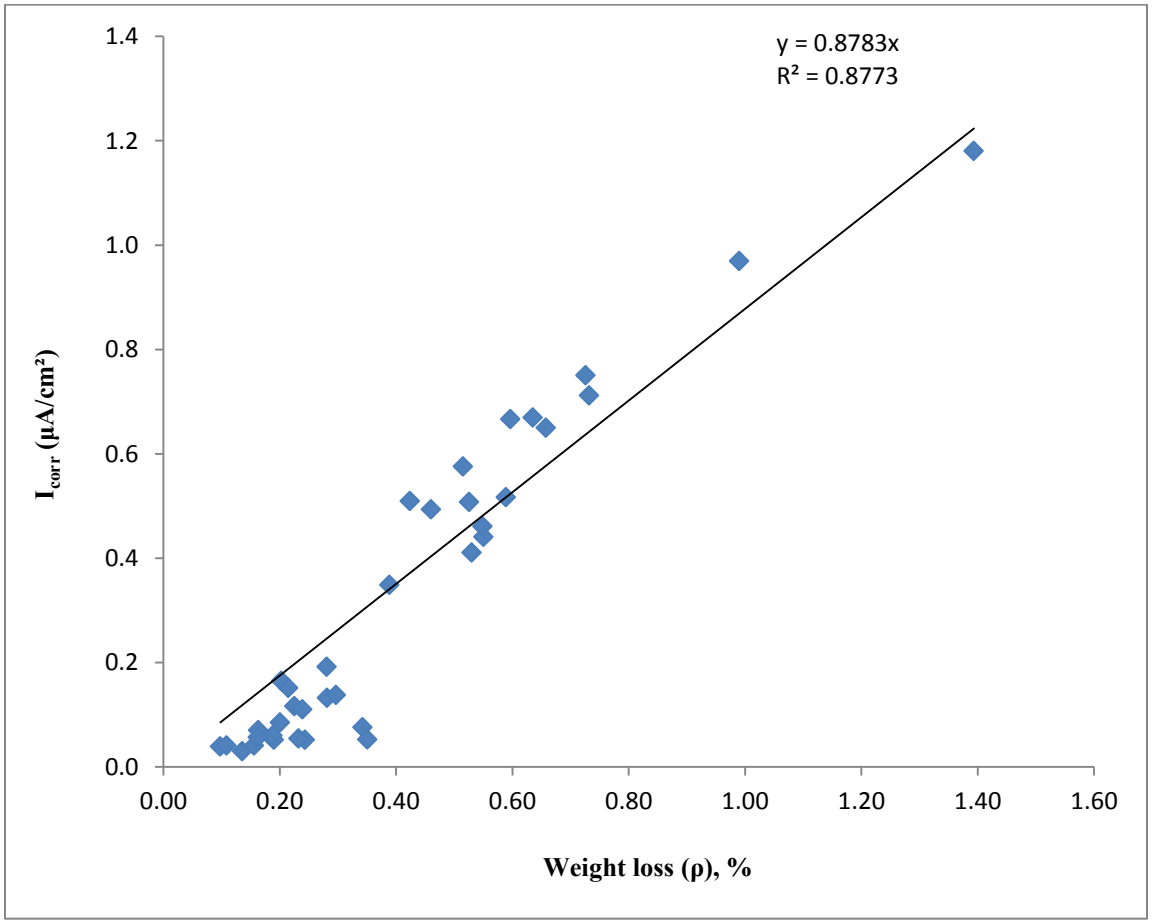

Figure 5.10: Comparison of I_{corr} measured with IR drop compensation using developed setup with gravimetric weight loss.

A comparison of data in Figure 5.9 and 5.10 indicates that the I_{corr} determined with Ohmic drop compensation is more than that without ohmic drop compensation.

5.4.3 Measured using commercial equipment # 1 without IR compensation

The I_{corr} measured with commercial equipment No.1 without Ohmic drop compensation and gravimetric weight loss is as shown in Figure 5.11. It can be observed from Figure 5.11 that the I_{corr} does not correlate well with the weight loss as R^2 is less than 0.85. Although the weight loss increases with an increase in corrosion current density and the relationship is not very encouraging being value of 0.702.

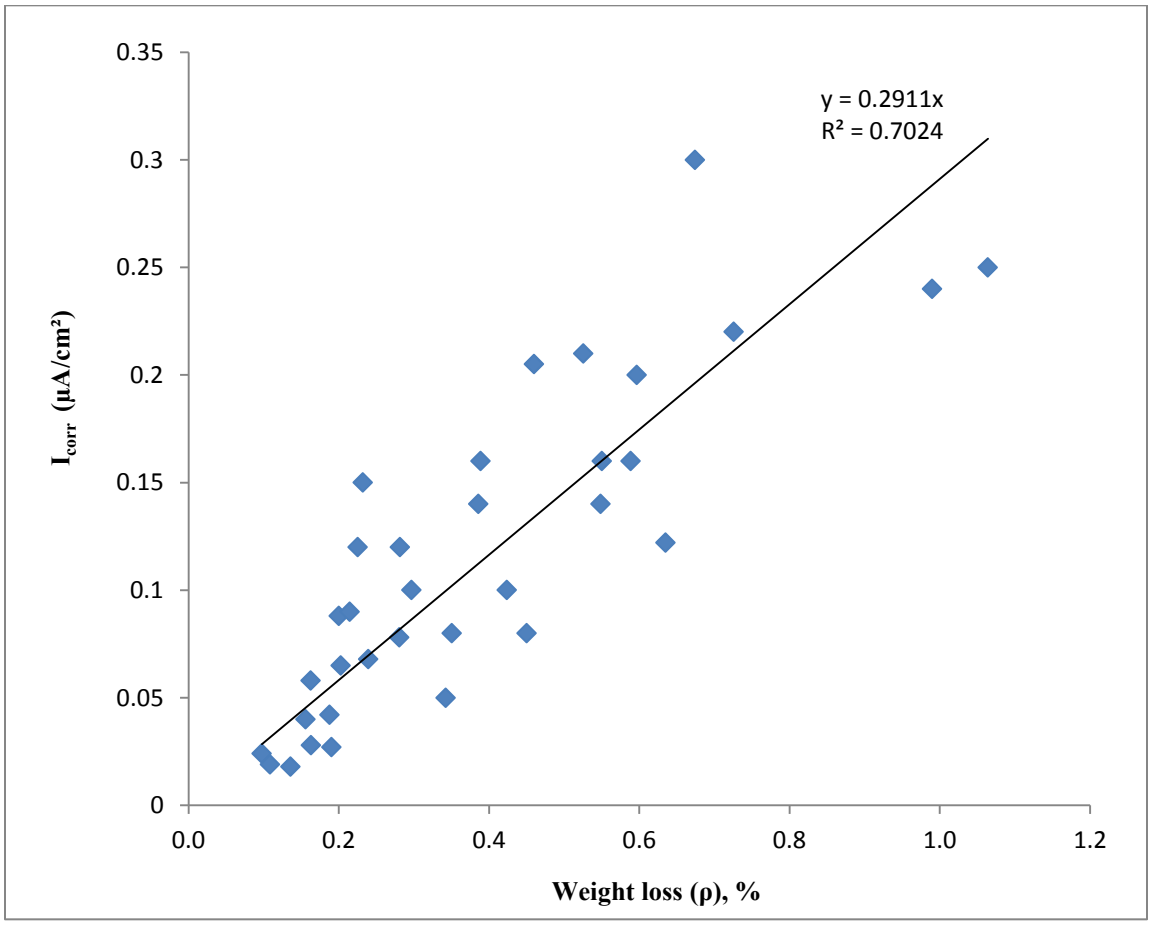

Figure 5.11: Comparison of I_{corr} without Ohmic drop compensation with commercial Equipment No-1 with gravimetric weight loss.

5.4.4 Measured using commercial equipment # 1 with IR compensation

Figure 5.12 shows the comparison of I_{corr} measured with Ohmic drop compensation using commercial equipment No.1.with gravimetric weight loss. A large scatter (R^2=0.17) was noted between the two values, indicating that the I_{corr} values measured using commercial equipment #1 with Ohmic drop compensation do not correspond to the gravimetric weight loss.

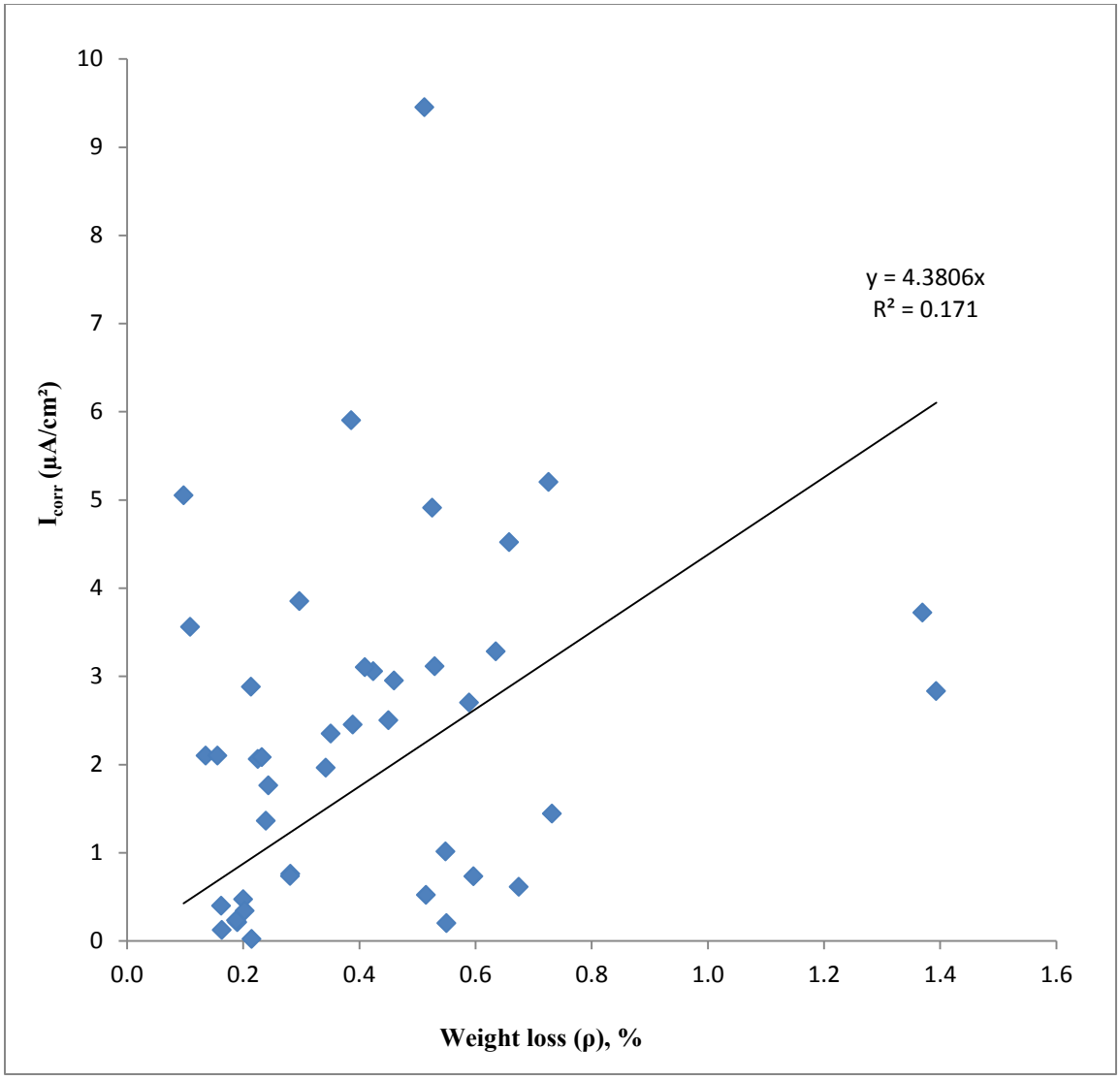

Figure 5.12: Comparison of I_{corr} measured with IR drop compensation using commercial equipment No-1with percentage weight loss

5.4.5 Measured using commercial equipment # 2 without IR compensation

Figure 5.13 compares I_{corr} measured with commercial equipment #2 without Ohmic drop and the gravimetric weight loss. It can be observed from Figure 5.13 that there is an acceptable relationship (R^2=0.77) between weight loss and I_{corr} measured using commercial equipment #2 without Ohmic drop.

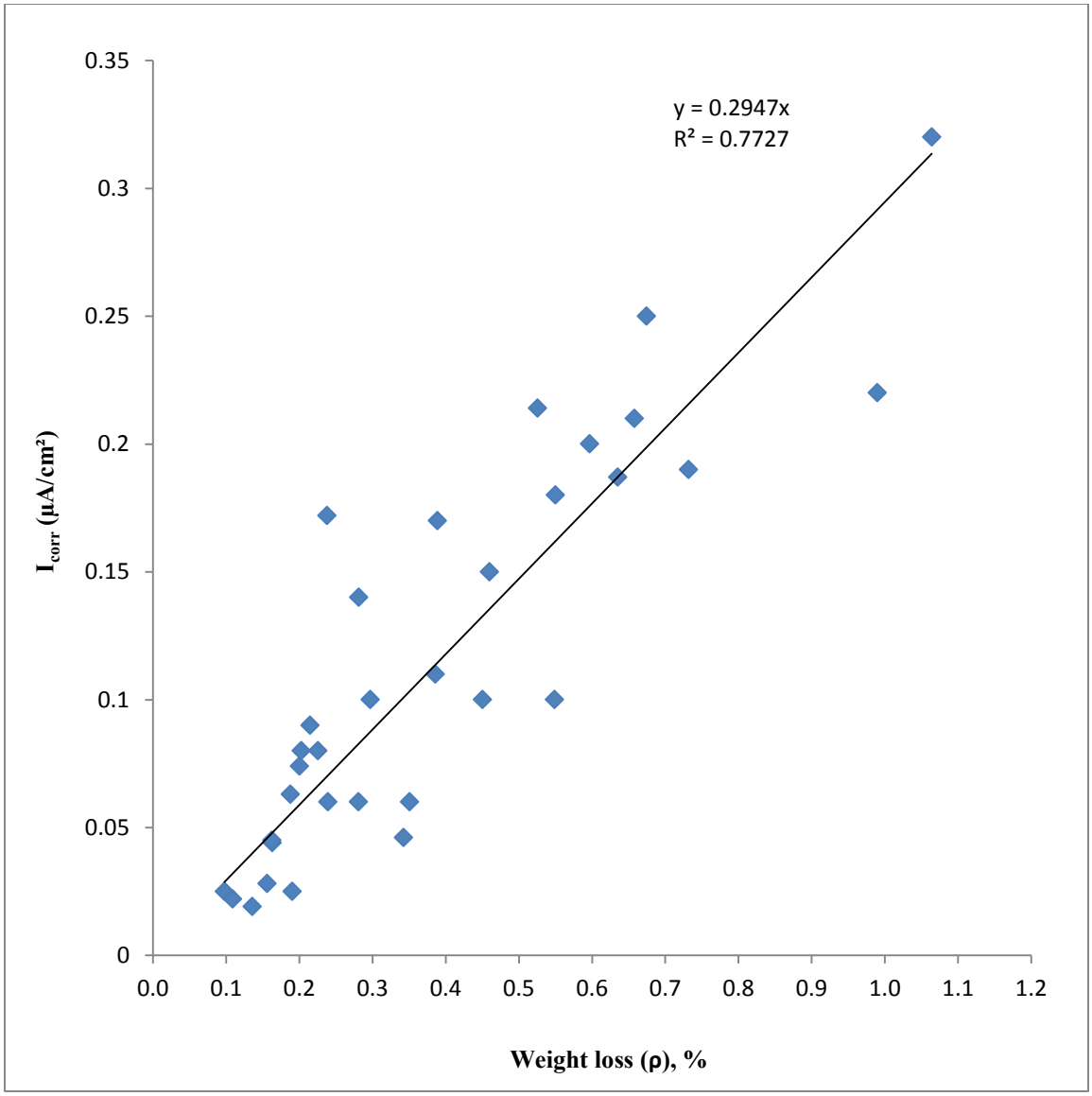

Figure 5.13: Comparison of I_{corr} without Ohmic drop compensation with commercial equipment No-2 with gravimetric weight loss.

5.4.6 Measured using commercial equipment # 2 with IR compensation

Figure 5.14 compares I_{corr} measured with IR compensation using commercial equipment # 2 with gravimetric weight loss. The relationship is not linear and a large scatter can be observed with a R^2 value of 0.464.

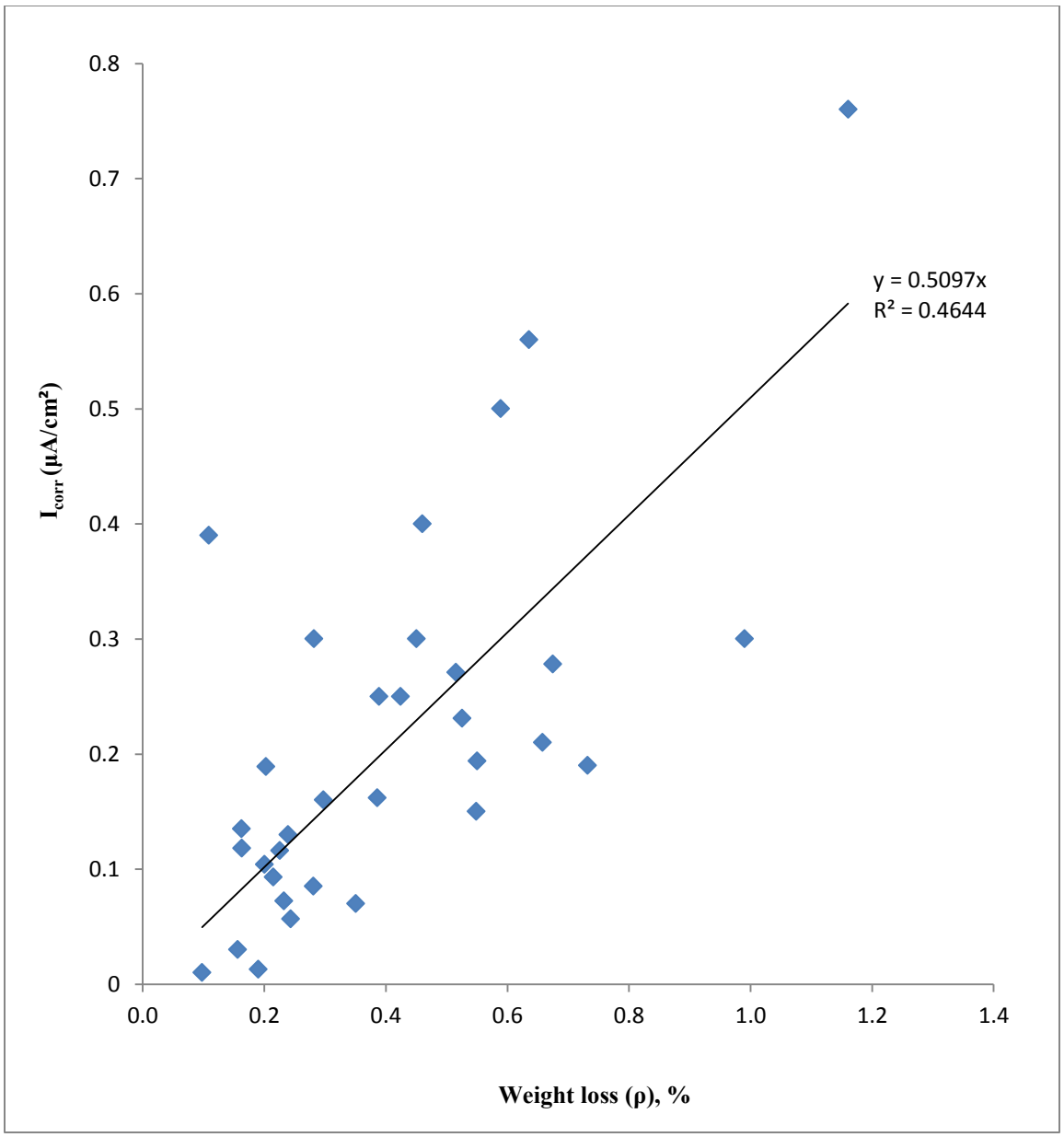

Figure 5.14: Comparison of I_{corr} measured with Ohmic drop compensation using commercial equipment No.2with gravimetric weight loss (ϱ).

Table 5.2 summarizes the relation obtained between I_{corr} measured by all three setups and the gravimetric weight loss. It can be observed that the developed setup and two commercially equipment were effective in measuring corrosion rate without Ohmic drop compensation. The I_{corr} measured using the developed setup is closer to the gravimetric weight loss with highest R^2 = 0.887.Hence it can be concluded that the developed setup is more accurate in measuring corrosion rate without Ohmic drop compensation than commercial equipment.

Table 5.2: Comparison of I_{corr} with three setups without Ohmic drop compensation with gravimetric weight loss.

Equipment	Slope*	R^2
Developed Set-up	I_{corr} = 0.343	0.887
C.E-1	I_{corr} = 0.291	0.702
C.E-2	I_{corr} = 0.294	0.772

*I_{corr}= slope × (ϱ)

I_{corr}: Corrosion current density, μA/cm²; ϱ: weight loss,%.

It should be noted that the relations shown in column #2 of Table 5.2 are valid for the conditions investigated in this study and are used to compare the performance of the developed setup and the two selected commercial equipment. As such, they may not be applicable for other situations.

Table 5.3 shows the relation between I_{corr} measured with all the three setups and the gravimetric weight loss. It can be observed that both commercial equipment gave varying results when compared with gravimetric weight loss. Both, Commercial equipment No.1 and commercial equipment No.2 are not capable of measuring I_{corr} with Ohmic drop compensation as evidence with poor I_{corr} = 4.38ϱ, R^2=-0.17 and I_{corr} =0.51ϱ, R^2=0.464, respectively. The developed setup is capable of measuring corrosion rate both with and without Ohmic drop compensation as indicated I_{corr} = 0.343ϱ, R^2 =0.887 for without Ohmic drop compensation and I_{corr}=0.878ϱ with R^2 =0.88 with Ohmic drop compensation.

Table 5.3: Comparison of I_{corr} with three setups with Ohmic drop compensation with gravimetric weight loss.

Equipment	Slope*	R^2
Developed Set-up	I_{corr} = 0.878	0.88
C.E-1	I_{corr} = 4.380	0.17
C.E-2	I_{corr} = 0.510	0.464

$$*I_{corr} = \text{slope} \times (\varrho)$$

I_{corr}: Corrosion current density, $\mu A/cm^2$; ϱ: weight loss, %.

It should be noted that the relations shown in column #2 of Table 5.3 are valid for the conditions investigated in this study and are used to compare the performance of the developed setup and the two selected commercial equipment. As such, they may not be applicable for other situations.

5.5 Correlation Between Icorr Measured Using Developed Setup and Commercial Equipment

5.5.1 Developed setup versus commercial equipment # 1 (without IR)

The I_{corr} measured using the developed setup and commercial equipment #1, both without Ohmic drop compensation is plotted in Figure 5.15. It can be noted that most of the values are close to each other and as indicated by R^2 value of 0.803.

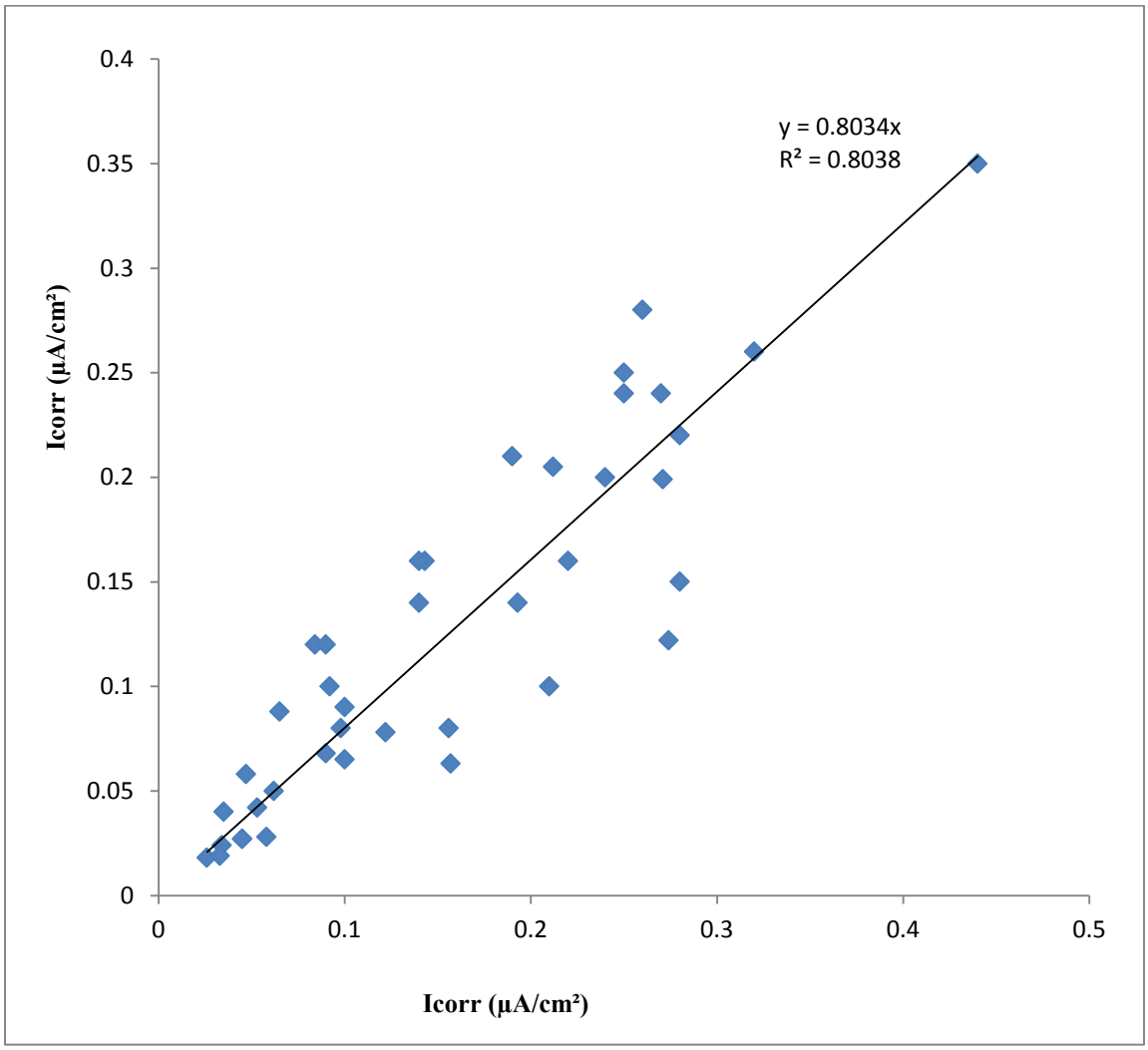

Figure 5.15: Comparison of I_{corr} without Ohmic drop compensation with developed setup and commercial equipment #1.

5.5.2 Developed setup versus commercial equipment # 1 (with IR)

The I_{corr} measured with the developed setup and commercial equipment #1, both with Ohmic drop compensation, is plotted in Figure5.16. It can be observed from Figure 5.16 that results obtained using Commercial equipment No.1 are highly varying when compared with the developed setup. The relation between the I_{corr} measured using the developed setup and commercial equipment # 1 is poor (R^2=0.313).

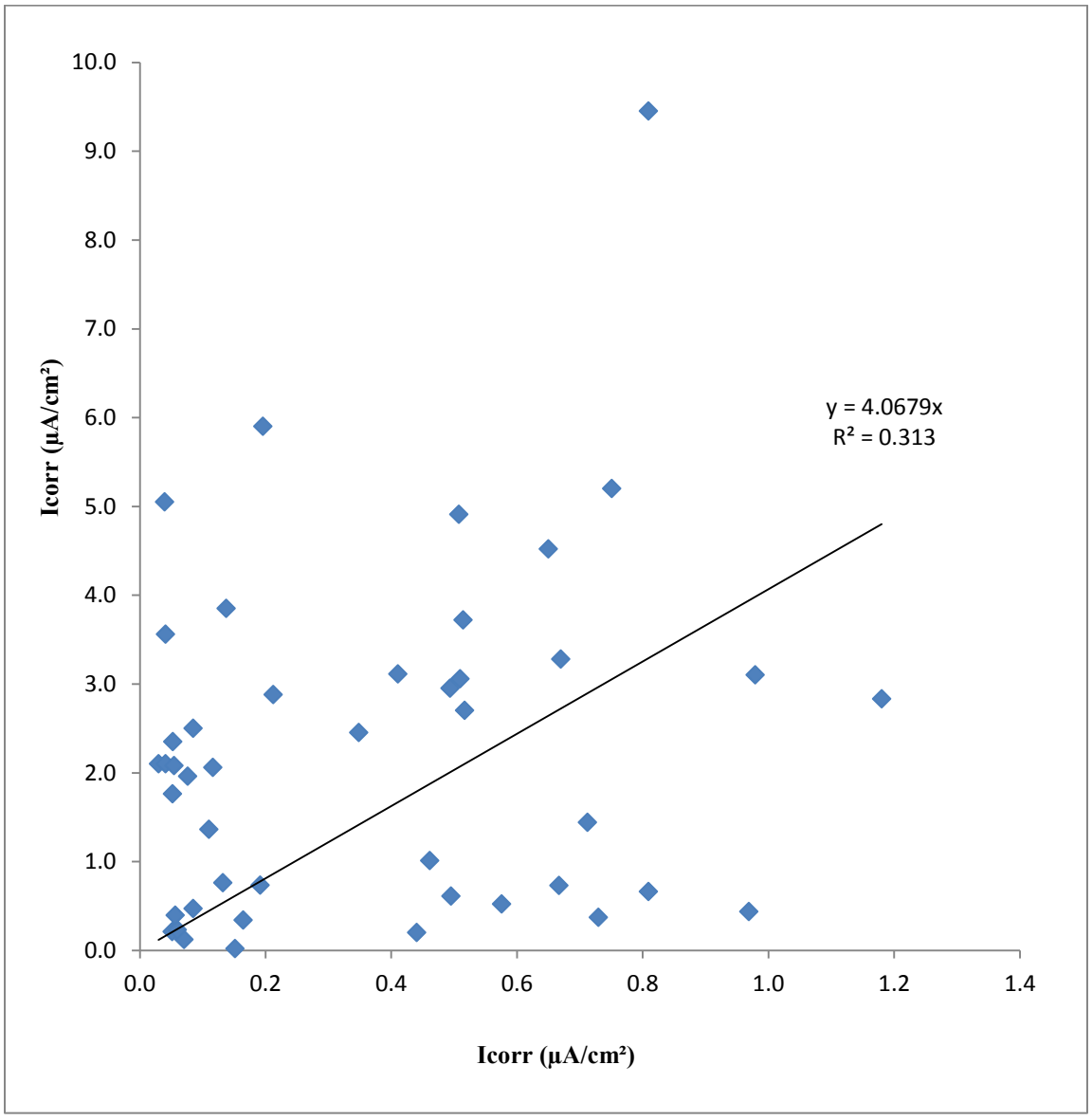

Figure 5.16: Comparison of I_{corr} with Ohmic drop compensation with developed setup and commercial equipment #1.

5.5.3 Developed setup versus commercial equipment # 2 (without IR)

The I_{corr} measured with the developed setup and commercial equipment #2, both without Ohmic drop compensation is shown in Figure 5.17. The resulting plot is quiet linear (R^2=0.814). Hence, it can be concluded that I_{corr} values measured by commercial equipment #2 are similar to those measured by the developed setup without Ohmic drop compensation.

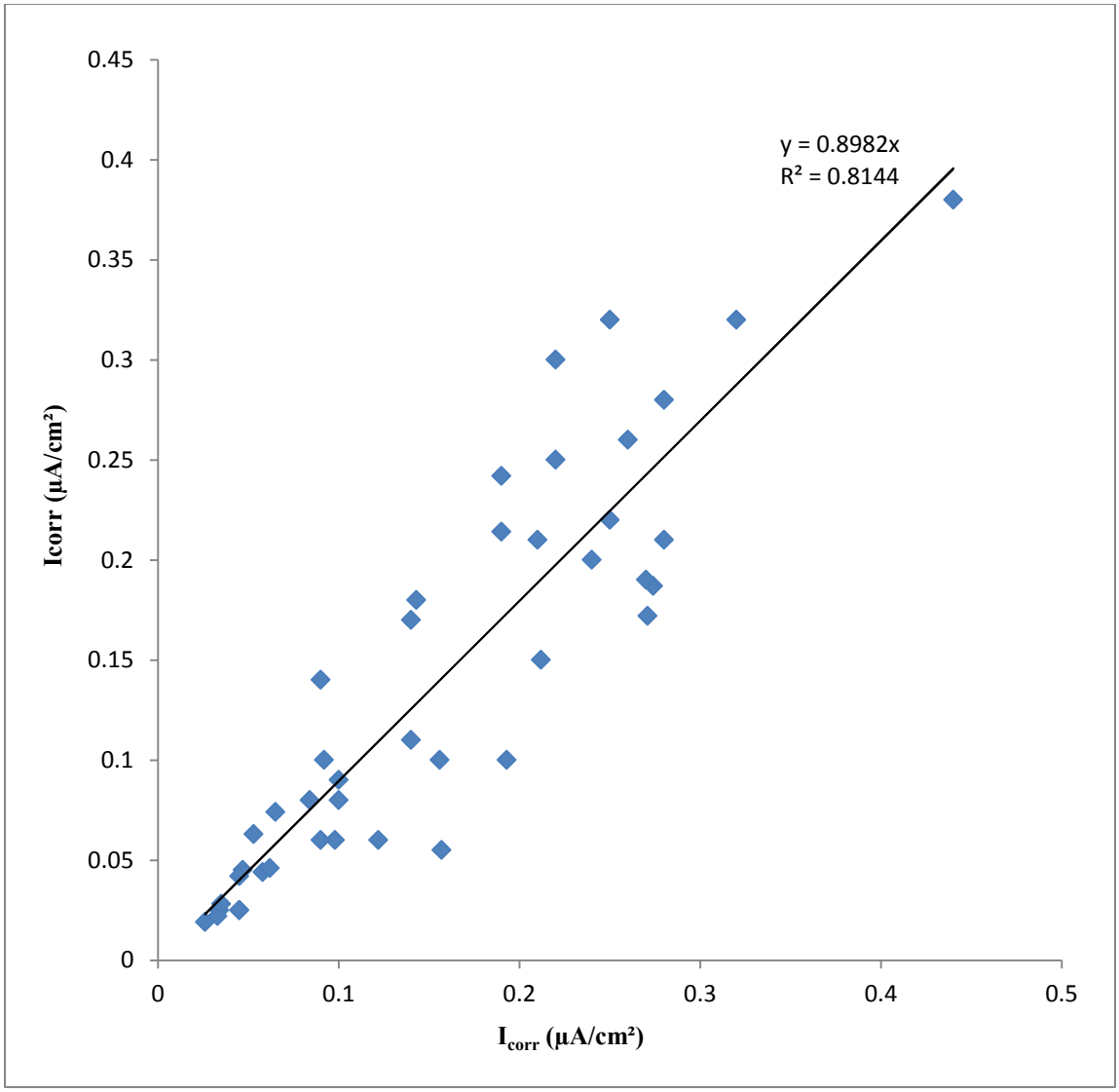

Figure 5.17: Comparison of I_{corr} without Ohmic drop compensation with developed setup and commercial equipment #2

5.5.4 Developed setup versus commercial equipment # 2 (with IR)

The I_{corr} measured with the developed setup and commercial equipment #2, both with Ohmic drop compensation is plotted in Figure5.18. From Figure 5.18 it can be observed that results obtained using Commercial equipment No.2 when compared with the developed setup gave a low relation with a value of R^2=0.473.

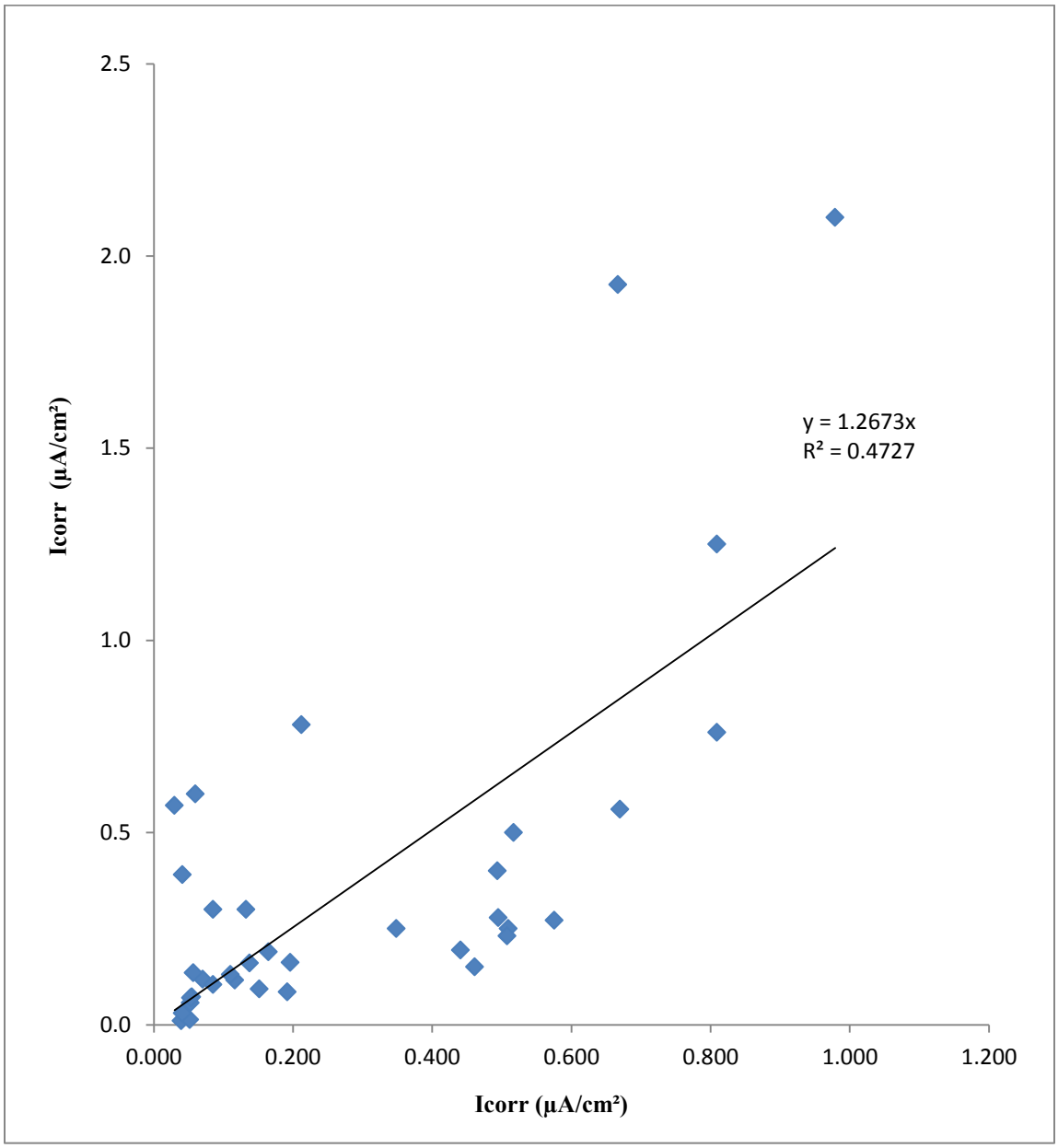

Figure 5.18: Comparison of I_{corr} with Ohmic drop compensation with developed setup and commercial equipment #2.

It can be observed from Table 5.4 that the I_{corr} without Ohmic drop compensation using developed setup and commercial equipment are very much similar. However, the I_{corr} measured with the commercial equipment, with Ohmic drop compensation do not match with I_{corr} measured with the developed setup. It should be noted that the I_{corr} measured using the developed setup are very close to the gravimetric weight loss.

Table 5.4: Comparison of I_{corr} measured using the commercial equipment and developed setup.

Type of Comparison	Correlation Equation	R^2
D.S Vs C.E # 1 (without IR)	$(I_{corr})_{CE1} = 0.803\ (I_{corr})_{DS}$	0.803
D.S Vs C.E # 1 (with IR)	$(I_{corr})_{CE1} = 4.067\ (I_{corr})_{DS}$	0.31
D.S Vs C.E # 2 (without IR)	$(I_{corr})_{CE2} = 0.898\ (I_{corr})_{DS}$	0.814
D.S Vs C.E # 1 (with IR)	$(I_{corr})_{CE2} = 1.267\ (I_{corr})_{DS}$	0.472

5.6 Correlation Between Icorr values with and without IR Compensation Measured using Developed Setup

In order to examine the usefulness of the developed setup for measuring varying intensities of corrosion (low, medium, and high) and also to correlate the I_{corr} values measured with and without IR, 13 more corroded specimens were tested using the developed setup. The corrosion rates of steels in these specimens were in the range of 0.2 $\mu A/cm^2$ to 3.38 $\mu A/cm^2$ without Ohmic drop compensation. This confirmed that the setup developed can measure corrosion rates for all types of specimens both with and without Ohmic drop compensation effectively. Table 5.5 shows the values of corrosion rate with and without Ohmic drop compensation measured with developed setup.

For developing the correlations between I_{corr} values with and without Ohmic drop for different ranges of the degree of corrosion, the results in Table 5.5 were divided into following three groups:

[1] Low corrosion (I_{corr}< 0.1 μA/cm²)

[2] Medium corrosion (I_{corr} = 0.1 to 1.0 μA/cm²)

[3] High corrosion (I_{corr}> 1 μA/cm²)

Table 5.5: I_{corr} with and without IRcompensation measured using developed setup.

Specimen ID	I_{corr} without IR (μA/cm²)	I_{corr} with IR (μA/cm²)
S-1-1-A	0.026	0.030
S-1-2-B	0.034	0.039
S-1-3-C	0.033	0.041
S-4-1-A	0.045	0.052
S-4-2-B	0.084	0.116
S-4-3-C	0.058	0.070
S-2-1-A	0.035	0.041
S-2-2-B	0.062	0.076
S-2-3-C	0.053	0.060
S-3-1-A	0.065	0.085
S-3-2-B	0.1	0.165
S-3-3-C	0.047	0.057
S-5-1-A	0.045	0.052
S-5-2-B	0.045	0.055
S-5-3-C	0.045	0.053
S-8-1-A	0.09	0.132
S-8-2-B	0.14	0.196
S-8-3-C	0.122	0.192
S-9-1-A	0.286	0.509
S-9-2-B	0.065	0.085
S-9-3-C	0.156	0.212
S-12-1-A	0.24	0.667
S-12-2-B	0.143	0.441
S-12-3-C	0.1	0.152
S-13-1-A	0.09	0.111
S-13-2-B	0.21	0.650
S-13-3-C	0.19	0.508
S-10-1-A	0.212	0.493
S-10-2-B	0.44	0.809

Specimen ID	I_{corr} without IR (μA/cm²)	I_{corr} with IR (μA/cm²)
S-10-3-C	0.32	0.979
S-11-1-A	0.286	0.751
S-11-2-B	0.14	0.349
S-11-3-C	0.092	0.138
S-14-1-A	0.254	0.576
S-14-2-B	0.22	0.495
S-14-3-C	0.25	0.969
S-15-1-A	0.28	0.809
S-15-2-B	0.41	1.180
S-15-3-C	0.193	0.461
S-6-1-A	0.274	0.670
S-6-2-B	0.19	0.411
S-6-3-C	0.271	0.514
S-7-1-A	0.25	0.730
S-7-2-B	0.22	0.517
S-7-3-C	0.27	0.712
S-1	0.2	0.28
S-2	0.25	0.35
S-3	0.21	0.35
S-4	0.24	0.38
S-5	0.56	0.66
S-6	0.431	0.87
S-7	0.56	0.85
S-8	2.25	9.7
S-9	2.96	10.5
S-10	2.44	8.1
S-11	3.38	14.3
S-12	1.72	5.6
S-13	1.082	3.18

5.6.1 Correlation for low corrosion (Icorr< 0.1 µA/cm²)

The relation obtained in this zone is shown in Figure 5.19. I_{corr} with Ohmic drop compensation is almost 1.3 times of I_{corr} without Ohmic drop compensation. This is considered as the passive state for reinforcement corrosion so effect of Ohmic drop compensation is very less in this zone.

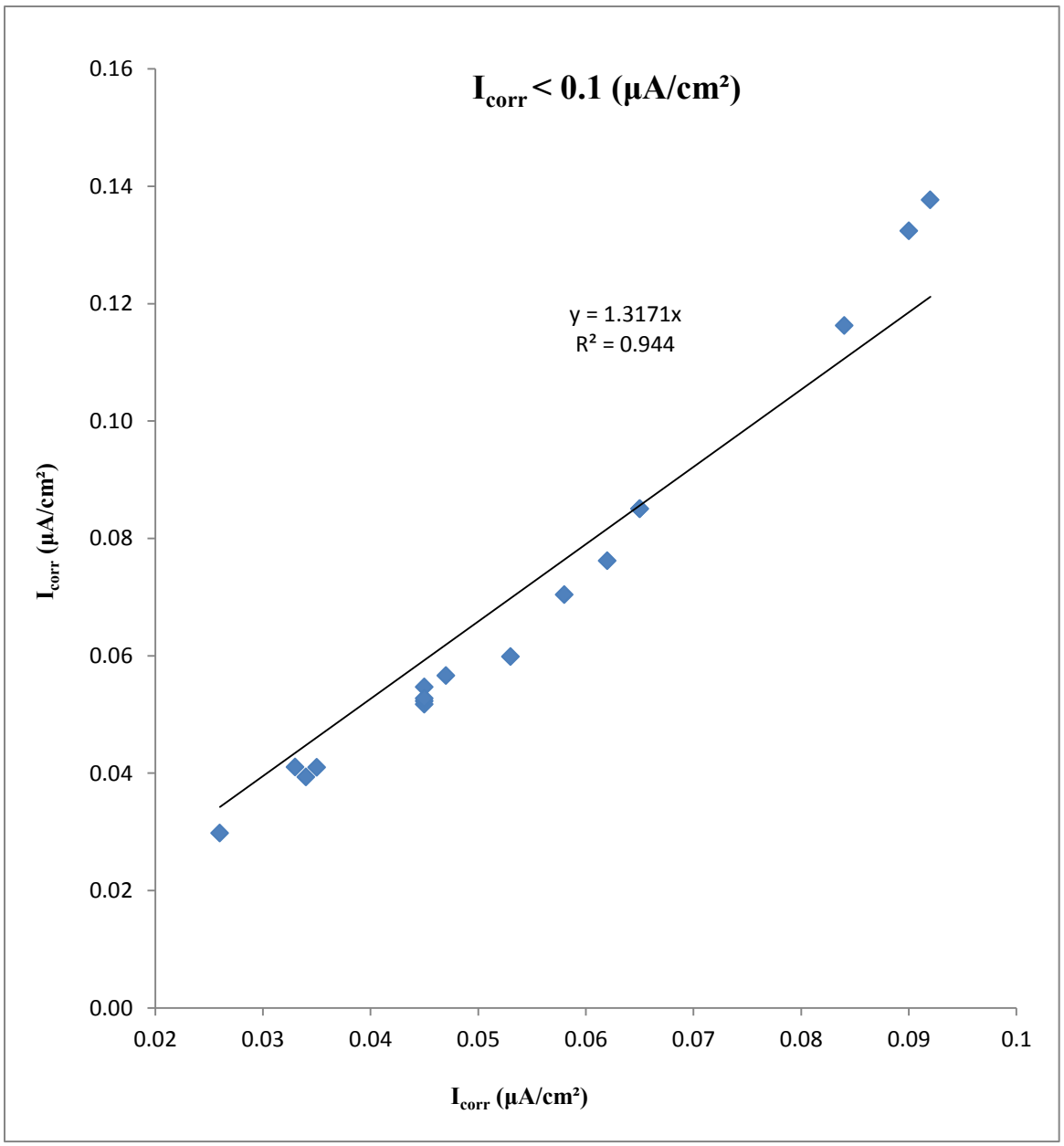

Figure 5.19: Relation between $I_{corr}$with Ohmic drop and that without Ohmic drop for low corrosion (I_{corr}< 0.1µA/cm²).

5.6.2 Correlation for medium corrosion (Icorr = 0.1 to 1.0 µA/cm²)

The relation obtained for this corrosion zone is shown in Figure 5.20. I_{corr} with Ohmic drop compensation is almost 2.35 times of I_{corr} without Ohmic drop compensation. This zone is considered as the medium state of reinforcement corrosion rate so the effect of Ohmic drop compensation increases in this region which may be due to increase in the corrosion current.

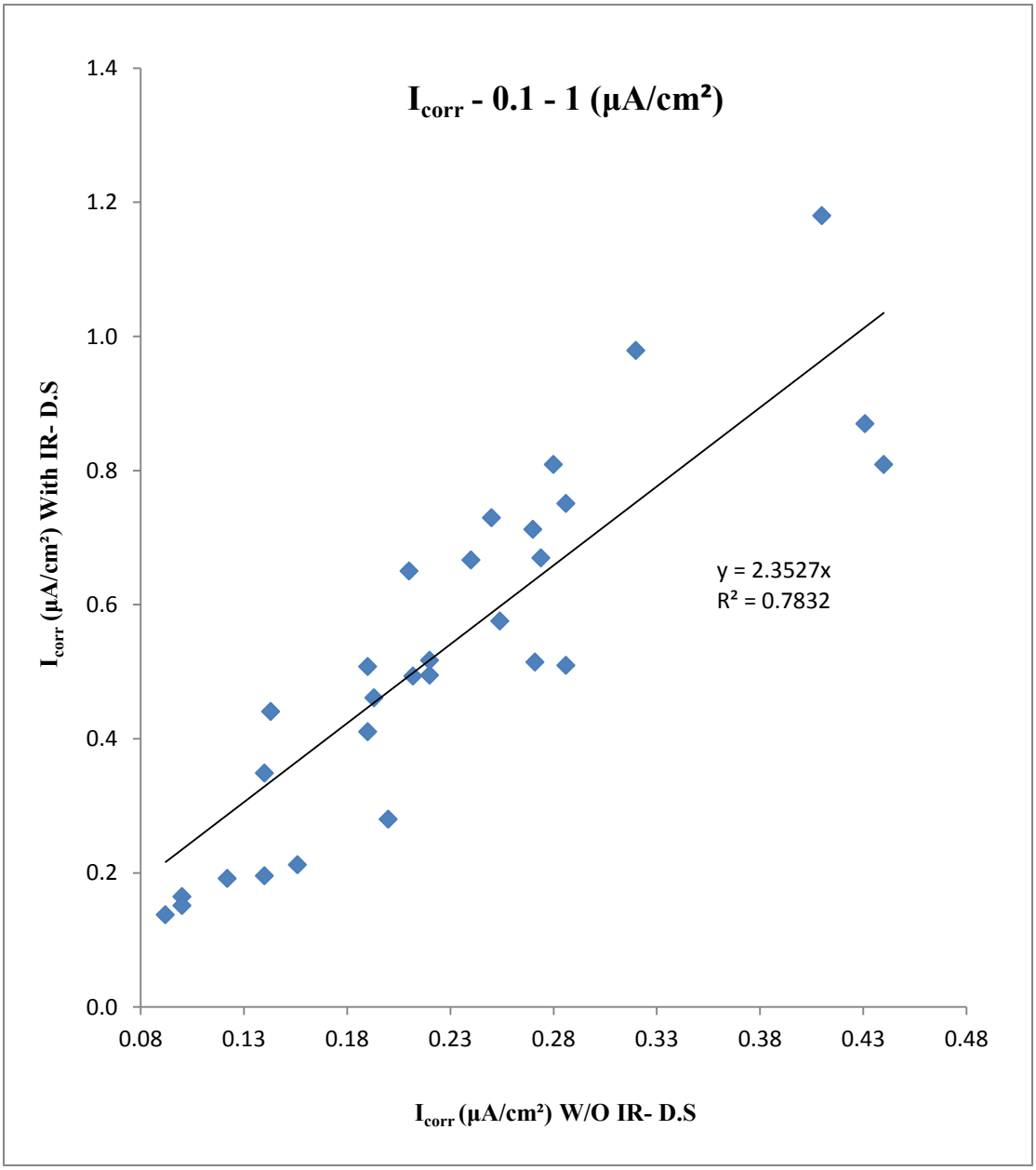

Figure 5.20: Relation betweenI_{corr}measured with Ohmic drop and without Ohmic drop (I_{corr} 0.1 To 1.0 µA/cm²).

5.6.3 Correlation for high corrosion (Icorr> 1 μA/cm²)

The relation obtained in this zone is shown in the Figure 5.21. The I_{corr} with Ohmic drop compensation is almost 3.8 times the I_{corr} without Ohmic drop compensation. This zone is considered as very high state of reinforcement corrosion rate. The high compensation is due to the high polarizing current.

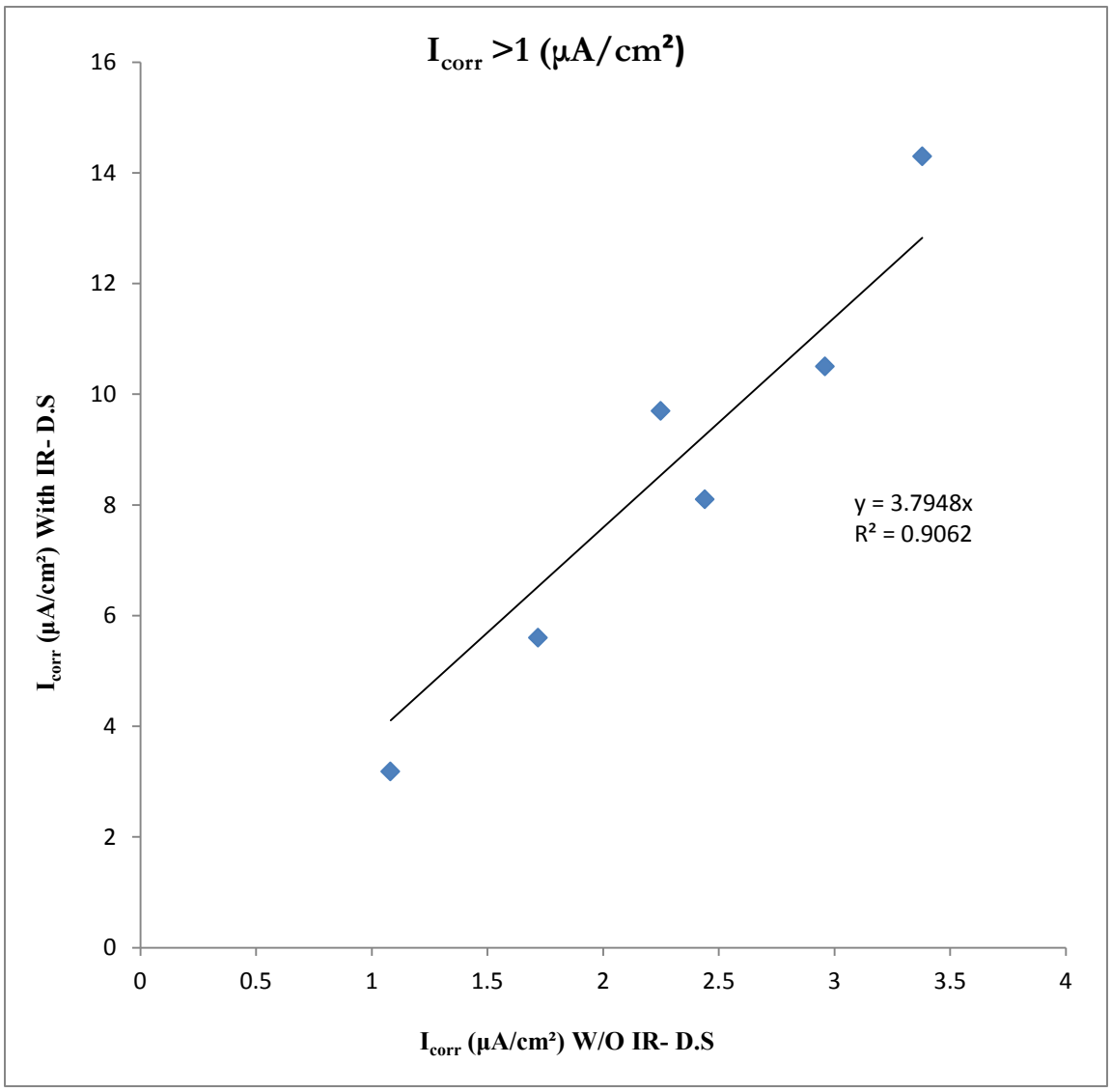

Figure 5.21: Relation Between with and without Ohmic Drop for (I_{corr}> 1μA/cm²).

The relationships obtained between I_{corr} measured with and without ohmic drop compensation for various zones have been tabulated in Table 5.6.

Table 5.6: Relation between I_{corr} without and with Ohmic drop for various degrees of corrosion.

Icorr(μA/cm²)	Degree of Corrosion	Relation Between Without & With Ohmic Drop using developed setup
< 0.1	Low	$(I_{corr})_{WITH\ IR} = 1.317\ (I_{corr})_{W/O\ IR}$
0.1 to 1	Medium	$(I_{corr})_{WITH\ IR} = 2.35\ (I_{corr})_{W/O\ IR}$
>1	High	$(I_{corr})_{WITH\ IR} = 3.794\ (I_{corr})_{W/O\ IR}$

From Table 5.6 it is clear that Ohmic drop compensation is the least when the corrosion rate is low. Thus, in this zone I_{corr} measurements can be carried out without Ohmic drop compensation. In the range of medium corrosion rate the effect of Ohmic drop compensation is in the range of 2 to 2.5. But when the corrosion rate goes beyond 1 μA/cm², the I_{corr} with Ohmic drop compensation is about 3.8 times of the corrosion rate without Ohmic drop compensation.

From the foregoing, data Ohmic drop compensation is critical to very critical in the medium to high corrosion rate.

5.7 Effect of Moisture Content and Resistivity on Corrosion Rate in a Reinforced Concrete Specimen

The effect of moisture content and resistivity on corrosion rate was studied. In this study 10 prismatic specimens of size 100 x 70 x 300 mm that were already corroded were utilized to study effect of moisture content and resistivity on corrosion current density.

5.7.1 Methodology

Specimens were first immersed in water for 48 hours so that the pores inside the specimen may be filled with moisture. Then they were taken out and the wet weight was obtained after surface drying and at that very instance the resistivity was measured by two probe method and immediately the corrosion rate was measured.

Finally, the specimens were oven dried at 110°C for 24 hours and the moisture content was obtained. The data so obtained were utilized to obtain relation between moisture content, electrical resistivity and corrosion current densityand is summarized in Table 5.7.

Table 5.7: Moisture content, corrosion current density, electrical resistivity.

Specimen ID	MoistureContent(%)	Icorr(μA/cm²)	R(KΩ-cm)
S-1	3.39	3.324	0.8
	3.18	4.69	1.1
	3.08	6.18	1.7
	2.81	7.07	2
	2.62	3.5	2.5
	2.50	2.25	3.5
	2.23	1.95	4.8
	2.06	1.52	6
	1.64	1.3	9.2
	1.31	0.9	13
	0.81	0.72	18
	0.55	0.7	24
S-2	2.65	1.55	3.5
	2.45	1.8	4.6
	2.25	2.1	6.2
	1.90	2.6	7.9
	1.64	1.5	9.5
	1.51	0.79	11.4
	1.34	0.358	13.5
	0.93	0.25	21.8
	0.62	0.092	35
	0.32	0.084	56.5
S-3	2.59	0.6	11
	2.40	0.67	11.2
	2.08	0.85	11.5
	1.75	1.127	12
	1.32	1	13.2
	1.23	0.85	14
	1.13	0.39	15
	0.99	0.187	22
	0.86	0.123	28.5
	0.74	0.0985	45
	0.52	0.0934	65

Specimen ID	Moisture Content (%)	Icorr(μA/cm²)	R(KΩ-cm)
S-4	3.74	2.2	1.4
	3.20	2.18	2
	2.72	2.95	4.1
	2.36	1.74	5.9
	2.15	1.336	7.4
	1.67	0.58	13.5
	1.41	0.4	17
	1.18	0.39	19.5
	1.02	0.36	25
	0.80	0.12	30
S-5	2.11	0.186	20.5
	2.02	0.186	20.7
	1.97	0.195	21
	1.80	0.25	21.5
	1.44	0.256	23.5
	1.29	0.2	25
	1.10	0.181	28
	0.70	0.123	40
	0.60	0.09	47
	0.49	0.08	55
S-6	4.00	1.495	7
	3.58	1.525	7.4
	2.94	2.21	8.3
	2.75	1.3	7.3
	2.52	0.91	8
	1.90	0.7	10.5
	1.64	0.73	12.2
	1.37	0.62	14.9
	1.13	0.46	18
	0.84	0.35	21.5
	0.64	0.22	27
	0.47	0.2005	32

Specimen ID	Moisture Content (%)	Icorr(μA/cm²)	R(KΩ-cm)
S-7	4.19	7.318	1.8
	4.05	7.77	2.1
	3.59	8.73	2.7
	3.40	5.24	3
	3.07	3.92	4.1
	2.70	2.98	5.2
	2.07	2.41	5.7
	1.80	1.65	8
	1.60	1.1	10
	1.35	0.85	14.5
	1.08	0.755	19.5
S-8	4.24	4.17	3.3
	3.96	4.1	4.6
	3.66	5.264	5
	3.26	2.7	5.4
	2.94	2.45	6.2
	2.41	2.11	7.6
	1.84	1.28	9
	1.39	1.09	13.5
	0.99	0.59	18.5
	0.63	0.42	22
S-9	4.59	7	2.9
	4.40	7.22	3.2
	4.06	8.2	3.3
	3.81	6.5	3.5
	3.36	4.65	3.8
	2.85	3.66	4.4
	2.46	2.47	5.8
	2.09	1.39	7
	1.56	1.41	10
	1.17	1.4	12.4
	0.72	1.39	16
S-10	5.09	6.29	2
	4.90	10.1	2.3
	4.43	10.7	2.7
	4.22	11	3.3
	3.62	6.32	3.5
	3.24	3.2	3.8
	2.88	2.48	4.9
	2.35	2.5	5.5
	1.84	1.65	7.4
	1.34	1.18	9.8
	0.79	0.36	19

5.7.2 Effect of moisture content on resistivity

Figure 5.22 shows the relationship between the moisture content and the electrical resistivity. It can be seen that the electrical resistivity decreases with the moisture content.

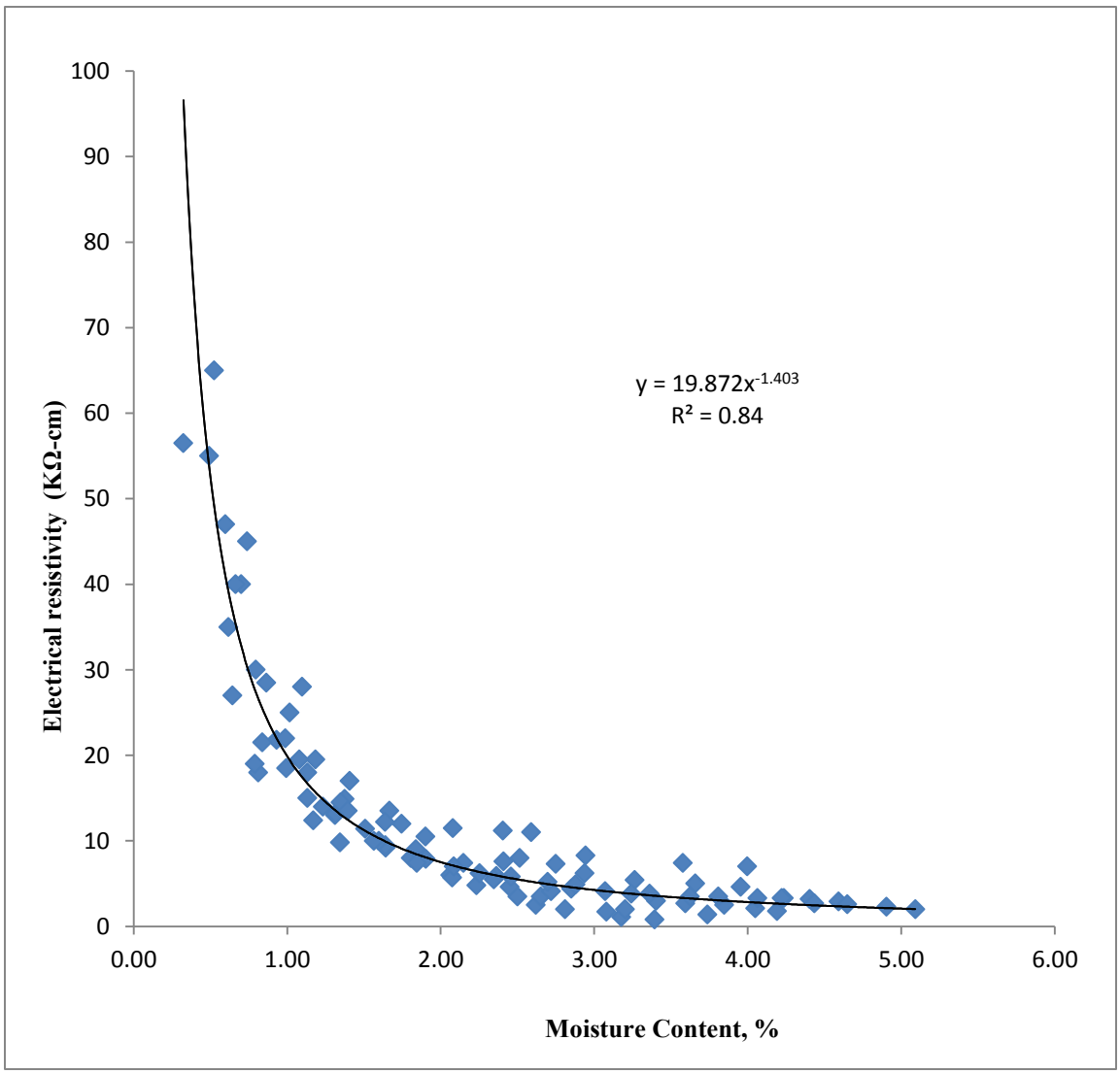

Figure 5.22: Relation between moisture content and electrical resistivity.

By using the data developed between the electrical resistivity and moisture content a relation was developed to determine moisture content using the resistivity of concrete. Following typical relation was developed to determine the moisture content using the resistivity of concrete.

$$R = \frac{19.87}{(M.C)^{1.4}}$$

M.C = Moisture content (%)

R = Resistivity (KΩ-cm)

Another prospective of the data in Figure 5.22 is that the resistivity is very low for a moisture content of more than 2.5%. Consequently, if the moisture content is 2.5% or more Ohmic drop compensation may not be necessary.

5.7.3 Effect of moisture content on corrosion rate

Figure 5.23 shows the relation between moisture content and I_{corr} in specimen A. It can be observed from Figure 5.23 that when the specimen is in wet condition the corrosion rate obtained at that instance is not the highest. But, when the specimen slowly starts losing its moisture the corrosion rate increases up to a certain point and then starts decreasing. The point were the highest corrosion is measured is the point where the specimen has the optimum moisture content. The optimum moisture content for this specimen recorded was 2.8%.

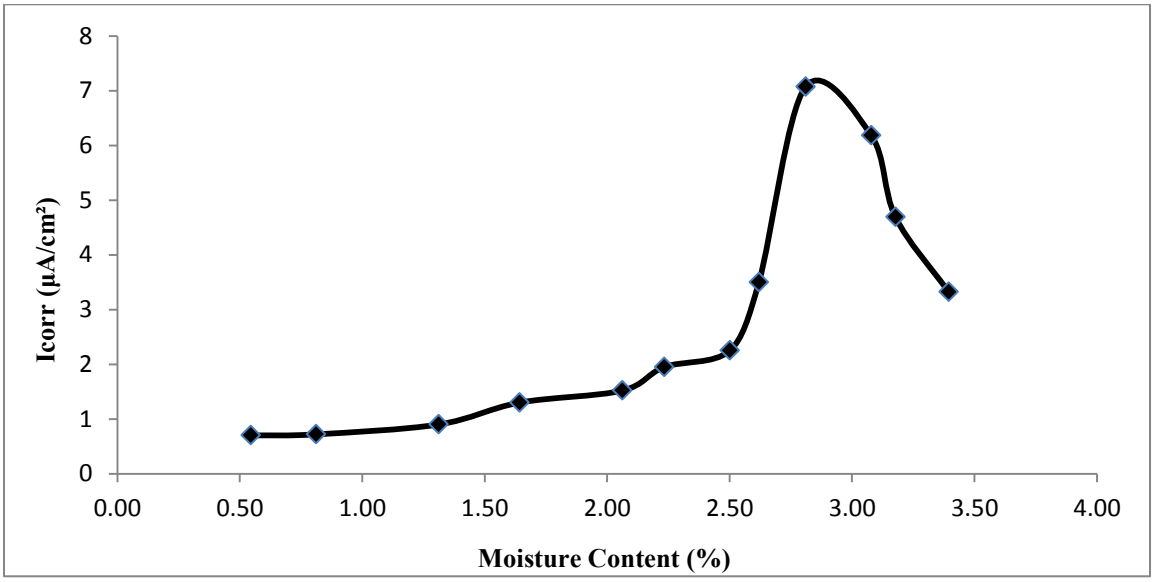

Figure 5.23: Relation between moisture content and corrosion rate – Specimen A.

The increase in I_{corr} with increasing moisture content is understandable since moisture is necessary for the cathodic reaction. However, the decrease in I_{corr} after optimum moisture content is attributed to a decrease in the oxygen content with increasing moisture content oxygen is not available for the cathodic reaction. Both oxygen and moisture content are required for the corrosion process to proceed. The optimum content was 2.8% in specimen A.

Figure 5.24 shows the relation between moisture content and corrosion current density for specimen B. The trend of this data is similar to that noted in specimen A. The optimum moisture content in this specimen was 2.94%.

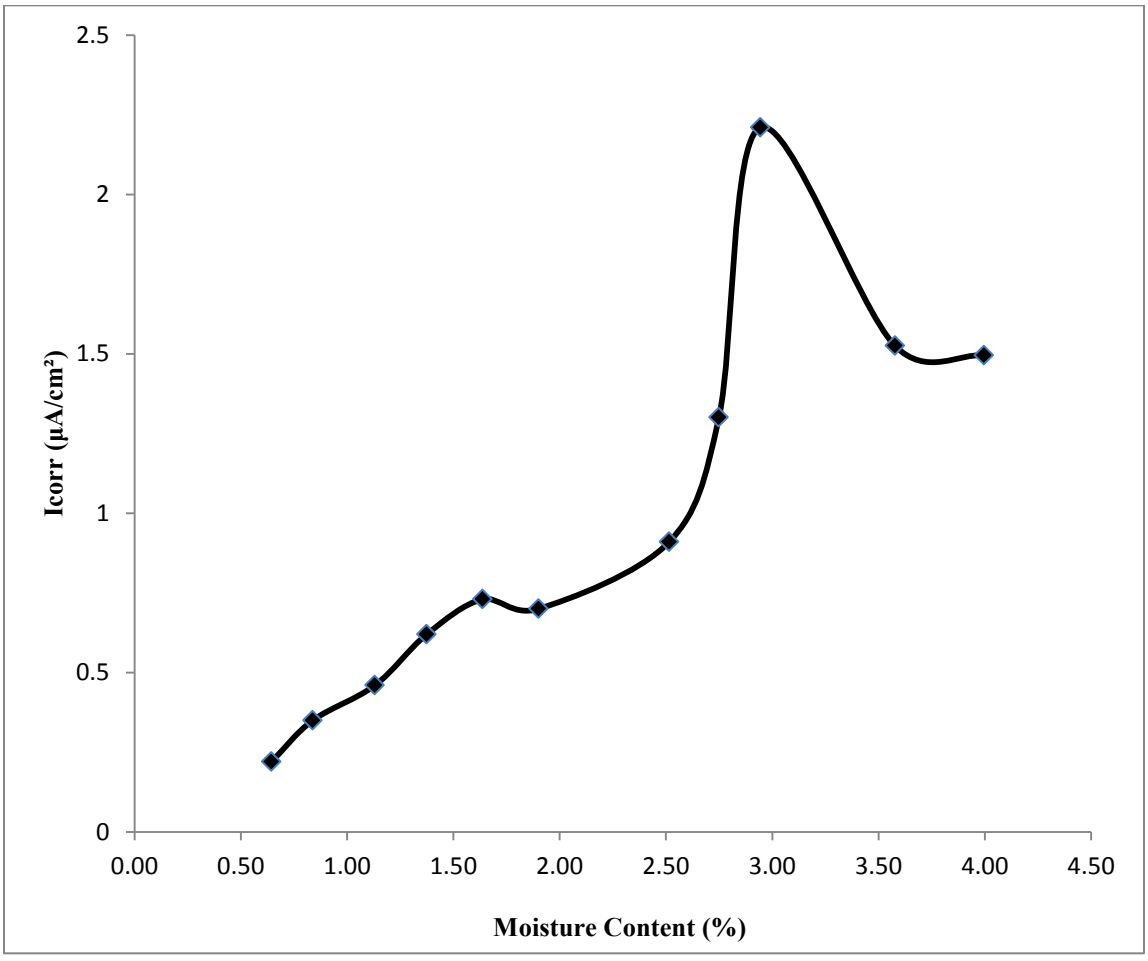

Figure 5.24: Relation between moisture content and corrosion rate – Specimen B.

5.7.4 Effect of resistivity on corrosion current density

Figure 5.25 shows the relation between electrical resistivity and corrosion current density. The corrosion current density decreases with the electrical resistivity. This drop was very rapid up to value of about 20 kΩ-cm. However, after this value the increase in electrical resistivity does not affect the I_{corr} significantly.

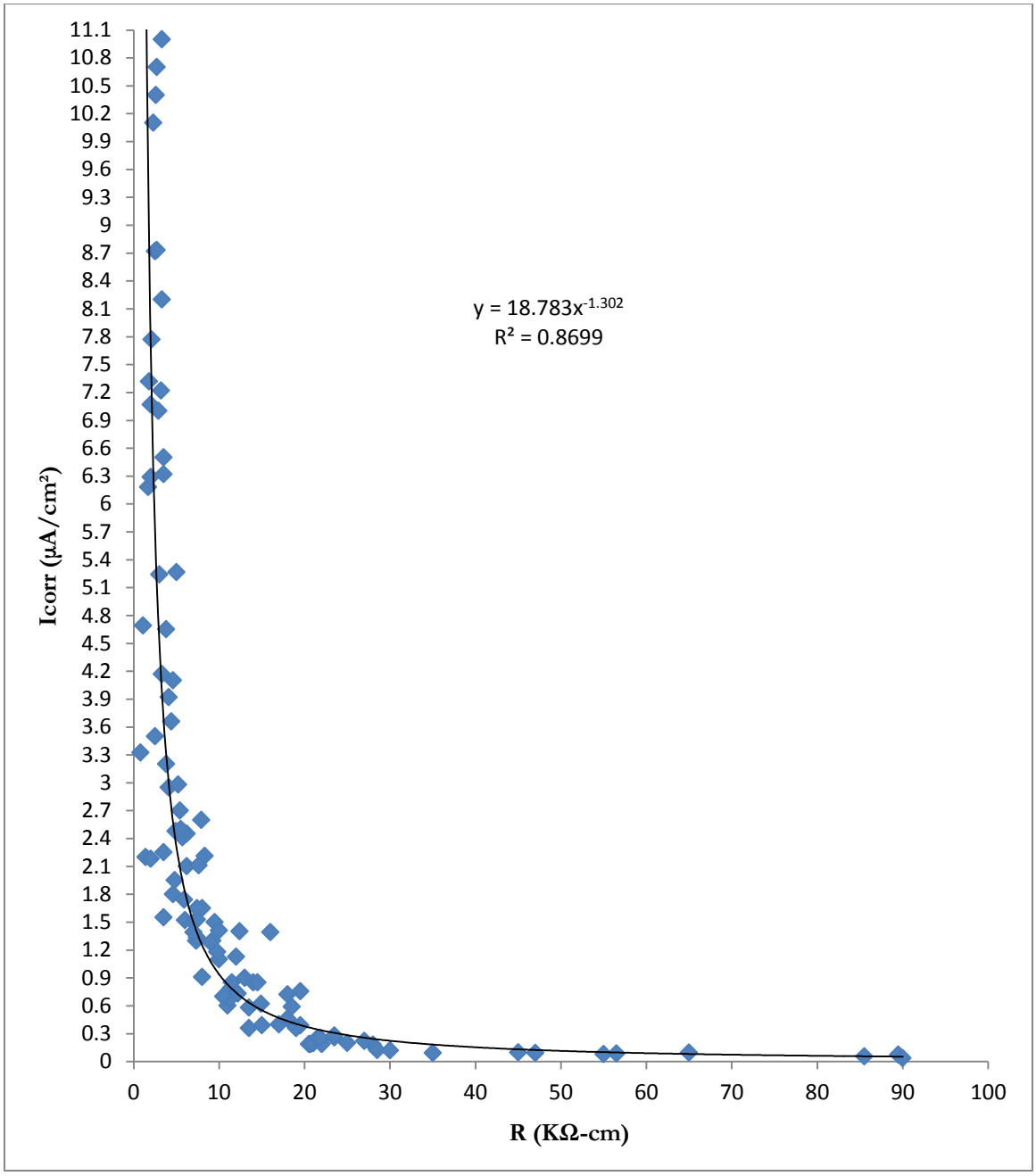

Figure 5.25: Relation between I_{corr} and Resistivity.

By using the resistivity and corrosion current density data a relation was developed to determine corrosion current density using the resistivity of concrete, as shown:

$$I_{corr} = \frac{18.84}{R^{1.3}}$$

I_{corr} = Corrosion Current Density ($\mu A/cm^2$)

R = Resistivity (KΩ-cm)

The data in Figure 5.25 were utilized to classify the risk of corrosion based on the electrical resistivity, as shown in Table 5.8.

Table 5.8: Relation between corrosion rate and resistivity.

R(kΩ-cm)	**Risk of Corrosion Damage**	**I_{corr}($\mu A/cm^2$)**
> 30	Very Low	< 0.1
20 to 30	Low	0.1 to 0.3
10 to 20	Medium	0.3 to 1
< 10	High	>1

CHAPTER 6

CONCLUSIONS AND RECOMMENDATIONS

6.1 Conclusions

The study was conducted to develop a reliable and low-cost setup for measuring corrosion rate both with and without Ohmic drop compensation. Fifteen reinforced concrete slab specimens each consisting of three bars were prepared and the bars were corroded using impressed current technique. Reinforcement corrosion rate results obtained using developed the set-up were compared with those obtained using two commercial equipment and by gravimetric weight loss measurements. The effect of moisture content and electrical resistivity on corrosion rate was also studied. Based on the results obtained, the following conclusions are made:

1. A setup and calculation procedure were developed that are capable of measuring the corrosion over a wide range.
2. The corrosion current density determined using the developed setup and other two commercial equipment without Ohmic drop compensation compared very well with gravimetric weight loss. However, the best trend was noted in the data obtained from the developed setup.
3. The corrosion current density determined with Ohmic drop compensation utilizing the developed setup, correlated very well with the gravimetric weight loss. However, the corrosion current density measured with Ohmic drop compensation utilizing the two commercial equipment did not correlate well with the gravimetric weight loss.

4. A good correlation was noted between the corrosion current density measured with and without compensation using the developed set-up. The corrosion current density measured with Ohmic drop compensation was more than that measured without Ohmic drop compensation. The following relation between corrosion current density measured with and without Ohmic drop compensation was observed.

Icorr (μA/cm²)	**Degree of Corrosion**	**Relation Between Without & With Ohmic Drop using developed setup**
< 0.1	Low	$(\mathbf{I_{corr}})_{\mathbf{WITH\ IR}} = 1.317\ (\mathbf{I_{corr}})_{\mathbf{W/O\ IR}}$
0.1 to 1	Medium	$(\mathbf{I_{corr}})_{\mathbf{WITH\ IR}} = 2.35\ (\mathbf{I_{corr}})_{\mathbf{W/O\ IR}}$
>1	High	$(\mathbf{I_{corr}})_{\mathbf{WITH\ IR}} = 3.794\ (\mathbf{I_{corr}})_{\mathbf{W/O\ IR}}$

Ohmic drop compensation is the least when the corrosion rate is low. Thus, in this zone I_{corr} measurements can be carried out without Ohmic drop compensation. In the range of medium corrosion the effect of Ohmic drop compensation is in the range of 2 to 2.5. But when the corrosion is more than 1 μA/cm², the I_{corr} with Ohmic drop compensation is about 3.8 times is that of I_{corr} measured without Ohmic drop compensation.

5. The electrical resistivity decreased with an increase in the moisture content. Further, the electrical resistivity was very low for a moisture content of more than 2.5%. Consequently, Ohmic drop compensation may not be necessary if the moisture content is more than 2.5%. The following relationship could be noted between the moisture content and the electrical resistivity:

$$R = \frac{19.87}{(M.C)^{1.4}}$$

Where: M.C = Moisture content (%)

R = Resistivity (KΩ-cm)

6. The corrosion current density decreased with an increase in the electrical resistivity. The decrease was very rapid up to 20 kΩ-cm. However, after this value the increase in the electrical resistivity did not affect I_{corr} significantly. The following relationship between the electrical resistivity and I_{corr} was noted:

$$I_{corr} = \frac{18.84}{R^{1.3}}$$

Where: I_{corr} = Corrosion Current Density ($\mu A/cm^2$)

R = Resistivity (KΩ-cm)

7. The electrical resistivity and I_{corr} values were utilized to classify the risk of corrosion, as shown below :

R(kΩ-cm)	**Risk of Corrosion Damage**	**I_{corr}($\mu A/cm^2$)**
> 30	Very Low	< 0.1
20 to 30	Low	0.1 to 0.3
10 to 20	Medium	0.3 to 1
< 10	High	>1

6.2 Recommendations

Based on the results obtained from this research work and the analysis provided, the following recommendations are made:

1. The setup developed under this research work is quiet effective in measuring corrosion rates with and without Ohmic drop compensation so it should be packed in a portable form so that the set-up can be utilized for field measurements.
2. Developed setup should be validated for field applications.
3. Long-term studies should be carried out to relate I_{corr} and gravimetric weight loss.
4. Further, studies on the effect of moisture content and relative humidity on resistivity and corrosion rate should be carried out.

CHAPTER 7

REFERENCES

[1] Pradhan, B. and Bhattacharjee, B. "*Performance Evaluation of Rebar in Chloride Contaminated Concrete by Corrosion Rate*", Journal of Construction and Building Materials, vol. 23, pp. 2346-2356, 2009.

[2] Sathiyanarayanan, S., Natarajan, P., Saravanan, K., Srinivasan, S. and Venkatachari G. "*Corrosion Monitoring of Steel in Concrete by Galvanostatic Pulse Technique*",Journal of Cement and Concrete Composites, vol. 28 , pp. 630-637, 2006.

[3] Ganesan, K., Rajagopal, K. and Thangavel, K. "*Evaluation of bagasse ash as corrosion resisting admixture for carbon steel in concrete*", Journal of Anti-corrosion Methods and Materials, vol. 54, pp. 230-236, 2007.

[4] Hausman, D.A. "*Steel corrosion in concrete-how does it work*", Materials protection, vol. 11, No.6, pp. 19-23, 1967.

[5] http://www.cement.org/tech/cct_dur_corrosion.asp.

[6] Mozer, J.D., et al. "*Corrosion of reinforcing bars in concrete*", Journal american concrete institute, pp. 909-931, 1965.

[7] ACI Committee 222 "*Corrosion of Metals in Concrete*", ACI manual of concrete practice, Part-1, Materials and General Properties of concrete, 1992.

[8] Khan, M.S., "*Corrosion State of Reinforcing Steel in Concrete at Early Ages*",ACI Materials journal, vol. 88, pp. 444-448, 1991.

[9] Sagoe-crentsil, K.K.,and glasser, F.P. "*Steel in Concrete : Part I; a Review of the Electrochemical and Thermodynamic Aspects*",Magazine of concrete Research, vol. 46, pp. 205-212, 1989.

[10] Cahyadi, J.H. and Uomoto, T. "*Influence of Environmental Relative Humidity on Carbonation of Concretre (mathematical modeling)*", Durability of building materials and components, vol. 6, pp. 1142–1151, 1993.

[11] Uhlig, H.H., "*Corrosion and Corrosion Control – an Introduction to Corrosion Science and Engineering* ", John Wiley and Sons, Inc. 1971.

[12] Berkely, K.G.C. and Pathmanaban, S. "*Cathodic Protection of Reinforcement Steel in Concrete*", Butterworths& Co. Ltd, London , 1990.

[13] Slater, J.E., "*Corrosion of Metals in Association with Concrete*", 1983.

[14] Rasheeduzzafar, Dakhil, F.H., Al-Gahtani, A.S., Al-Saadoun, S.S. and Bader, M.A., "*Influence of Cement Composition on the Corrosion of Reinforcement and Sulfate Resistance of Concrete*", ACI Materials Journals, **vol. 87** , pp. 114–122,1990.

[15] ACI Committee 201 "guide to durable concrete", ACI Materials Journal 1991.

[16] Jaegermann,C. "*Effect of Water–Cement Ratio and Curing on Chloride Penetration into concrete*

exposed to Mediterranean sea climate", ACI Materials Journals, pp. 333–339**,** 1990.

[17] Ho D.W.S. and Lewis R.K. "*Carbonation of Concrete and its Prediction*", Cement Concrete Research, Vol. 17 , pp. 489–504,1987.

[18] Maslehuddin, M., and Al-Amoudi, O.S.B. "*Corrosion of Reinforcing Steel in Concrete: Its Monitoring and Prevention*",Preprint, Symposium on Corrosion and Its Control, King Saud University, pp. 110-125, May 1992.

[19] Bertolini L., Elsener, B., Pedeferri, P., and Polder, R., "*Corrosion of Steel in Concrete-prevention, diagnosis, repair*", Wiley-VCH, 2004.

[20] Polder, R. B., "*Test Methods for on Site Measurement of Resistivity of Concrete – a RILEM TC-154 Technical Recommendation*", Construction and Building Materials, vol. 15, pp. 125-131, 2001.

[21] Ahmad S. and Bhattacharjee, B."*A Simple Arrangement and Procedure for In-Situ Measurement of Corrosion Rate of Rebar Embedded in Concrete*", Corrosion Science, vol. 37, pp. 781-791, 1995.

[22] Cavalier, P.G. and Vassie, P.R. "*Investigation and repair of reinforced corrosion in a bridge deck*", In Proceedings of Institution of Civil Engineers, vol. 70, pp. 461-480, 1981.

[23] MacDonald, D. "*Evaluation of Electrochemical Impedance Technology for Detecting Corrosion of Rebar in Reinforced Concrete*", National Research Council, vol. 1, 1991.

[24] ASTM C876-91, "*Standard Test Method for Half-Cell Potentials of Uncoated Reinforcing*,"1999.

[25] Soleymani, H.R. and Ismail, M.E. Cement and concrete Research, vol. 34, pp. 1073-1079, 2004.

[26] Elsener, B., Molina, M. and Bonhi H., Corrosion Science, vol. 35, p. 1563, 1993.

[27] Elsener, B., Bönhi, H."*Corrosion Rates of Steel in Concrete*", ASTM STP 1065, p. 143, 1990.

[28] Broomfield, J.P., Langford, P.E., Ewins A.J. "*Corrosion Rates of Steel in Concrete*," ASTM STP 1065, p. 157, 1990.

[29] Elsener, B. and Bönhi, H. Material Science Forum, vol. 111-112, p. 635, 1992.

[30] Arup, H."*Corrosion of Reinforcement in Concrete Construction*", London,UK, p. 151, 1983.

[31] Browne, R.D., Geoghegan M.P. and Baker, A.F."*Corrosion of Reinforcement in Concrete Construction*", London, UK, p. 193, 1983.

[32] Flis, J., Pickering, H.W. and Osseo-Asare K. Electrochim. Acta, vol. 43, p. 1921, 1998.

[33] Videm, K. "*Corrosion of Reinforcement in Concrete, Monitoring, Prevention and Rehabilitation*", European Federation of Corrosion,London, pp. 104–121, 1998.

[34] Aguilar, A., Sagüés, A., Powers, R. "*Corrosion Rates of Steel in Concrete*", American Society for Testing and Materials,Philadelphia, pp. 66–85, 1990.

[35] Escalante, E., In: Page, C.L. ,Treadaway K. and Bamforth P. "*Corrosion of Reinforcement in Concrete*", Elsevier Applied Science, London–New York, p. 281, 1990.

[36] Sagües, A. "*Corrosion Measurement Techniques for Steel in Concrete*",Corrosion, p. 353,

1993.

[37] Yeih, W. and Huang, R. cement concrete research , vol. 28, p. 1071, 1998.

[38] Eden,D.A.andRothwell, A.N." *Electrochemical Noise Data: Analysis, Interpretation and Presentation Conference on Corrosion*", NACE International, Houston, TX p. 292, 1992.

[39] Gowers, K.R., Milliard, S.G."*Electrochemical Technology for Corrosion Assessment of Reinforced*",Civil Engineers Structutes and Buildings, vol. 134, pp. 129-134, 1999.

[40] Bertocci, U. and Huet, F. Corrosion, vol. 51, p. 131, 1995.

[41] Legat,A. and Dolecek,V. "*Chaotic Analysis of Electrochemical Noise Measured on Stainless Steel*",Journal of the Electrochemical Society, vol. 142, no. 6, pp. 1851–1858, 1995.

[42] Leban, M., Dolecek, V. and Legat, A. "*Comparative Analysis of Electrochemical Noise Generated during Stress Corrosion Cracking of AISI 304 Stainless Steel*", Corrosion , vol. 56, p. 921, 2000.

[43] Cottis, R.A. "*Interpretation of Electrochemical Noise Data*", Corrosion", Vol. 57, p.265, 2001.

[44] Cottis, R.A., Al-Awadhi, M.A.A., Al-Mazeedi H. and Turgoose, "*Measures for the Detection of Localized Corrosion with Electrochemical Noise*", S. Electrochemical Acta, vol. 46, p.3665, 2001.

[45] Leban M., Dolecek,V., and Legat,A., "*Electrochemical Noise DuringNon-Stationary Corrosion Processes*",Materials and Corrosion, vol. 52 , p. 418, 2001.

[46] Aballe, A., Bethencourt, M., Botana, F.J. and Marcos, M. "*Using Wavelets Transform in the Analysis of Electrochemical Noise Data*", ElectrochimicaActa, Vol. 44 No. 26, pp. 4805-16, 1999.

[47] Kearns U., Scully, J.R., Roberge, P.R.,Reichert, D.L., Dawson, J.L. Bertocci, "*Electrochemical Noise Measurement for Corrosion Applications*", ASTM STP 1277, ASTM, West, vol. 39, 1996.

[48] Mariaca, L., Bautista , A., Rodriguez , P., Gonzalez J. A. "*Use Of Electrochemical Noise For Studying The Rate Of Corrosion Of Reinforcements Embedded In Concrete*", Materials and structures, VOL.30, pp.613, 1997.

[49] Tullmin, M. and Hansson, C. M., "*Proceedings of the Corrosion*", San Diego, CA, NACE, Houston, TX, 1998, p. 372.,1998

[50] Stern, M. and Geary, L., "*Electrochemical Polarization, No.1 Theoretical Analysis of the Shape of Polarization Curves*", Journal of Electrochemical Society, Vol. 104, pp. 56-63, 1957.

[51] Andrade, C., Alonso, C., Gulikers, J., Polder, R., Cigna, R., Vennesland, O., Salta, M., Raharinaivo, A., and Elsener, B., "*Test methods for on-site Corrosion Rate Measurement of Steel Reinforcement in Concrete by Means of the Polarization Resistance Method*", RILEM Materials and Structures, vol.37, pp. 623-643, 2004.

[52] Bertolini, L., Elsener, B., Pedeferri, P., and Polder, R., "*Corrosion of Steel in Concrete-Prevention, Diagnosis, Repair"*, Wiley-VCH, 2004.

[53] Walter, G.W. "*Problems Arising in the Determination of Accurate Corrosion Rates from Polarization Resistance Measurements*", Corrosion Science, vol.17, pp. 983-993, 1977.

[54] Gonzalez, J.A., Molina, A., Escudero, M.L., and Andrade, C., "*Errors in the Electrochemical Evaluation of very Small Corrosion Rates-I: Polarization Resistance Method applied to Corrosion of Steel in Concrete*", Corrosion Science, Vol.25, pp.917-930, 1985.

[55] Feliu, S., Gonzalez, J.A., Miranda, J.M., and Feliu, V., "*Possibilities and Problems of in Situ Techniques for Measuring Steel Corrosion Rates in Large Reinforced Concrete Structures*",Corrosion Science, Vol. 47, pp.217-238, 2005.

[56] Andrade, C., Alonso, M.C., Gonzalez,J.A., "*An Initial Effort to use Corrosion Rate Measurements for Estimating Rebar Durability Corrosion Rates of Steel in Concrete*," ASTM STP 1065, N.S.Berke et al., pp. 29-37, 1990.

[57] ASTM G 1-03 ,"*Standard Practice for Preparing, Cleaning, and Evaluating Corrosion Test Specimens*", West Conshohocken, PA, 2003.

[58] Frank, E. "*Electrical Measurements Analysis*", Mc-Graw Hill, New York, 1959.

[59] Jones, D.A. "*The Advantageous of Galvanostatic Polarization Resistance Measurements*", Corrosion, Vol.39, No. 1 , January-February , PP.37-40, 1983.

[60] Rocchini, G. "*Numerical Methods for the Determination of the Polarization Resistance in Corrosion Rate Monitoring and Inhibitor Testing*", Vol.44, No.3, pp.158-164, March, 1988.

[61] Mansfeld, F. "*Tafel Slopes and Corrosion Rates from Polarisation Resistance Measurements*", Corrosion,Vol.29, No.10, October , pp.397-402, 1973.

[62] LeRoy, R.L. "*Evaluation of Corrosion Rates Polarisation Measurements*", Corrosion, Vol.31, No.5, May , pp.173-177, 1975.

[63] Gonzalez, J.A., et al. "*Effect of Carbonation,Chloride and Relative Ambient Humidity on the Corrosion of GalvanisedRebars Embedded in Concrete*" , British Corrosion Journal, Vol.17, No.1, pp.21-28, 1982.

[64] Feliu, S., et al. "*On-situ Determination of the Polarization Resistance in a Reinforced Concrete Beam*", Corrosion , Vol.44, No.10, October, pp.761-765, 1988.

[65] ASTM C 128-07a, "*Standard Test Method for Density, Relative Density (Specific Gravity) and Absorption of Fine Aggregate*",ASTM, West Conshohocken, Pa.

[66] Neville, A. M., "*Properties of Concrete*," Fourth Edition, Pearson Prentice hall, England, 2010.

[67] PowerCORR User's Manual, "*Corrosion Measurement Software*", Princeton Applied Research, USA, 2001.

VITAE

Name : Mohammed Abdul Azeem Jibran

Nationality : Indian.

Date of Birth : February 29, 1988.

Permanent Address : H.No: 22-3-947/33/A/2/1, Purani Haveli,
Hyderabad – 500002, Andhra Pradesh, INDIA.

Present Address : Room#803/306, KFUPM, Dhahran, K.S.A.

Email : azeem_jibran@yahoo.com

Phone : +966-557953924/548731659
+91-9885244923

Degrees:

Bachelor of Science in Civil Engineering from Osmania University (Sept. 2005 – June 2009).

Experiences:

Research Assistant in Civil Engineering Department of King Fahd University of Petroleum & Minerals (KFUPM) (Feb. 2010 – Feb. 2012).